# INSTITUTO CARLOS CHAGAS

Doutorado em Biociências

CARACTERIZAÇÃO FUNCIONAL DO COMPLEXO ADAPTADOR 1 (AP-1) EM *Trypanosoma cruzi*

CLAUDIA MARIA DO NASCIMENTO MOREIRA

Curitiba/PR

2017
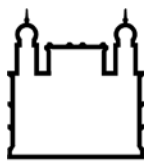
Ministério da Saúde

FIOCRUZ
Fundação Oswaldo Cruz

INSTITUTO CARLOS CHAGAS

Pós-graduação em Biociências e Biotecnologia

CLAUDIA MARIA DO NASCIMENTO MOREIRA

CARACTERIZAÇÃO FUNCIONAL DO COMPLEXO ADAPTADOR 1 (AP-1) EM *Trypanosoma cruzi*

Tese apresentada ao Instituto Carlos Chagas

como parte dos requisitos para obtenção do

título de Doutor em Biociências

Orientadores: Dr. Stenio Perdigão Fragoso

Dr. Maurilio José Soares

Curitiba/PR

2017

AGRADECIMENTOS

Dedico esse trabalho ao meu amor Giancarlo Lupatini, aos meus pais, irmãos e aos que não estão mais aqui, mas que me acompanham sempre em pensamento:

Franscisco Gomes Barbosa

Francisca Moreira

Gabriel Erick dos Santos

RESUMO

O AP-1 é um complexo adaptador heterotetramérico formado pelas subunidades γ, β, μ e σ. Esse complexo auxilia a montagem do revestimento de vesículas com clatrina na rede trans-Golgi, as quais transportam enzimas deste para os lisossomos em células eucarióticas. No entanto, o papel do AP-1 no protozoário *Trypanosoma cruzi* – o agente causador da doença de Chagas – é totalmente desconhecido. Nesse trabalho, estudamos a função do complexo AP-1 em diferentes formas do ciclo de vida de *T. cruzi*. Para tanto, foi produzido uma linhagem mutante nulo para subunidade gama (TcAP1-γ) através da técnica de nocaute gênico por recombinação homóloga a fim de aferir uma função para esse adaptador nesse parasita. Outra abordagem foi identificar proteínas associadas à duas subunidades de TcAP-1 (β e μ) por imunoprecipitação e análise por espectometria de massas. Nossos dados com o parasita nocaute para AP1-γ (TcAP1-γKO) mostraram que formas epimastigotas tiveram sua proliferação e diferenciação para a forma infectiva tripomastigota metacíclicos reduzidas (comparando com parasita selvagem) após a deleção da proteína. Os parasitas TcAP1-γKO também mostraram uma significativa redução na capacidade de infectar células de mamíferos (HeLa e VERO). Outro aspecto relevante é que o nocaute de AP1-γ prejudicou o processamento e o transporte da cruzipaína (principal cisteíno-proteínase de *T. cruzi)* do complexo de Golgi para os reservossomos (organelas relacionadas aos lisossomos) em *T. cruzi*. Para confirmar que a ausência da cruzipaína nos reservossomos nos parasitas nocaute era devido à ausência da expressão de TcAP1-γ, parasitas TcAP1-γKO foram transfectados com plasmídeo para expressão epissomal de TcAP1-γ. A complementação da expressão de TcAP1-γ no parasita TcAP1-γKO restaurou a maturação e a localização da cruzipaína nos reservossomos, sugerindo que o complexo TcAP-1 atue na rede trans-Golgi, na formação de vesículas contendo cruzipaína direcionadas aos reservossomos em *T. cruzi*. Além disso, análise de proteômica das proteínas associadas com TcAP1-β e TcAP1-μ fusionadas à etiqueta GFP, detectaram as subunidades TcAP1-γ e TcAP1-σ do complexo AP-1, mas não detectaram outras possíveis interações. Esse resultado indica que a etiqueta GFP provavelmente interferiu com as associações de AP-1 com outras proteínas auxiliares.

Palavras-chave: Complexo adaptador 1, tráfego de vesículas, cruzipaína, *Trypanosoma cruzi*

ABSTRACT

The AP-1 Adaptor Complex assists clathrin-coated vesicle assembly in the *trans*-Golgi network of eukaryotic cells. However, the role of AP-1 in the protozoan *Trypanosoma cruzi* — the Chagas disease parasite — has not been addressed. Here, we studied the function of AP-1 in different *T. cruzi* life cycle forms, by generating a gene knockout of the large AP-1 subunit gamma adaptin (TcAP1-γ). Epimastigote (insect form) parasites lacking TcAP1-γ (TcAP1-γKO) have reduced proliferation and differentiation into infective metacyclic trypomastigotes (compared with wild-type parasites). TcAP1-γKO parasites have also displayed significantly reduced infectivity towards mammalian cells. Importantly, TcAP1-γ knockout impaired maturation and transport to lysosome-related organelles (reservosomes) of a key cargo – the major cysteine protease cruzipain, which is important for parasite nutrition, differentiation and infection. To confirm that the absence of cruzipain in the reservosomes of TcAP1-γKO parasites was due the lack of TcAP1-γ expression, TcAP1-γKO parasites were transfected with an episomal construct constitutively expressing TcAP1-γ. Complementation of TcAP1-γ expression in AP1-γKO mutants restored maturation and cruzipain localization to the reservosomes, implicating the AP-1 complex in the formation of reservosome-bound vesicles containing cruzipain, at the *trans*-Golgi network. In addition, proteomics analysis of complexes associated with GFP-tagged TcAP1-β and TcAP1-μ detected the subunits of AP-1, TcAP1-γ and TcAP1-σ, but not others possible targets, indicating that GFP probably interfered with the association of AP-1 with other auxiliary proteins.

Keywords: Adaptor complex 1, vesicles traffic, cruzipain, *Trypanosoma cruzi.*

SUMARIO

1 INTRODUÇÃO

1.1 Transporte vesicular

As células eucarióticas desenvolveram características próprias como a presença de um sistema de endomembranas, originando compartimentos quimicamente distintos entre si. Para manter a homeostase celular e a identidade de cada compartimento, existe um elaborado sistema de comunicação através de vesículas revestidas que, seletivamente, direciona moléculas entre esses compartimentos (FAINI *et al*., 2013).

A formação do revestimento envolve o recrutamento de um conjunto de proteínas citoplasmáticas para a região de brotamento das vesículas, na membrana do compartimento de origem, promovendo o aumento na concentração local de receptores transmembranares e suas cargas correspondentes. As proteínas associadas à formação do revestimento, além de selecionar a carga a ser transportada, aplicam uma força mecânica à membrana, causando uma invaginação, que auxilia, posteriormente, na liberação da vesícula. Faz-se igualmente necessário estabelecer interações específicas para ancorar e fundir a vesícula com o compartimento aceptor. Assim, a captura de uma carga a partir do compartimento doador e a sua entrega para um compartimento aceptor requerem um conjunto de interações de alta fidelidade (KIRCHHAUSEN, 2000a).

Vesículas revestidas trafegam em vias essenciais para célula, tais como as vias endocítica e biossintética. Na endocitose, macromoléculas e porções da membrana plasmática são acomodadas em vesículas que seguem para o sistema endossomal. No endossomo inicial, o conteúdo endocitado pode ser reciclado de volta à membrana plasmática ou seguir para os lisossomos onde será degradado (SCOTT *et al*., 2014). Já na via biossintética, vesículas contendo proteínas e lipídios sintetizados no retículo endoplasmático e complexo de Golgi podem, dependendo da carga, seguir para (a) o meio extracelular, (b) para recomposição de membrana plasmática ou (c) para os lisossomos através do sistema endossomal (MATTEIS & LUINI, 2008) (Fig.1.1). O tráfego intracelular de vesículas é essencial para célula, pois atua em processos como nutrição, sinalização, integridade das membranas celulares, proteção contra patógenos, etc.

Dentre as proteínas de revestimento, as mais estudadas são as COP-I, COP-II e a clatrina (Fig.1.1) (FAINI *et al*., 2013).

O tráfego intracelular de vesículas é intenso e também altamente dinâmico, mas além disso, ele é muito seletivo. Somente um determinado grupo de proteínas e lipídios é

internalizado e transportado em vesículas até seu destino, permitindo que cada organela mantenha sua identidade através do ciclo celular. O quão seletivo é, como ocorre exatamente esse transporte e como a identidade de cada organela é mantida, são questões que tem intrigado cientistas por décadas.

1.1.1 Via biossintética

A via biossintética é responsável pela síntese, classificação e distribuição tanto das proteínas com destino às membranas como daquelas que seguem para o meio extracelular e para o interior de outros compartimentos intracelulares. Essa via também é responsável pelo destino da maior parte dos lipídeos na célula. A via biossintética é composta pelo retículo endoplasmático, complexo de Golgi e por compartimentos tubulares que permeiam essas organelas (Fig.1.1)(CAMPBELL & CHOY, 2001).

O retículo endoplasmático fica localizado adjacente ao núcleo e é formado por uma rede intrincada de túbulos e sacos achatados envoltos por membrana, que se estende pelo citosol. O caminho das proteínas destinadas ao sistema de endomembranas é sinalizado pela presença de peptídeos sinais que, durante o processo de tradução, as direcionam, juntamente com os ribossomos, para o retículo endoplasmático, onde são sintetizadas e sofrem modificações pós-traducionais, como a glicosilação (MANDON *et al*., 2013). O retículo endoplasmático também é o principal sítio de síntese dos lipídios constituintes das membranas em células de mamíferos (FAGONE & JACKOWSKI, 2009). Proteínas e lipídios são então transportados para o complexo de Golgi por uma região especializada do retículo endoplasmático, denominada local de saída do retículo endoplasmático (LSRE). A seleção dessa carga é realizada por vesículas revestidas pela proteína COP-II (Fig. 1.1) (SZUL & SZTUL, 2011) que entregarão seu conteúdo à região intermediária entre retículo endoplasmático e o complexo de Golgi (RIRECG). Essa é uma região de triagem onde componentes de membrana e proteínas residentes do retículo endoplasmático retornam para sua origem, através de vesículas revestidas por COP-I e as demais seguem pela via através do complexo de Golgi (Fig.1.1) (SZUL & SZTUL, 2011).
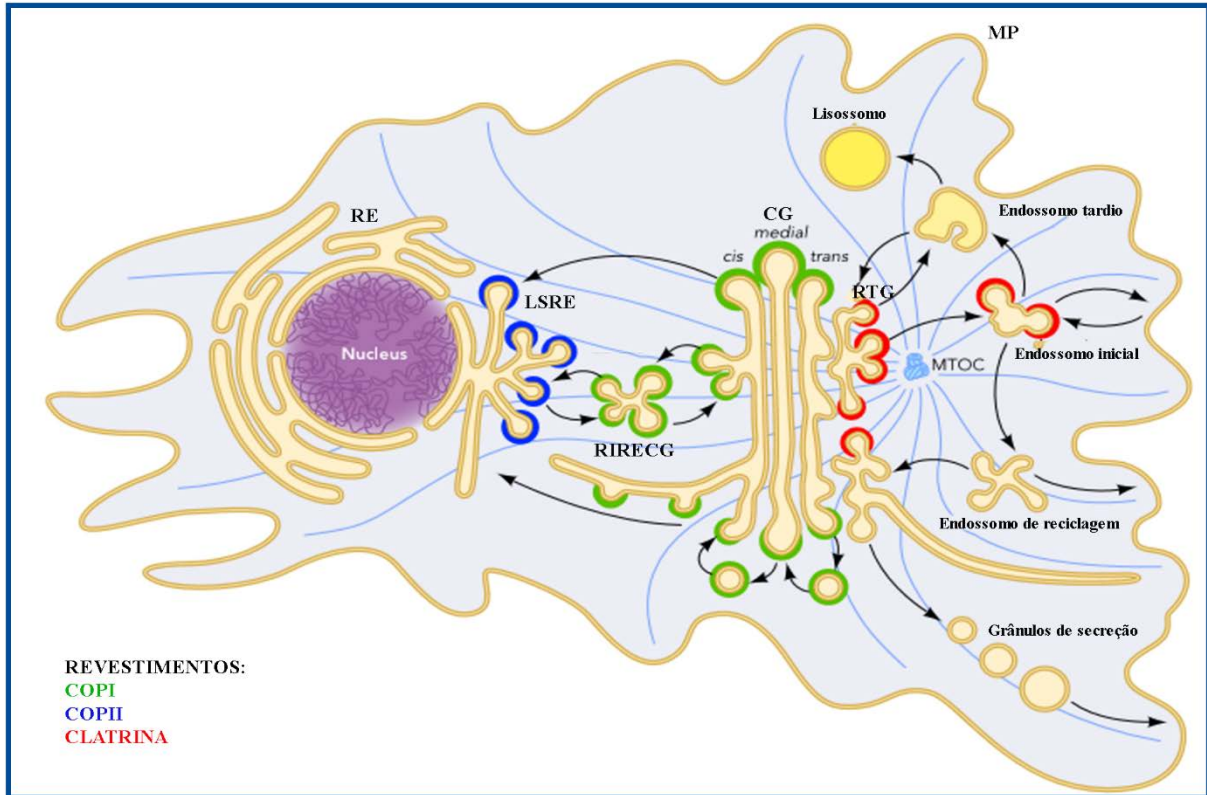
Figura 1.1. Vias de trafégo intracelular com vesículas revestidas: Proteínas COP-II (azul) formam o revestimento de vesículas de transporte, a partir do local de saída do retículo endoplasmático (LSRE) para a região intermediária entre retículo endoplasmático e complexo de Golgi (RIRECG). Proteínas COP-I (verde) revestem vesículas que atuam tanto no transporte entre as cisternas do Golgi quanto para o transporte retrógrado deste para o retículo endoplasmático. A clatrina (vermelho) atua no transporte endocítico na membrana plasmática e no complexo de Golgi, a partir da rede trans-Golgi (RTG). As flechas indicam a direção da via. Adaptado de (SZUL & SZTUL, 2011).

O complexo de Golgi é o principal centro de processamento, triagem e distribuição de proteínas e lipídios na célula. É uma organela peculiar, formada por discos achatados ou cisternas envolvidas por membrana, morfologicamente heterogêneas e que se organizam em pilhas. Possuem uma superfície lisa (sem ribossomos) e, dependendo da célula, podem variar quanto ao número, forma e localização. Normalmente essas pilhas se arranjam em número de quatro a seis cisternas e localizam-se próximo ao retículo endoplasmático e a membrana plasmática (FARQUHAR & PALADE, 1998). Em invertebrados e plantas, o complexo de Golgi pode se organizar em uma única pilha ou em centenas de pilhas individuais dispersas no citosol. No caso de alguns fungos, o complexo de Golgi se organiza na forma de algumas cisternas espalhadas pela célula (MUNRO, 2011).

Quanto à estrutura, o complexo de Golgi é classicamente dividido nas seguintes regiões: (a) rede cis do Golgi que é a mais próxima do retículo endoplasmático, (b) cisternas do complexo de complexo de Golgi propriamente ditas, divididas em cisternas cis, medial e trans e (c) rede trans do Golgi que está orientada para membrana plasmática. Essas regiões diferem entre si quanto ao conteúdo e composição de membrana, permitindo que realizem diferentes funções dentro da organela (FARQUHAR & PALADE, 1981).

As cisternas do complexo de Golgi possuem funções tais como processamento e maturação de N- e O-glicanos, formação de proteoglicanos, sulfatação e modificação lipídica (MUNRO, 2011). A rede trans-Golgi é a última estação do complexo de Golgi e desempenha a importante função de triagem de macromoléculas que serão enviadas, pela via secretória, aos seus locais de destino (MATTEIS & LUINI, 2008).

A triagem das macromoléculas a partir da rede trans-Golgi depende de seus receptores transmembranares, dentre os quais, o melhor caracterizado é o receptor de manose-6-fostato. Nesse processo, hidrolases lisossomais adquirem no Golgi um grupamento de manose-6-fosfato, que é reconhecido pelos receptores de manose-6-fostato (LE BORGNE & HOFLACK, 1997). O complexo carga-receptor é empacotado em vesículas com revestimento de clatrina, para então alcançar o sistema endossomo/lisossomo. A diminuição do pH do lúmem das vesículas leva à dissociação do complexo com concomitante reciclagem dos receptores de manose-6-fostato de volta a rede trans-Golgi. As enzimas seguem para os lisossomos, onde com o pH apropriado, são ativadas (TRAUB & KORNFELD, 1997).

1.1.2 Clatrina

Inicialmente descrita por Barbara Pearse (PEARSE, 1976), a clatrina recebeu esse nome por formar uma estrutura que lembra uma gaiola (do latim *clatratus*). É uma das proteínas de revestimento de vesícula mais estudadas e está presente em todas as células eucarióticas. A clatrina consiste em três cadeias polipeptídicas pesadas (190 kDa) que interagem entre si pela porção C-terminal formando um "vértice". A extremidade amino da cadeia possui o domínio globular, que se associa com proteínas adaptadoras presentes na membrana. Cada uma das cadeias pesadas se associa com uma cadeia leve (25 kDa) (Fig 1.2 A e B). Este conjunto, conhecido como trisquélion se polimeriza em grades poliédricas de forma regular, com diferentes formas e tamanhos (EDELING *et al.*, 2006).
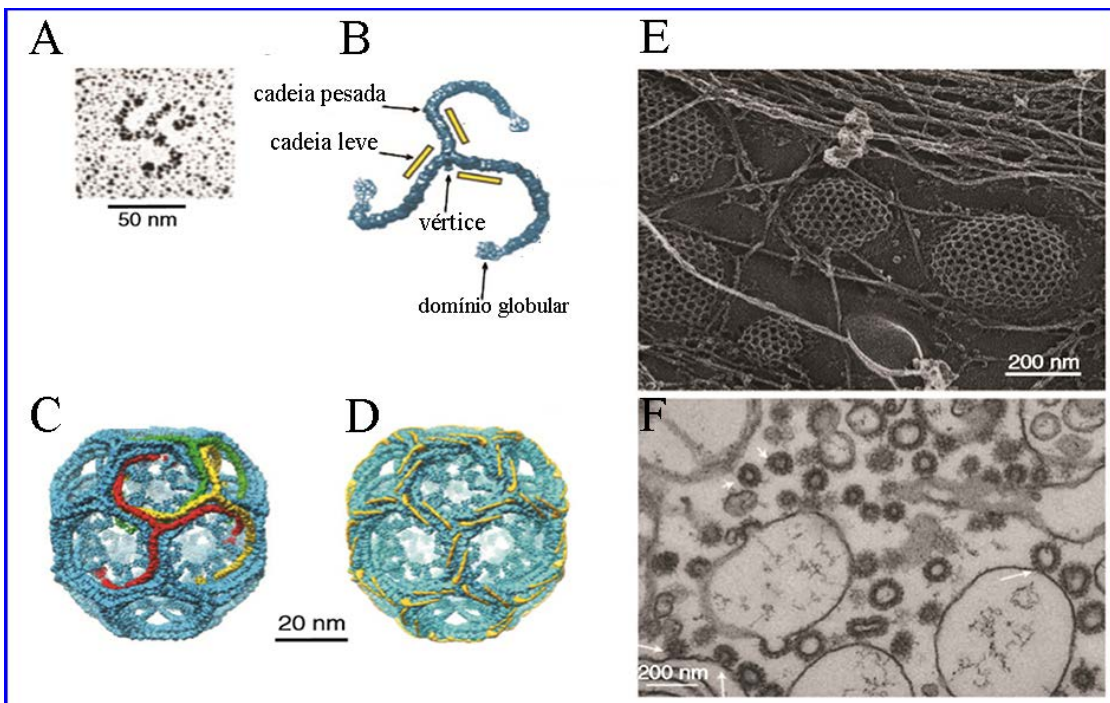
Figura 1.2. Estrutura da clatrina: A) Micrografia do trisquélion de clatrina. B) Esquema do trisquélion de clatrina mostrando a cadeia pesada com o domínio globular, o vértice e a cadeia leve. C) Reconstrução da imagem do barril de hexágono mostrando as cadeias pesadas de clatrina e em D) mostrando as cadeias leves. E) Micrografia eletrônica de varredura mostrando poços revestidos com clatrina na membrana plasmática. E) Micrografia eletrônica mostrando brotamento de vesículas revestidas com clatrina no lipossomo. Adaptado de (ROBINSON, 2015).

As vesículas revestidas com clatrina participam de processos mediados por receptores, tais como a endocitose na membrana plasmática e o transporte de macromoléculas entre a rede trans-Golgi e os compartimentos endossomais (KIRCHHAUSEN, 2000b). Entretanto, em condições fisiológicas, a clatrina não se associa diretamente com os receptores ou com a membrana celular para montar o revestimento. Para tanto, diversas proteínas se associam previamente à membrana e recrutam a clatrina para formação do revestimento. Dentre elas estão aquelas que constituem os complexos adaptadores, as proteínas mais abundantes em vesículas revestidas com clatrina, depois da própria clatrina.

1.1.3 Complexos adaptadores

Diversas proteínas citoplasmáticas são necessárias para a formação do revestimento de clatrina na membrana celular. Dentre elas, estão as que compõem os complexos adaptadores heterotetraméricos, que desempenham importante função como mediadores do tráfego

vesicular entre diferentes compartimentos dentro da célula. São eles que definem o local da membrana onde o revestimento deve ser montado. Eles interagem com componentes de membrana, segregam receptores e sua carga e se associam com diversos fatores citoplasmáticos para formar as vesículas revestidas (BOEHM & BONIFACINO, 2001; PARK & GUO, 2014). Os primeiros complexos adaptadores foram identificados a partir do isolamento de vesículas revestidas por clatrina (revisto por HIRST & ROBINSON, 1998) e, devido a sua capacidade de montar o revestimento *in vitro*, foram nomeados em inglês "assembly protein" (AP) ou "adaptins" (PEARSE & ROBINSON, 1984), embora, por conveniência, tem-se usado atualmente o nome "adaptor protein".

Já foram descritos cinco complexos adaptadores que são estruturalmente relacionados. Todos possuem quatro subunidades protéicas ou adaptinas, sendo duas grandes (~90 a 130 kDa), uma média (~40 kDa) e uma menor (~20 kDa), conforme a seguir: AP-1 (γ, β1, μ1, σ1) AP-2 (α, β2, μ2, σ2), AP-3 (δ, β3, μ3, σ3), AP-4 (ϵ, β4, μ4, σ4) e AP-5 (ζ, β5, μ5, σ5) (BOEHM & BONIFACINO, 2001; HIRST *et al*., 2011) (Fig. 1.3). Entre AP-1 e AP-2, β é a subunidade mais conservada mostrando 84% de identidade de sequência, enquanto as subunidades μ e σ são aproximadamente 40% idênticas, apenas 25% dos aminoácidos são conservados entre γ e α, principalmente devido à divergência dos domínios da "orelha" (EDELING *et al.*, 2006). Apesar das diferenças na sequência primária, as análises da estrutura secundária e dos perfis de hidrofobicidade indicam que todos os quatro complexos são altamente homólogos (COLLINS *et al*., 2002).
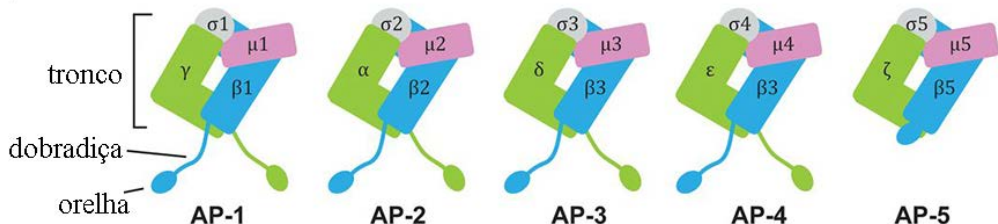
Figura 1.3. Estrutura dos complexos adaptadores: Esquema dos complexos AP heterotetraméricos. Adaptado de (PARK & GUO, 2014).

A maioria dos complexos AP tem três regiões. O tronco, a orelha e a dobradiça (Fig. 1.3). O núcleo ou tronco é constituído pelos domínios N-terminais das duas subunidades grandes e a cadeia completa das subunidades μ e σ. A orelha é constituída pelos domínios C-terminais das duas subunidades grandes e interage com algumas proteínas reguladoras e acessórias. A região da dobradiça faz a ligação entre os outros dois domínios e é importante para interação

com a clatrina através da adaptina β (SHIH *et al*., 1995). O AP-5 funciona de forma independente de clatrina (HIRST *et al*., 2011).

A interação com a membrana celular é realizada pelo tronco dos adaptadores, que interage com lipídeos e proteínas locais. Para que o receptor transmembrana e sua carga sejam incorporados em vesículas, é necessário que este seja reconhecido pelo complexo AP. Já foram identificados alguns sinais de classificação presentes na região citoplasmática desses receptores. Um deles é o motivo de tirosina YXXØ (onde X é qualquer aminoácido e Ø é um resíduo de aminoácido com cadeia lateral hidrofóbica), que é reconhecido pelas subunidades µ1 - µ4 (BONIFACINO & TRAUB, 2003). Outro sinal é o motivo di-leucina [DE]XXXL[LI] que, por sua vez, é identificado pelo dímeros γ-σ1, α-σ2 ou δ-σ3 dos complexos AP-1, AP-2 e AP-3 (BONIFACINO & TRAUB, 2003; MATTERA *et al*., 2011; PARK & GUO, 2014). Os sinais reconhecidos pelo AP-5 ainda não são conhecidos (HIRST *et al*., 2011).

Em células eucarióticas, cada um destes complexos realiza a seleção de macromoléculas em organelas distintas na célula. O AP-1 localiza-se no complexo de Golgi, atuando no transporte para os lisossomos. O AP-2 atua na via endocítica dependente de clatrina na membrana plasmática. O AP-3 encontra-se nos endossomos e medeia o transporte de carga dos endossomos tubulares para os endossomos tardios, atuando na biogênese das ORL (organelas relacionadas aos lisossomos) e pode se associar ou não com clatrina. O AP-4 localiza-se na rede trans-Golgi e está envolvido com o transporte desta organela para os endossomos. O AP-5 foi recentemente identificado e sua localização foi descrita nos endossomos tardios, atuando no tráfego endossomal (Fig. 1.4) (HIRST *et al*., 2011; PARK & GUO, 2014).
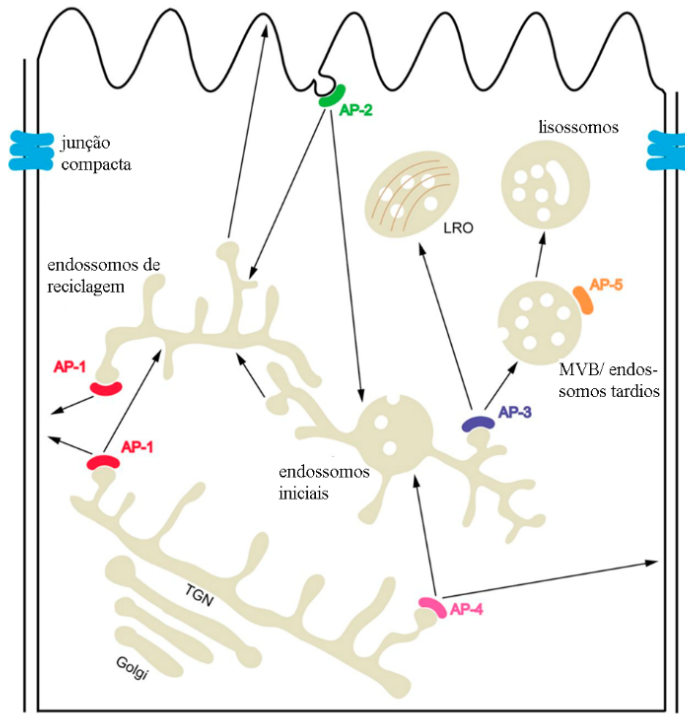
Figura 1.4. Vias de tráfego e localização dos complexos adaptadores AP. (PARK & GUO, 2014).

Entretanto, nem todos eucariotos codificam todos os complexos AP. Por exemplo, *Caenorhabditis elegans* e as leveduras *Saccharomyces cerevisiae* e *Schizosaccharomyces pombe* possuem apenas AP-1, AP-2 e AP-3 (BOEHM & BONIFACINO, 2001; HIRST *et al.*, 2011).

A formação do revestimento na membrana celular segue pelos menos quatro passos que foram caracterizados para os complexos AP-1 e AP-2, mas que, devido à similaridade estrutural, pode ser extendido aos demais. O primeiro é a iniciação, onde uma GTPase ativa o complexo adaptador para associação deste com componentes de membrana, tais como lipídeos e receptores transmembranares. Só então a clatrina é recrutada para membrana. A propagação é o segundo passo e consiste na formação do revestimento e a incorporação da carga, assim como a deformação da membrana. Posteriormente, há o brotamento da vesícula com o auxílio da dinamina que faz a fissão do pescoço da vesícula (terceiro passo). O quarto passo é caracterizado pela perda do revestimento com o auxílio das proteínas auxilina e a chaperona Hsc70, que se associam com a clatrina (revisto KIRCHHAUSEN, 2000). A perda do revestimento acontece logo após o brotamento da vesícula e é importante para expor marcadores, tais como as SNAREs (do inglês, soluble NSF Attachment Receptor) e Rabs, que direcionaram a vesícula para o compartimento correto (SANDERFOOT, 1999), com o auxílio do citoesqueleto (COLE & LIPPINCOTT-SCHWARTZ, 1995; PRESLEY *et al.*, 1997).

1.1.4 Complexo adaptador 1

O complexo adaptador 1 (AP-1) atua na formação de revestimento de vesículas com clatrina no transporte anterógrado entre a rede trans-Golgi e os lisossomos (via formação de endossomos). O AP-1 também participa no transporte retrógado a partir do endossomo inicial ou de reciclagem (HIRST *et al*., 2012). Essa via recicla receptores residentes do Golgi que seguiram para o sistema endossomal ou, equivocadamente, para membrana plasmática e que necessitam ser endocitados.

O AP-1 pode ocorrer como isoformas codificadas por diferentes genes (γ1 / 2, β1, μ1A / B e σ1A / B / C), formando os complexos AP-1A e AP1-B. O AP1-A é encontrado em todas as células eucarióticas, enquanto que o AP1-B é epitelial-específico agindo no tráfego basolateral. O AP-1 está associado às vesículas revestidas com clatrina e medeia o transporte entre a RTG e o sistema endossomo/lisossomo (NAKATSU *et al*, 2014). Entre as moléculas transportadas via AP-1, estão as hidrolases lisossomais que possuem resíduo de manose-6-fosfato, que devem seguir da via biossintética para atuarem nos lisossomos (GHOSH *et al*, 2003).

A forma pela qual o revestimento é formado na membrana é similar entre os adaptadores. Entretanto, algumas moléculas são características de cada adaptador. Para saber em qual membrana o adaptador deve iniciar o revestimento, pelo menos dois fatores são importantes: a GTPase e o fosfolípideo da membrana. Por exemplo, a GTPase Arf1 recruta o AP-1 para a membrana do Golgi através da interação com a região N-terminal da subunidade γ. Essa GTPase também tem a função de ativar o adaptador para que este exponha os sítios de interação com a região citoplasmática dos receptores transmembranares, que é alcançada pela interação com a região N-terminal da subunidade β, bem como de uma região mais central da subunidade γ (Fig. 1.5) (REN *et al*., 2013; TRAUB *et al*, 1993). Outra molécula importante para a ancoragem do AP-1 é o fosfatidil-inositol-4-fosfato. Esse fosfolipídio é enriquecido na membrana da rede trans-Golgi e interage através da região N-terminal da subunidade γ (DI PAOLO & DE CAMILLI, 2006; HELDWEIN *et al*., 2004; WANG *et al*., 2003). Diversas proteínas acessórias estão envolvidas com a formação de revestimento envolvendo AP-1, tais como a γ-sinergina (PAGE *et al*., 1999), a Rabaptina 5, a epsinaR e a GGA (Golgi localized, gamma-ear-containing, ADP-ribosylation factor-binding protein). A GGA é uma proteína adaptadora monomérica que possui homologia com a subunidade γ do complexo AP-1. Esse adaptador está envolvido com o transporte de vesículas a partir da RTG e já foi descrita sua associação com complexo AP-1 (BAI *et al*., 2004).

AP-1 desativado   AP-1 ativado por Arf1
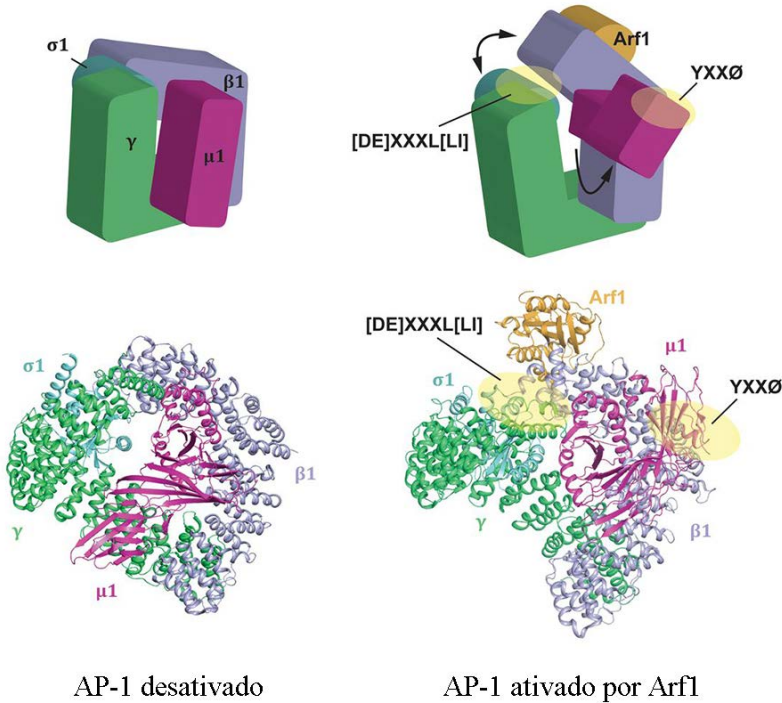
Figura 1.5. Complexo AP-1 desativado e ativado por Arf1 expondo sítios de interação com receptor e membrana. (PARK & GUO, 2014).

Apesar da elevada conservação de AP-1 entre mamíferos e levedura, a função desse adaptor parece ser distinta entre esses organismos. Estudos mostraram que camundongos deficientes em AP-1 morrem precocemente no desenvolvimento embrionário (MEYER *et al*., 2000; ZIZIOLI *et al*., 1999). O nocaute da adaptina γ interfere com o desenvolvimento do blastocisto, enquanto que os camundongos deficientes em μ1 sobrevivem apenas até ao dia 13.5 do desenvolvimento embrionário, sugerindo que as funções de AP-1 são essenciais para o desenvolvimento de um organismo multicelular. Em contraste, a depleção de todas as adaptinas do AP-1 não causa um fenótipo letal em *S. cerevisiae* (YEUNG *et al.*, 1999), sugerindo que, em diferentes organismos, AP-1 transporta cargas que, dependendo da sua função, são vitais para o funcionamento normal da célula.

1.2 Tripanossomatídeos e o transporte vesicular

Os tripanossomatídeos são protozoários flagelados, que pertecem ao reino Protozoa, sub-reino Eozoa, filo Euglenozoa, classe Kinetoplastea, ordem Kinetoplastida e família Trypanosomatidae e diversas características apontam que esses organismos divergiram cedo do ramo principal dos eucariotos na árvore evolutiva (CAVALIER-SMITH, 2010). A família Trypanosomatidae compreende um grande número de protozoários parasitas, muitos dos quais

causam graves doenças em humanos. Entre eles estão *Trypanosoma brucei*, *Leishmania* spp. e *Trypanosoma cruzi*. *Trypanosoma brucei* é o agente causador da doença do sono em humanos e da nagana em gado. Essas enfermidades são as principais causas de morbidade e dificuldades econômicas em regiões endêmicas da África. Espécies de *Leishmania* são causadoras de diversos tipos de leishmaniose, que variam desde pequena úlcera na pele até doença visceral fatal, atingindo África, Ásia, partes da Europa e América Latina (WHO, 2017).

Todos os parasitas descritos acima são transmitidos por insetos vetores hematófagos infectados e invadem uma gama de células e tecidos no hospedeiro mamífero. Eles possuem um ciclo de vida complexo durante o qual sofrem transformações morfológicas e metabólicas dramáticas para se adaptarem aos diferentes ambientes onde vivem. Para que esses organismos tenham sucesso em seus hospedeiros, o transporte de moléculas entre seus compartimentos e também para sua superfície é extremamente importante para sua nutrição, adaptação aos diferentes ambientes e para o escape do sistema imune do hospedeiro vertebrado.

1.2.1   A doença de Chagas e o *Trypanosoma cruzi*

A doença de Chagas ou tripanossomíase americana é causada pelo parasita *T. cruzi* e é uma das mais importantes doenças tropicais negligenciadas (TARLETON *et al*., 2014). Esta doença é endêmica da América latina, porém, tem se espalhado pelos diversos continentes em decorrência da imigração humana (COURA & VINAS, 2010). Estima-se que entre 6 a 7 milhões de pessoas estão infectadas no mundo, principalmente na América Latina (WHO, 2017). A forma de transmissão do protozoário é principalmente pela via vetorial, através das excretas do inseto barbeiro, mas pode ocorrer também por outras vias, como exemplo: via transfusional, via congênita (através da placenta), por transplante de órgãos, via oral (alimento contaminado) ou acidentes laboratoriais (COURA, 2007).

Trypanosoma cruzi possui um ciclo de vida complexo (Fig. 1.6), que se alterna entre dois hospedeiros: um hospedeiro invertebrado, representado por insetos triatomíneos (ordem Hemíptera, família Reduviidae, subfamília Triatominae) conhecidos popularmente como barbeiros, e um hospedeiro mamífero, incluindo o homem.
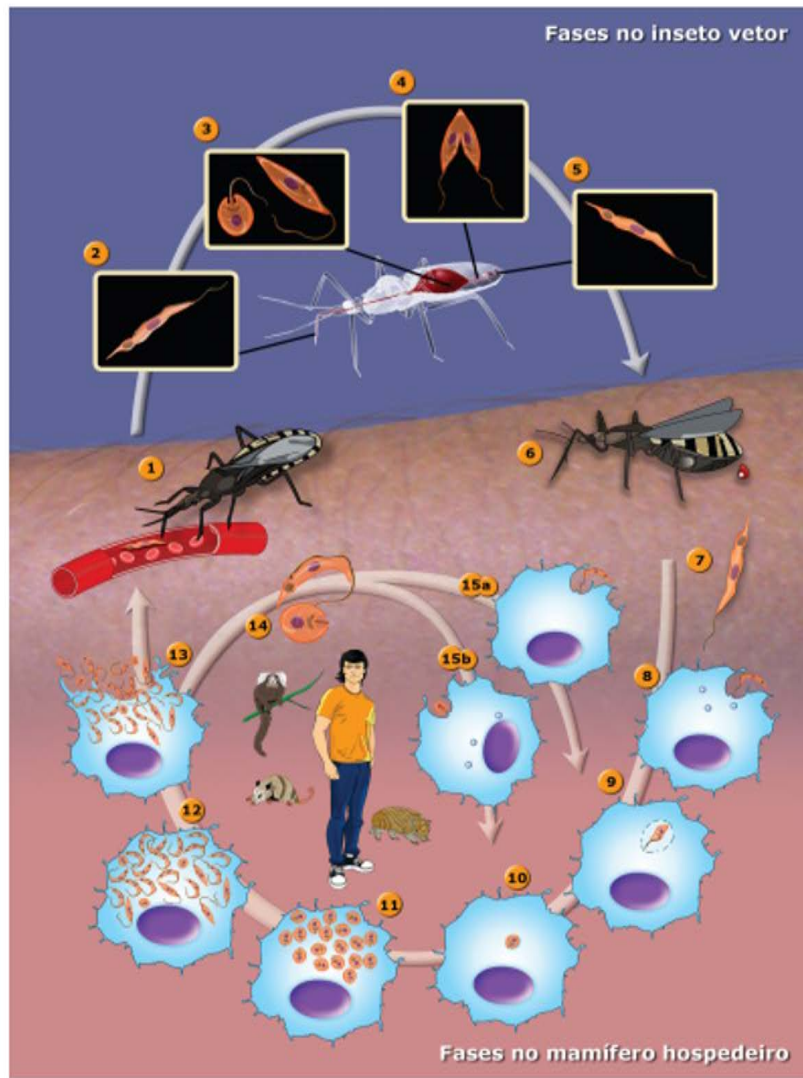
Figura 1.6. Ciclo de vida do *Trypanosoma cruzi*. A contaminação do barbeiro (1) ocorre durante o repasto sanguíneo em um mamífero infectado e ingere formas tripomastigotas sanguíneas (2). Na porção anterior do estômago os tripomastigotas se diferenciam em epimastigotas (3). As epimastigotas sobreviventes à digestão, alcançam o intestino e começam a se multiplicar sucessivamente por divisão binária (4) e aderem-se às membranas perimicrovilares. Posteriormente, os epimastigotas se soltam e movem-se para o intestino posterior, onde iniciam o processo de diferenciação em tripomastigotas metacíclicos (5) que aderem à cutícula que reveste o epitélio do reto e do saco retal do inseto. Ao se soltarem do epitélio, podem ser eliminados na urina ou fezes do inseto em seu próximo repasto sanguíneo. A contaminação de um hospedeiro vertebrado ocorre quando o barbeiro infectado pica o mamífero. Neste processo, o inseto geralmente defeca e urina (6), depositando, assim, sobre a pele ou mucosa do mamífero a forma tripomastigota metacíclica, que é a forma infectiva (7), porém não replicativa. A invasão do parasito ocorre quando o hospedeiro se coça, o que gera lesões da pele por onde o parasita pode penetrar ou quando ele entra em contato com a

mucosa. Os tripomastigotas metacíclicos acessam a circulação sanguínea, aderindo e invadindo uma gama de células nucleadas como, por exemplo, macrófagos (8), células musculares e epiteliais. Inicialmente, a forma tripomastigota é fagocitada pelo macrófago, seguindo-se a formação do vacúolo parasitóforo (9). No interior do vacúolo parasitóforo, a forma tripomastigota se diferencia para a forma amastigota e ocorre a lise da membrana do vacúolo parasitóforo (10). No citoplasma, esta forma se multiplica por fissões binárias sucessivas, podendo tomar todo o citoplasma (11). Após as sucessivas divisões, os amastigotas iniciam sua diferenciação para a forma tripomastigota (12) antes de a célula hospedeira ser rompida pelo excesso de parasitas (13). A ruptura da célula hospedeira pode ocorrer antes da total diferenciação de amastigotas para tripomastigotas, o que gera o aparecimento de diferentes formas no meio externo (14). No meio extracelular, os tripomastigotas (15a) e amastigotas (15b) podem infectar novas células que ali estejam presentes (Atlas Didático – O ciclo de vida do *Trypanosoma cruzi*).

1.2.2 Estrutura celular do *Trypanosoma cruzi*

Trypanosoma cruzi possui organelas que são encontradas em outras células eucarióticas, assim como também possui estruturas que são próprias desse organismo (Fig. 1.7).
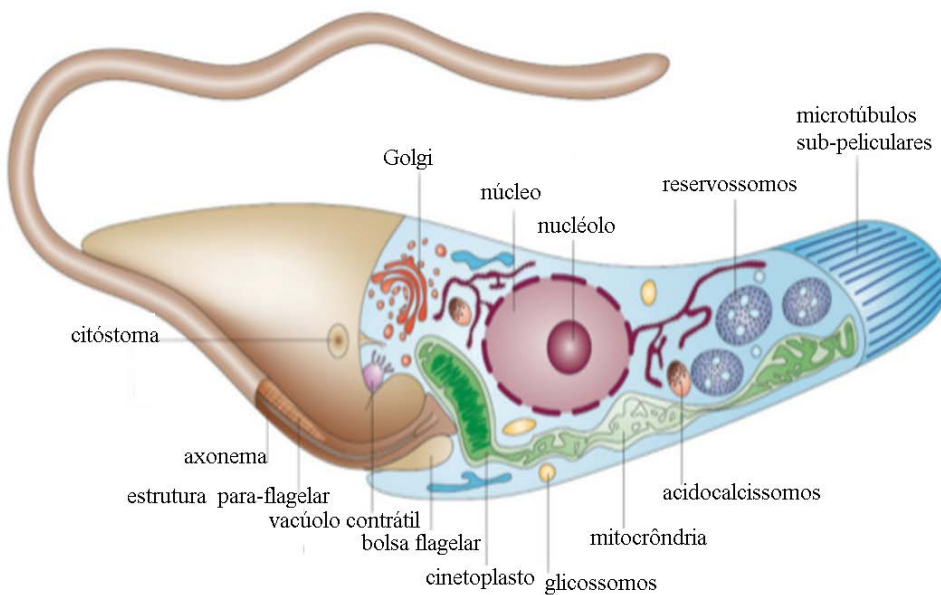
Figura 1.7. Forma epimastigota de *Trypanosoma cruzi* e suas principais organelas (DOCAMPO *et al*., 2005)**.**

Uma das diferenças está na superfície dos tripanossomatídeos. Ela é caracterizada pela presença de uma membrana plasmática disposta sobre uma rede sub-pelicular de microtúbulos unidos por filamentos, de natureza desconhecida. A associação do citoesqueleto com a membrana plasmática já é bem descrita na maioria das células eucarióticas, mas em tripanossomatídeos essa associação forma uma rede extremamente resistente, que permanece associada mesmo após a lise do parasita (DE SOUZA, 2002a) .

A única região onde não há microtúbulos é a bolsa flagelar. Trata-se de uma invaginação da membrana plasmática, na região anterior do parasita, de onde emerge o flagelo. Essa é uma região altamente especializada nos tripanosomatídeos, pois é o local de intensa atividade endocítica e exocítica (DE SOUZA *et al.*, 2009). Entretanto, *T. cruzi* além da bolsa flagelar possui outra estrutura especializada, o complexo citóstoma/citofaringe. Essa estrutura é uma invaginação da membrana plasmática na região anterior do parasita que penetra profundamente dentro da célula alcançando a região nuclear. Nesse parasita, esse é o principal sítio de endocitose (DE SOUZA *et al.*, 2009).

O retículo endoplasmático liso e rugoso é encontrado por todo o corpo de todas as formas evolutivas de *T. cruzi* (DE SOUZA, 2002). Observa-se apenas a presença de um único complexo de Golgi, que possui de 4 a 10 cisternas achatadas as quais, são quase sempre observadas na porção anterior do corpo celular, próximo à bolsa flagelar (Fig. 1.7). A rede trans-Golgi normalmente está orientada para a bolsa flagelar e é formada de túbulos e vesículas (FIGUEIREDO & SOARES, 1995).
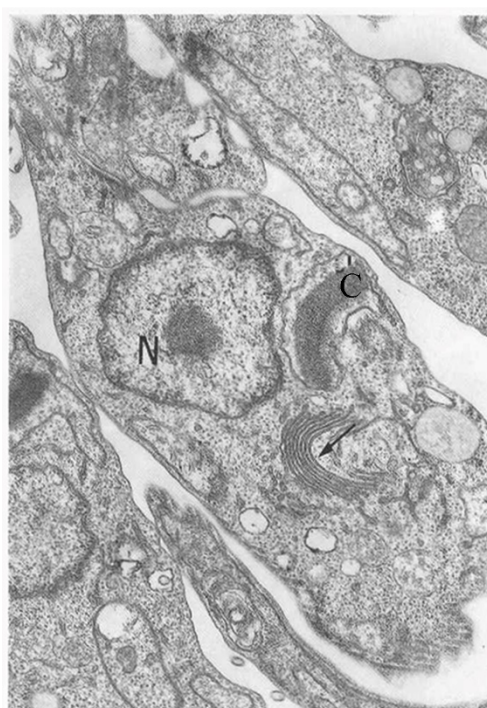
Figura 1.7. Micrografia da forma epimastigota de *T. cruzi*. Seta: complexo de Golgi; núcleo (N) e cinetoplasto (C) (adaptado de FIGUEIREDO & SOARES, 1995).

Na região posterior das formas epimastigotas de *T. cruzi* são encontrados os reservosomos. Estes são compartimentos esféricos onde se acumulam proteínas e lipídios oriundos do processo de endocitose pela bolsa flagelar e citóstoma bem como diversas hidrolases produzidas pelo retículo endoplasmático e o complexo de Golgi. É o último ponto da via endocítica e evidências experimentais sugerem que sejam compartimentos pré-lisosomais (SOARES *et al*, 1992). Entre as proteinases presentes nessa organela destaca-se, pela quantidade, a cruzipaína (SOARES *et al.*, 1992). A cruzipaina é a principal cisteino proteínase em *T. cruzi* e é diferencialmente expressa ao longo do ciclo de vida do parasita, tendo alta atividade na forma epimastigota. Está envolvida com diversos processos biológicos importantes como adesão do parasita ao intestino do inseto, diferenciação e interação do parasita com a célula hospedeira e no processo infectivo. Durante o processo de metaciclogênese, os reservossomos desaparecem, possivelmente pelo consumo de seu conteúdo (proteínas e lipídeos), para servir de fonte de energia para esta atividade (SOARES, 1999; VIDAL et al., 2017).

Todos os membros da família Trypanosomatidae possuem um único flagelo, que emerge a partir da bolsa flagelar. O tamanho do flagelo pode variar dependendo do estágio de desenvolvimento do parasita. Nas formas epimastigotas e tripomastigotas de *T. cruzi*, o flagelo, além da função de motilidade, também é importante para a adesão a diferentes células e superfícies. Nessas formas, parte do flagelo está aderida ao corpo do parasita. Já na forma intracelular de amastigota, o flagelo é muito curto e não é aderido ao corpo (DE SOUZA, 2002b). Os tripanosomatídeos possuem somente uma mitocôndria, que se ramifica ao longo da célula. Na porção anterior do parasita, a mitocôndria forma uma região especializada, conhecida como cinetoplasto e que contém o DNA mitocondrial (kDNA) (DE SOUZA, 2002b). Essa estrutura caracteriza a ordem Kinetoplastida a qual a família tripanosomatidae pertence.

Distribuídos pelo citoplasma estão os glicossomos, um tipo especializado de peroxisomo que acumula enzimas da via glicolítica envolvidas na conversão da glicose a fosfoglicerato (HANNAERT *et al*., 2003). Outras organelas particulares são os acidocalcisomos, envolvidos na estocagem intracelular de cálcio e polifosfato e provavelmente estão envolvidos em diversos processos biológicos, tais como adaptação a condições de estresse ambiental, manutenção do pH intracelular e osmo-regulação (DOCAMPO *et al*., 2005).

1.2.3   AP-1 em Tripanosomatídeos

O tráfego intracelular de vesículas revestidas com clatrina e seus adaptadores (principalmente AP-1 e AP-2) tem sido amplamente estudado em diversos modelos eucarióticos. Entretanto, os tripanosomatídeos possuem características próprias quanto aos processos de endocitose e exocitose. Uma delas é que, diferentemente do que acontece com a maioria das células eucarióticas, esses processos são altamente polarizados, ocorrendo na região da bolsa flagelar, onde também se localiza o complexo de Golgi (DE SOUZA, 2002a).

Em *T. brucei*, vesículas com revestimento de clatrina brotam tanto da bolsa flagelar como no complexo de Golgi (MORGAN *et al*., 2001). Análises usando a técnica de RNA de interferência mostraram que o silenciamento da expressão de clatrina é letal para o parasita. As formas sanguíneas apresentaram um grande inchaço na bolsa flagelar, indicando que apesar da endocitose ter sido prejudicada, o processo exocítico permaneceu em atividade (ALLEN *et al*., 2003). Já nas formas procíclicas observou-se um fenótipo diferente, no qual grandes vesículas se acumularam no citoplasma do parasita, sugerindo uma deficiência no transporte a partir do Golgi (ALLEN *et al.*, 2003).

O silenciamento das subunidades γ e μ1 do complexo AP-1 em *T. brucei* também foi letal nas duas formas evolutivas do parasita, indicando uma função crítica da maquinaria desse adaptador (ALLEN *et al*., 2007; TAZEH *et al*., 2009). Além disso, foi mostrado que o transporte da proteína de membrana p67 e da cisteíno-proteínase, tripanopaína do Golgi para os lisossomos é dependente de AP-1 somente no estágio procíclico (TAZEH *et al*., 2009).

Em *L. mexicana,* diferentemente do que acontece em *T. brucei,* o nocaute das subunidades μ1 e σ1 de AP-1 não foi letal para o parasita (GOKOOL, 2003), mas impediu a infecção do parasita *in vitro* e *in vivo*, bem como interferiu em processos, tais como: biogênese do flagelo, homeostase lipídica, entre outros (VINCE *et al*., 2008).

Em *T. cruzi*, estudos sobre a caracterização e função das proteínas de revestimento e sua participação no tráfego vesicular são escassos. Moreira (2013) mostrou que a subunidade AP1-γ se localiza no complexo de Golgi, sugerindo a participação de AP-1 no tráfego vesicular a partir da rede trans-Golgi, semelhante ao que ocorre em outras células. A triagem de hidrolases lisossomais na rede trans-Golgi é majoritariamente dependente do receptor manose-6-fostato, em células eucarióticas (LE BORGNE & HOFLACK, 1997). Porém, em tripanosomatídeos, esse receptor não está presente (BROOKS *et al*., 2000; SOARES *et al.*, 1992) sugerindo uma via diferente de seleção dessas moléculas.

Mais recentemente, Kalb e colaboradores (KALB et al., 2014) demonstraram a presença de clatrina na bolsa flagelar e no complexo de Golgi do *T. cruzi*, bem como

sugeriram, por ensaios de endocitose, que a captação de albumina ocorre na bolsa flagelar de forma dependente de clatrina, enquanto que a captação de transferrina pelo citóstoma (SOARES & SOUZA, 1991) é feita de forma independente de clatrina. As moléculas ingeridas por essas duas vias seguem pela via endocítica até alcançarem os reservossomos, onde serão degradadas (SOARES & SOUZA, 1991).

Análises *in silico* a partir de dados do genoma de *T. cruzi*, *T. brucei* e *Leismania* spp. mostraram que esses três tripanossomatídeos possuem repertórios distintos de complexos adaptadores. *T. brucei* apresenta em seu genoma somente o conjunto de genes que codificam os complexos AP1, AP3 e AP4. *Leishmania* spp. não possuem o AP-4. É provável que isso se deva a uma perda secundária, uma vez que *T. cruzi* apresenta quatro desses complexos adaptadores, AP1, AP2, AP3 e AP4 (CORRÊA *et al.*, 2007; MANNA *et al.*, 2013). O complexo AP-5 não foi encontrado em nenhum dos três tripanosomatídeos (MANNA *et al.*, 2013). Essas diferenças entre esses organismos não são compreendidas, mas a hipótese é que a ausência do AP-2 em *T. brucei* está relacionada com a elevada taxa de endocitose da glicoproteína variante de superfície (VSG), pois se a endocitose das VSGs fosse dependente da montagem do adaptador, isso tornaria o processo mais lento, com consequente redução da capacidade do parasita de escapar do sistema imune do hospedeiro (FIELD & CARRINGTON, 2009). A função de AP-4 em outros organismos não é totalmente clara, de modo que o significado funcional da perda de AP-4 em *Leishmania* não é conhecido. *T. cruzi* é um parasita intracelular que pode infectar uma gama de células hospedeiras, necessitando de uma modulação da expressão de moléculas de superfície para invasão e escape ativo do vacúolo parasitóforo para o citoplasma da célula hospedeira (TAN & ANDREWS, 2002), o que poderia explicar a presença de todos os quatro complexos nesse parasita. Assim, essas diferenças podem estar relacionadas com os mecanismos que cada parasita desenvolveu para evadir do sistema imune do hospedeiro e estabelecer a infecção (DENNY *et al.*, 2005; MANNA *et al.*, 2013).

O tráfego vesicular permite a realização de diversos processos biológicos essenciais para as células eucarióticas. Contudo em tripanosomatídeos, o conhecimento sobre as vias de tráfego de vesículas ainda é escasso, mas já foi demonstrado que o tráfego vesicular dependente de AP-1 é um importante componente para sobrevivência de *T. brucei* e infectividade de *L. mexicana* (GOKOOL, 2003; TAZEH *et al.*, 2009). Entretanto, ainda não se sabe qual a função e quais moléculas atuam concomitantemente com esse adaptador no complexo de Golgi em *T. cruzi*. Dessa forma, essa tese tem como objetivo a caracterização funcional de AP-1 de *T. cruzi* para avaliar seu papel na proliferação, diferenciação e

infectividade do parasita, bem como definir possíveis associações com proteínas de revestimento.

2 OBJETIVOS

2.1 Objetivo Geral

Caracterização funcional do complexo AP-1 de *Trypanosoma cruzi*.

2.2 Objetivos específicos

- Gerar uma linhagem mutante de *T. cruzi* para a subunidade AP1-γ (TcAP1-γ KO), por técnica de substituição gênica por recombinação homóloga (nocaute gênico);

-Avaliar as alterações morfológicas da linhagem TcAP1-γ KO por microscopia óptica e eletrônica de transmissão;

-Analisar o efeito da ausência da expressão da subunidade AP1-γ na proliferação, diferenciação e infectividade de *T. cruzi in vitro*;

-Verificar se o nocaute de AP1-γ interfere no transporte da cruzipaína do complexo de Golgi para os reservossomos;

-Verificar se os fenótipos da linhagem mutante são revertidos com a expressão ectópica de TcAP1- γ;

- Identificar as proteínas que interagem com as subunidades AP1-β e AP1-μ de *T. cruzi*.

CAPÍTULO 1

Caracterização do complexo AP-1 em *T. cruzi* por nocaute gênico da adaptina TcAP1-γ

Os dados referentes a esse capítulo foram submetidos ao periódico PLoS One (fator de impacto: 4,41/ Qualis: A1 na área CB-I), em janeiro de 2017.

Título: Knockout of the Gamma Subunit of the AP-1 Adaptor Complex in the Human Parasite *Trypanosoma cruzi* Impairs Infectivity and Differentiation and Prevents the Maturation and Targeting of the Major Protease Cruzipain
Autores: Claudia Maria do Nascimento Moreira, Cassiano Martin Batista, Jessica Chimene Fernandes, Rafael Luis Kesller, Maurilio José Soares e Stenio Perdigão Fragoso

RESUMO: O complexo adaptador 1 (AP-1) é um do mais estudados em células eucarióticas. Sua função está relacionada com a segregação de moléculas em vesículas revestidas com clatrina, as quais seguem para os lisossomos a partir da rede *trans*-Golgi. Esse complexo possui quatro subunidades, dentre elas, a subunidade AP1-γ, que é uma das que caracteriza o complexo por definir o local de montagem deste. Existem poucos trabalhos sobre AP-1 em tripanosomatídeos, sendo esses concentrados em *T. brucei* e *Leishmania* spp. Em *T. brucei,* o silenciamento tanto da subunidade AP1-μ quanto da AP1-γ foi letal, enquanto que, em *L. mexicana*, o nocaute das subunidades AP1-μ e AP1-σ não interferiram na viabilidade, mas afetaram a infectividade desse parasita em macrófagos e camundongos. Esses dados mostram que, mesmo em organismos filogeneticamente relacionados, o complexo adaptador AP1 parece desempenhar diferentes funções. O *Trypanosoma cruzi* é o agente causador da doença de Chagas, enfermidade que afeta milhões de pessoas no mundo. A função de AP-1 nesse parasita é totalmente desconhecida. Para elucidar o papel de AP-1 em *T. cruzi*, utilizamos técnicas de genética reversa como o nocaute gênico, construindo uma linhagem mutante para TcAP1-γ (TcAP1-γ KO). Mostramos que os parasitas mutantes são apenas ligeiramente afetados quanto à sua proliferação em meio axênico. Contudo, o processo de metaciclogênese *in vitro* foi drasticamente reduzido, assim como a infectividade do parasita em linhagens celulares VERO e HeLa. Nossos dados mostraram que o processamento da cruzipaína, principal cisteíno-proteínase de *T. cruzi,* foi drasticamente reduzido no complexo de Golgi dos parasitas TcAP1-γ KO. O silenciamento da expressão de AP1-γ por nocaute gênico também levou a inibição do transporte da cruzipaína para os reservossomos das formas epimastigotas, sugerindo que o complexo AP1 atue na rede trans-Golgi na formação de vesículas contendo hidrolases direcionadas aos reservossomos.

Knockout of the gamma subunit of the AP-1 adaptor complex in the human parasite *Trypanosoma cruzi* impairs infectivity and differentiation and prevents the maturation and targeting of the major protease cruzipain
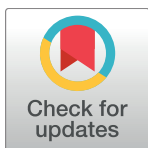
Claudia Maria do Nascimento Moreira[1], **Cassiano Martin Batista**[2], **Jessica Chimenes Fernandes**[2], **Rafael Luis Kessler**[3], **Maurilio José Soares**[2], **Stenio Perdigão Fragoso**[1] *

1 Laboratory of Molecular Biology of Trypanosomatids, Instituto Carlos Chagas/Fiocruz, Curitiba - PR, Brazil, **2** Laboratory of Cell Biology, Instituto Carlos Chagas/Fiocruz, Curitiba - PR, Brazil, **3** Laboratory of Functional Genomics. Instituto Carlos Chagas/Fiocruz, Curitiba - PR, Brazil

* sfragoso@fiocruz.br

Abstract

The AP-1 Adaptor Complex assists clathrin-coated vesicle assembly in the *trans*-Golgi network (TGN) of eukaryotic cells. However, the role of AP-1 in the protozoan *Trypanosoma cruzi*—the Chagas disease parasite—has not been addressed. Here, we studied the function and localization of AP-1 in different *T. cruzi* life cycle forms, by generating a gene knockout of the large AP-1 subunit gamma adaptin (TcAP1-γ), and raising a monoclonal antibody against TcAP1-γ. Co-localization with a Golgi marker and with the clathrin light chain showed that TcAP1-γ is located in the Golgi, and it may interact with clathrin *in vivo*, at the TGN. Epimastigote (insect form) parasites lacking TcAP1-γ (TcγKO) have reduced proliferation and differentiation into infective metacyclic trypomastigotes (compared with wild-type parasites). TcγKO parasites have also displayed significantly reduced infectivity towards mammalian cells. Importantly, TcAP1-γ knockout impaired maturation and transport to lysosome-related organelles (reservosomes) of a key cargo—the major cysteine protease cruzipain, which is important for parasite nutrition, differentiation and infection. In conclusion, the defective processing and transport of cruzipain upon AP-1 ablation may underlie the phenotype of TcγKO parasites.

Introduction

The protozoan *Trypanosoma cruzi* (Euglenozoa: Kinetoplastea) is the causative agent of Chagas disease, which affects an estimated 6 to 7 million people worldwide, mostly in Latin America (WHO, 2016, http://www.who.int/mediacentre/factsheets/fs340/en/). During its life cycle this parasite alternates between an invertebrate host (hematophagous triatomine insects) and a

mammalian host, with the four following well characterized developmental stages: bloodstream trypomastigotes and intracellular amastigotes, which are observed in the vertebrate hosts, and epimastigotes and metacyclic trypomastigotes, which are found in the insect digestive tract [1].

All *T. cruzi* developmental stages have lysosome-related organelles (LROs) [2]; however, in the epimastigote form, LROs have the additional and unique ability of storing cargo and they are called "reservosomes" [3]. Reservosomes are located at the posterior region of the parasite and accumulate proteins and lipids ingested from the extracellular medium by endocytosis, which occurs at the anterior region of the parasite. They also contain several hydrolases that are acquired from the secretory pathway and crucial for the digestion of the endocytosed material [4,5]. Reservosomes disappear during the differentiation of epimastigotes into metacyclic trypomastigotes (metacyclogenesis) [6,7], a process that can be triggered by nutritional stress [8]. It is possible that the content of reservosomes is mobilized as energy source during metacyclogenesis. Nutritional stress would trigger reservosome acidification, activating its hydrolases and altering organelle activity from a 'pre' to a 'full' lysosomal state. The consumption of stored material triggered by nutritional stress would explain reservosome disappearance during metacyclogenesis [7]. However, a recent study suggested that LROs from metacyclic trypomastigotes may arise directly from reservosomes [9].

Cruzipain, the major cysteine protease of *T. cruzi*, is highly expressed in epimastigotes [10] and accumulates in reservosomes [3] along with its inhibitor, chagasin [11]. Cruzipain plays an important role in parasite nutrition, differentiation and infectivity [12–16], and it is synthesized and processed in the endoplasmic reticulum/Golgi complex. However, it is not yet clear how cruzipain is targeted to reservosomes [17]. Newly formed reservosomes originate at the anterior region of the parasite, close to the Golgi complex [14,18], and cruzipain was detected in vesicles budding from the *trans*-Golgi network (TGN) that seemed to fuse with newly formed reservosomes [18]. These data indicate that the secretory pathway—which has the TGN as a key cargo-sorting hub—plays an important role in reservosome formation.

Cargo-containing vesicles bud from the TGN to different destinations by a regulated process that envolves the assembly of specific cytosolic cargo adaptors onto TGN membranes [19,20]. Cargo adaptors recognize an appropriate sorting signal in the cytosolic domain of cargo molecules and pack them, aided by auxiliary proteins, into vesicles that are delivered to their target sites at the endocytic or secretory pathways [21]. Eukaryotic cells have different cargo adaptors, including cytosolic proteins from the family of heterotetrameric adaptor complexes (APs) [22]. All five AP complexes identified to date (AP-1 to AP-5) consist of two large subunits of ~100 kDa (β1- β5, and either α, γ, δ, ε or ζ), a medium subunit of ~50 kDa (μ1–μ5) and one small subunit of ~20 kDa (σ1–σ5) [22,23].

The AP-1, AP3 and AP-4 complexes are involved in protein sorting at the TGN [19,20], while only AP-1 and AP-2 clearly recruit clathrin [24].

The *T. cruzi* genome contain the full set of genes for AP-1 to AP-4 complexes, but AP-5 appears to be absent in trypanosomatids [25,26]. The related parasites *T. brucei* and *Leishmania* spp. are only capable of assembling three of the AP adaptor complexes: *T. brucei* lacks AP-2, while AP-4 is absent in *Leishmania*. AP-1 is responsible for the transport of lysosomal hydrolases from the trans-Golgi Network (TGN) to endosomes in eukaryotic cells [19,27], a function that is conserved in primitive eukaryotes [28,29]. AP-1 appears to be ubiquitous in trypanosomatids [25] and studies indicate that it plays important roles in endosomal trafficking in *T. brucei* and *Leishmania mexicana*. Knockdown of the μ1 and γ subunits of the *T. brucei* AP-1 complex by RNA interference was lethal to both procyclic (insect form) and bloodstream forms of the parasite in axenic cultures [30,31]. In contrast, knockout mutants for the μ1 or σ1 subunits of the AP-1 complex in *L. mexicana* were viable in culture, but they were unable to

infect macrophages or mice [32]. Although viable, *Leishmania* AP-1 mutants displayed defects in lysosome and lipid transport as well as in flagellar biogenesis [33]. Both µ1 and σ1 adaptins of *L. mexicana* AP-1 are localized to endosomes and TGN vesicles [33]. Overall, these data indicate that the AP-1 complex plays important roles in endosomal trafficking in trypanosomatids. Nevertheless, the role of APs in the endocytic and secretory pathways in *T. cruzi* remains unexplored.

Here, we investigated the function of AP-1 in *T. cruzi*, taking advantage of the highly polarized endocytic and secretory pathways in the epimastigote stage, where secretion and exocytosis/endocytosis sites (the Golgi complex and flagellar pocket/cytostome, respectively) are found at the anterior while the final compartments of the endocytic pathway (the reservosomes) are in the posterior. We show here that gene knockout of the *T. cruzi* AP-1 gamma subunit TcAP1-γ blocks the transport of cruzipain to the reservosomes and impairs parasite proliferation, metacyclogenesis and infectivity *in vitro*.

Materials and methods

Parasite

Epimastigote forms of *T. cruzi* clone Dm28c [8] were kept at 28°C in liver infusion tryptose (LIT) medium supplemented with 10% inactivated fetal bovine serum (FBS), with weekly passages.

Metacyclic trypomastigotes were obtained from the differentiation of epimastigotes in the chemically defined medium TAU3AAG, as previously described [34,35]. Epimastigotes in late exponential growth phase (5–6×10^7 cells ml^{-1}) were harvested from LIT medium by centrifugation and subjected to nutritional stress by incubation for 2 h (at 28°C) in triatomine artificial urine (TAU) medium (190 mM NaCl, 17 mM KCl, 2 mM MgCl$_2$, 2 mM CaCl$_2$, and 8 mM sodium phosphate buffer, pH 6.0) at a density of 5×10^8 cells ml^{-1}. The cell suspension was then inoculated (to a density of 5×10^6 cells ml^{-1}) in culture flasks containing TAU3AAG medium (TAU medium supplemented with 50 mM sodium glutamate, 10 mM L-proline, 2 mM sodium aspartate and 10 mM glucose) pre-warmed at 28°C, and incubated for 72h. After incubation, the metacyclic trypomastigotes found in the culture supernatant were purified by DEAE cellulose chromatography, as previously described [36].

Intracellular amastigotes were obtained from the differentiation of metacyclic trypomastigotes in VERO cells (ATCC CCL-81). VERO cells were grown in Dulbecco's Modified Eagle's medium (DMEM; Sigma) supplemented with 5% FBS and cultivated (at 37°C, in a humidified atmosphere with 5% CO$_2$) until they reached 50–70% confluence. Cell monolayers were then infected with metacyclic trypomastigotes (150 parasites/host cell) obtained by metacyclogenesis as described above. After 24 h the medium was discarded (to remove non-adherent parasites), cultures were washed once with PBS and new medium was added to culture flasks. Amastigotes were obtained by disrupting VERO cells 10 days after infection and harvesting parasites by centrifugation at 1,000 x *g* for 5 min.

Growth Curve and Metacyclogenesis quantification

For growth curve analysis, epimastigote cultures were established at a density of 1×10^6 cells ml^{-1} and population growth was monitored for seven days, with cell counting in a Z series Coulter Counter (Beckman Coulter, CA, USA). Experiments were performed in technical and biological triplicates and the data were analyzed with the t-test using GraphPad software.

To quantify metacyclogenesis, epimastigotes were allowed to differentiate *in vitro* as described above (see "Parasite"), and the number of metacyclic trypomastigotes was counted in a Neubauer chamber after 72h of incubation in TAU3AAG medium (which corresponds to

the peak of differentiation into metacyclic trypomastigotes). Experiments were performed in technical triplicates.

Recombinant protein expression and purification

Nucleotides 1,609 to 2,091 (hinge region) of the gene encoding the *T. cruzi* AP-1 γ adaptin (TcAP1-γ, gene ID TcCLB.508257.260, from tritrypdb.org) were amplified by PCR using the primers HingeF and HingeR (Table 1), which contain the *attB*1 and *attB*2 recombination sites, respectively. These sites allowed the insertion of the PCR fragment into the pDONR 221 vector from the Gateway recombination cloning system (Thermo Scientific, MA, USA). The resulting recombinant plasmid (entry clone) was then used to transfer the hinge fragment DNA cassette (by recombination) into the expression vector pDEST17 from the Gateway platform. *Escherichia coli* strain BL21(DE3)STAR was used to produce the histidine-tagged TcAP1-γ hinge domain by induction with 1 mM IPTG. Inclusion bodies containing the insoluble recombinant protein were purified as previously described [37] and then solubilized in Laemmli sample buffer (60 mM Tris-HCl, pH 6.8, 10% glycerol, 2% SDS, 5% 2-mercaptoethanol and 0.01% bromophenol blue) at 100˚C, for 10 min. The recombinant protein was recovered by electroelution from SDS-PAGE gels, as previously described [37].

Monoclonal antibody (mAb) production

Four young adult male BALB/c mice (30–45 day-old) were inoculated five times with 20 μg of the histidine-tagged TcAP1-γ hinge domain at one-week intervals. The first four doses were administered by the intraperitoneal route using Alu-Gel-S (Serva, Heidelberg, Germany) as adjuvant. The fifth dose of antigen was inoculated by the intravenous route with no adjuvant. Three days after the last immunization, the animals were anesthetized with ketamine/xylazine solution (100 and 10 mg kg^{-1}, respectively) by the intraperitoneal route, bled by cardiac puncture to obtain post-immune sera and euthanized by cervical dislocation. The spleens were aseptically removed to obtain antibody-secreting cells, which were fused with Ag8XP3653 myeloma cells to produce hybridomas, as previously described [38]. Positive hybridomas were selected by indirect ELISA, Western blot, and indirect immunofluorescence, and stable hybridomas were cloned by limiting dilution. The Mouse Rapid ELISA mAb Isotyping Kit (Thermo Scientific) was used to identify immunoglobulin isotypes. A positive monoclonal antibody against TcAP1-γ—named 211.F7—was selected using the screening procedure described above and was used throughout this work.

Table 1. Primer sequences used in this work.

PRIMERS	SEQUENCES (5'- 3')
Hinge F	**GGGGACAAGTTTGTACAAAAAAGCAGGCTTC**ATGAAAATCGCCTCCAGGTATCC
Hinge R	**GGGGACCACTTTGTACAAGAAAGCTGGGTCCTA**ACAATCAAACACACATGCACTTCAGG
UPS_KpnI	GTG<u>GGTACC</u>GTGTGTTGTGTTGTCCCTTTTTTTTTGTGT
UPS_SalI	ACC<u>GTCGAC</u>CGGCAACGATCAAGTCACGAAGTCTCGCA
DOWN_BamHI	GCGTGTGTGTGTGT<u>GGATCC</u>CTTTGTCGTCACGGAGAGAA
DOWN_XbaI	CGCCAGCACAAT<u>CTAGA</u>CATAGCTAGACTGAAACT
AP-1-γ_attB1	**GGGGACAAGTTTGTACAAAAAAGCAGGCTTC**ATGGAGGGGAAACTTGAGTCG
AP-1-γ_attB2	**GGGGACCACTTTGTACAAGAAAGCTGGGTCC**AACTCCTGCGTCACCTGA

*attB*1 and *attB*2 recombination sequences (for use with the Gateway cloning system) are shown in bold. Restriction sites are underlined.

https://doi.org/10.1371/journal.pone.0179615.t001

Ethics statements

Experiments with animals were approved by the Ethics Committee for Animal Research of Fundação Oswaldo Cruz (Oswaldo Cruz Foundation, FIOCRUZ, attached to the Brazilian Ministry of Health, Rio de Janeiro, Brazil) under protocol number LW-15/13, which follows the guidelines on animal care of the Brazilian Council for the Control of Animal Experimentation (CONCEA).

Western blot

Epimastigotes, *in vitro*-derived metacyclic trypomastigotes and isolated intracellular amastigotes obtained as described above (see "Parasites") were washed in PBS, resuspended in PBS containing a protease inhibitor cocktail (Roche, Basel, Switzerland), and lysed by the addition of 4x Laemmli sample buffer, which was followed by heating at 100°C for 5 min. Lysates containing an equivalent of 1×10^6 cells μl^{-1} were fractionated by SDS-PAGE and transferred onto nitrocellulose membranes (Hybond C, GE Healthcare, PA, USA) according to standard protocols [39]. Membranes were blocked with 5% non-fat dry milk and 0.05% Tween 20 in PBS (blocking solution) then, they were probed with one of the following primary antibodies (diluted in blocking solution): the monoclonal antibody 211.F7, against the Tcγ hinge domain (1:300); anti-cruzipain (1:1500) antiserum that recognizes both the zymogen and the mature form of cruzipain [40]; or a mouse anti-TcGAPDH antiserum (1:8,000) [41], as a loading control. Membranes were then incubated with horseradish peroxidase-conjugated anti-mouse IgG antibodies (Thermo Scientific product #31430) and diluted to 1:7,500 in blocking solution. The SuperSignal West Pico Chemiluminescent System (Thermo Scientific) was used for antibody binding detection according to the manufacturer's instructions.

Immunofluorescence microscopy

Parasites were washed twice in PBS, fixed for 10 min at room temperature with 4% paraformaldehyde, washed twice in PBS and then adhered for 20 min to 0.1% poly-L-lysine-coated coverslips. Then, cells were permeabilized for 5 min with 0.5% Triton X-100 in PBS, washed with PBS and blocked with 1.5% bovine serum albumin in PBS for 1 h. For cell surface labeling of WT and γKO amastigotes and metacyclic trypomastigotes, the parasites were fixed with paraformaldehyde without Triton X-100 treatment. Samples were then incubated for 1 hour at 37°C with either the anti-TcAP1-γ mAb 211.F7 (1:80) or anti-cruzipain antiserum (1:500) diluted in PBS (pH 7.4) containing 1.5% BSA (blocking buffer). Coverslips were washed three times with PBS and then incubated with goat anti-mouse IgG secondary antibodies coupled to Alexa Fluor 488 or Alexa Fluor 594 (Thermo Scientific; both at 1:600) in blocking buffer. Finally, samples were washed three times in PBS, incubated for 5 min with Hoechst 33342 (1 µg ml^{-1}; Thermo Scientific), mounted with Prolong Gold (Thermo Scientific) and examined in a Leica SP5 confocal laser microscope (Leica Microsystems, Wetzlar, Germany).

For co-localization with TcAP1-γ, transfectant epimastigotes expressing the tagged Golgi marker Huntingtin interacting protein TcHIP/AC [42] or the tagged clathrin light chain TcCLC/AC [43] (where AC stands for the protein C/protein A 'PTP' epitope tag; [44]) were fixed, adhered and permeabilized as described above. Then, they were incubated for one hour at 37°C with the anti-TcAP1-γ mAb 211.F7 (1:80) and with a rabbit IgG anti-protein A antibody (1:40,000) (Sigma-Aldrich, MO, USA). Samples were washed three times in PBS, incubated with a goat anti-mouse antibody coupled to Alexa Fluor 488 (1:600) and a goat anti-rabbit antibody coupled to Alexa Fluor 546 (1:600), and processed for fluorescence microscopy as described above.

Transmission electron microscopy

Epimastigotes in exponential growth phase (2–3 x 10^7 cells ml^{-1}) were collected by centrifugation and washed in PBS. The cells were then fixed with 2.5% glutaraldehyde in 0.1 M phosphate buffer (pH 7.2). After that, cells were washed once with 0.1 M phosphate buffer, once with 0.1 M cacodylate buffer and post-fixed with 1% osmium tetroxide/0.8% potassium ferricyanide/5 mM $CaCl_2$ in 0.1 M cacodylate buffer (pH 7.2). Cells were dehydrated in graded acetone, infiltrated in acetone/PolyBed 812 mixture and embedded in PolyBed 812 resin (Poly-Sciences, Warrington, PA, USA). Ultrathin sections were stained with uranyl acetate and lead citrate before examination in a JEOL JEM-1400 Plus transmission electron microscope at 80kV.

Gene knockout

Flanking sequences of the *TcAP1-γ* gene were amplified from *T. cruzi* Dm28c genomic DNA by PCR using the primer pairs UPS_KpnI and UPS_SalI (5' flank, 658 bp) and DOWN_BamHI and DOWN_XbaI (3' flank, 652 bp) (Table 1). The 5' flank fragment was inserted into the KpnI and SalI sites of pTc2KO-neo and pTc2KO-hyg, which carry the neomycin and hygromycin B resistance genes, respectively [45]. The 3' flank fragment was then cloned into BamHI and XbaI of the recombinant plasmids containing 5' flank fragments. The resulting plasmids were named pTc2KO-AP-1γ-neo and pTc2KO-AP-1γ-hyg (S1 Fig).

To produce the *TcAP1-γ* gene knockout, the targeting cassettes (5'flank-NEO-3'flank and 5'flank-HYG-3'flank) were amplified using UPS_KpnI and DOWN_XbaI primers and transfected into *T. cruzi* epimastigotes as previously described [37]. First, parasites were transfected with the 5'flank-NEO-3'flank cassette and incubated for 24 h in LIT medium before selection in LIT medium with 500 µg ml^{-1} G418. After 4 to 5 weekly passages in selection medium, G418-resistant transfectants were recovered, while no growth was observed in control cultures transfected without DNA. The G418-resistant parasite population was then transfected with the 5'flank-HYG-3'flank cassette, incubated for 24h in LIT medium, and selected in LIT medium supplemented with 500 µg ml^{-1} G418 and 500 µg ml^{-1} hygromycin B. Resistant transfectants were selected after 5 to 8 weekly passages. Individual clones from the double resistant parasite population were obtained by flow cytometry sorting. Briefly, epimastigote forms (1 x 10^6 cells) were resuspended in 1 ml PBS. The parasites were analyzed by FACSAria II (BD) and *T. cruzi* autofluorescence helped to identify the cell population. The most homogeneous population was selected by forward scatter (FSc) vs. side scatter (SSc) contour plot and subjected to cell sorting. The single cell precision mode from FACSDiva (BD) software was used to directly sort single cells into 96-well plate containing 100 µl of LIT medium/well, that was supplemented with G418 (500 µg ml^{-1}) and hygromycin B (500 µg ml^{-1}). Parasites were kept at 28˚C in a humidified atmosphere with 5% CO2. Parasite growth was observed 15–20 days from cell sorting. Clones were screened for the lack of TcAP1-γ expression by Western blot.

Pulsed-field gel electrophoresis (PFGE) and Southern blot

To confirm TcAP1-γ knockout, chromosomes from wild-type (WT) and TcγKO parasites were fractionated by PFGE as previously described [46]. Chromosomes from *Hansenula wingei* (Biorad Laboratories, CA, USA) were used as molecular mass standards. After electrophoresis, gels were stained with 0.5 µg ml^{-1} ethidium bromide, imaged and processed by Southern blotting according to standard protocols [39]. After transfer to nylon membranes, specific DNA sequences were detected by hybridization with probes for the entire coding sequences of *TcAP1-γ, NEO* and *HYG* genes. Probes were radioactively labeled with [α-^{32}P]-dCTP using the megaprime DNA labeling system (GE Healthcare).

Complementation of TcAP1-γ KO parasites

For TcAP1-γ KO complementation, the *TcAP1-γ* gene was amplified by PCR (primers AP-1-γ_attB1 and AP-1-γ_attB2, Table 1), cloned (as described above) into pDONR 221 from the Gateway cloning system (entry clone), and then transferred to pTcGW-bsd, yielding pTcGW-AP-1γ-bsd (S2 Fig). The expression plasmid pTcGW-bsd is a modified version of the pTcGW 1.1 series Gateway expression vectors constructed for constitutive expression and selection in *T. cruzi* [47,48]. TcγKO parasites were transfected with 15 µg of pTcGW-AP-1γ-bsd and selected in LIT medium containing 15 µg ml^{-1} Blasticidin-S (Sigma-Aldrich). The expression and localization of TcAP1-γ in the complemented (add-back) cells were analyzed by Western blot and immunofluorescence microscopy, respectively, using the anti-TcAp1-γ mAb 211.F7. The TcAp1-γ-complemented parasites [TcγKO(pTc-AP1γ)] were further tested for their capacity to proliferate, differentiate and infect cells as well as for the restoration of cruzipain transport to the reservosomes.

High-content quantification of *T. cruzi* infectivity

Two mammalian cell lines from distinct cell lineages were used for *in vitro* high-content analysis of parasite infectivity, HeLa cells (ATCC CCL-2; epithelial lineage) and VERO cells (ATCC CCL-81; fibroblast lineage). Cells were kept at 37°C in DMEM medium containing 10% heat inactivated serum under a 5% CO_2 atmosphere. Cells were seeded into 96-well plates at a density of 5 x 10^3/well with *T. cruzi in vitro* derived metacyclic forms (100:1 parasite-host cell ratio). After 4 h of interaction, plates were washed twice with PBS, fresh medium was added, and plates were incubated for 72 h at 37°C (5% CO_2). After incubation, plates were washed in PBS and cells were fixed for 5 min with cold methanol. Then, plates were washed 3 times with PBS, incubated for at least 30 min in blocking buffer (1% saponin, 2% BSA in PBS), and incubated overnight at 4°C with the anti-TEMA rabbit hyperimmune antiserum (1:2,000 in blocking buffer) (kindly provided by Dr. Victor Tulio Contreras, University of Carabobo, Venezuela), which recognizes the cell body of all major stages of *T. cruzi*. Plates were then washed twice with blocking buffer, three times with PBS, and incubated for 60 min at 37°C with a secondary antibody (goat anti-rabbit IgG, Alexa Fluor 488) diluted 1:1,000 in blocking buffer. Finally, the plates were washed five times with PBS, incubated with 100 µl of DAPI (1µg ml^{-1}) in PBS, and analyzed in an Operetta High-Content Imaging System (Perkin Elmer, USA) using a 40X high WD objective. Fifty fields per well were imaged using five distinct Z focal planes that were spaced by 1 µm. Maximum projection images (of combined z focal planes) were automatically analyzed using the Harmony High-Content Imaging and Analysis Software (Perkin Elmer, USA). The user-optimized algorithm worked in the following steps: (i) identification of host cell nucleus by DAPI staining, (ii) host cell cytoplasm identification in the digital phase contrast (DPC) channel, (iii) identification of potential intracellular parasites as small spots of DAPI staining in the cytoplasm, and (iv) confirmation of parasite identification by anti-TEMA (Alexa-488) co-staining on small DAPI spots. For each well, the algorithm identified infected and non-infected cells, counted the number of intracellular amastigotes, and calculated the mean number of intracellular parasites per cell (a) and the % of infected cells (b). These data were used to calculate the intracellular parasite growth factor iGF = a x b. The relative intracellular growth (riGF) was calculated using the formula: riGF = iGF$_{mutant}$ / iGF$_{wt}$. Growth factor values for each condition represent data from eight replicate wells from ≥ 2 independent experiments. Statistical analysis was performed by ANOVA, which was followed by Tukey-Kramer multiple comparisons test, using GraphPad Prism version 5 software (GraphPad Software Inc, La Jolla, CA, USA).

Results

The *T. cruzi* AP-1 gamma adaptin (TcAP1-γ) is expressed in all life cycle forms and co-localizes with Golgi and TGN markers

Gamma adaptin is one of the largest subunits of the AP-1 complex. Bioinformatics analysis using the Pfam database (http://pfam.xfam.org/) showed that the *T. cruzi* γ adaptin (TcAp1-γ; TcCLB.508257.260; 800 aa, ~ 90 kDa) has the typical structure of eukaryotic γ-adaptins with an N-terminal 'trunk' domain (aa 30 to 577) (pfam 01602) and C-terminal appendage or 'ear' domain (aa 691 to 798) (pfam 02883), linked by a flexible hinge region. The hinge region of the large γ and β1 adaptins contain sequences that recognize and bind to clathrin [49–51] and the C-terminal 'ear' (appendage) domain recruits accessory proteins that modulate AP function to form clathrin-coated vesicles (CCVs) at the TGN [50,52]. By manual sequence analysis we identified a clathrin box candidate in the hinge region of Tcβ1 adaptin (811LFHLE815) that fits the canonical clathrin box motif LΦXΦ(D/E), where Φ is a bulky hydrophobic amino acid and X is any amino acid [53]. We identified two motifs in the hinge region of TcAP-1γ adaptin (627LFEVN630 and 657LFGLK661) that partially resemble the canonical clathrin box.

To study the function of TcAP1-γ, we produced a monoclonal antibody against the hinge domain of this protein (mAb 211.F7) assuming that this region is more accessible than the N- and C-terminal domains, which are likely to be obscured by a myriad of protein-protein interactions (within the AP-1 complex and with accessory and regulatory proteins) [22].

Hybridoma screening after mouse immunization with the histidine-tagged TcAP1-γ hinge domain led to the identification of monoclonal antibody 211.F7 (IgG isotype and kappa positive), which recognizes the recombinant protein (Fig 1A). Analysis of the TcAP1-γ expression pattern during the *T. cruzi* life cycle with 211.F7 showed that the TcAP1-γ is expressed in epimastigotes, amastigotes and metacyclic trypomastigotes (Fig 1B).

The AP-1 complex is important for the trafficking of vesicles from the TGN to endosomes [54]. In agreement with this function, immunofluorescence microscopy using the 211.F7 mAb showed that TcAP1-γ was mainly localized in a region adjacent to the kinetoplast in epimastigotes (Fig 1C-a) and intracellular amastigotes (Fig 2) and between the nucleus and the kinetoplast in trypomastigotes (Fig 1C-b), which corresponds to the region where the Golgi complex is located in *T. cruzi* [55]. We confirmed that TcAP1-γ was located in the Golgi by co-localization of TcAP1-γ with the Golgi marker Huntingtin interacting protein (TcHIP) [42] (Fig 3A–3C). An interesting result was that TcAp1-γ also co-localized with the clathrin light chain (TcCLC) in the Golgi complex (Fig 3E–3G), suggesting the involvement of both TcAP1-γ and TcCLC in vesicle formation at the TGN.

TcAP1-γ gene disruption delays epimastigote growth and decreases metacyclogenesis

To investigate TcAP-1 function in *T. cruzi*, we deleted the TcAP1-γ gene in epimastigotes by replacing both alleles with resistance markers *NEO* and *HYG* (S1 Fig). *TcAP1-γ* gene knockout was confirmed by Southern blot from PFGE of chromosomes from TcγKO parasites (Fig 4A). The *TcAP1-γ* radioactive probe recognized a 1.05 Mb chromosomal band only in WT parasites, but not in TcγKO parasites (γKO) (Fig 4A), indicating that the *TcAP1-γ* gene was deleted from the genome in TcγKO parasites. Additionally, *NEO* and *HYG* probes only hybridized with the 1.05Mb chromosomal band in the TcγKO parasites (Fig 4A), indicating that the NEO and HYG cassettes were correctly integrated into the *TcAP-1γ* locus. Western blot analysis with total protein extracts from WT and TcγKO parasites using the 211.F7 mAb showed that
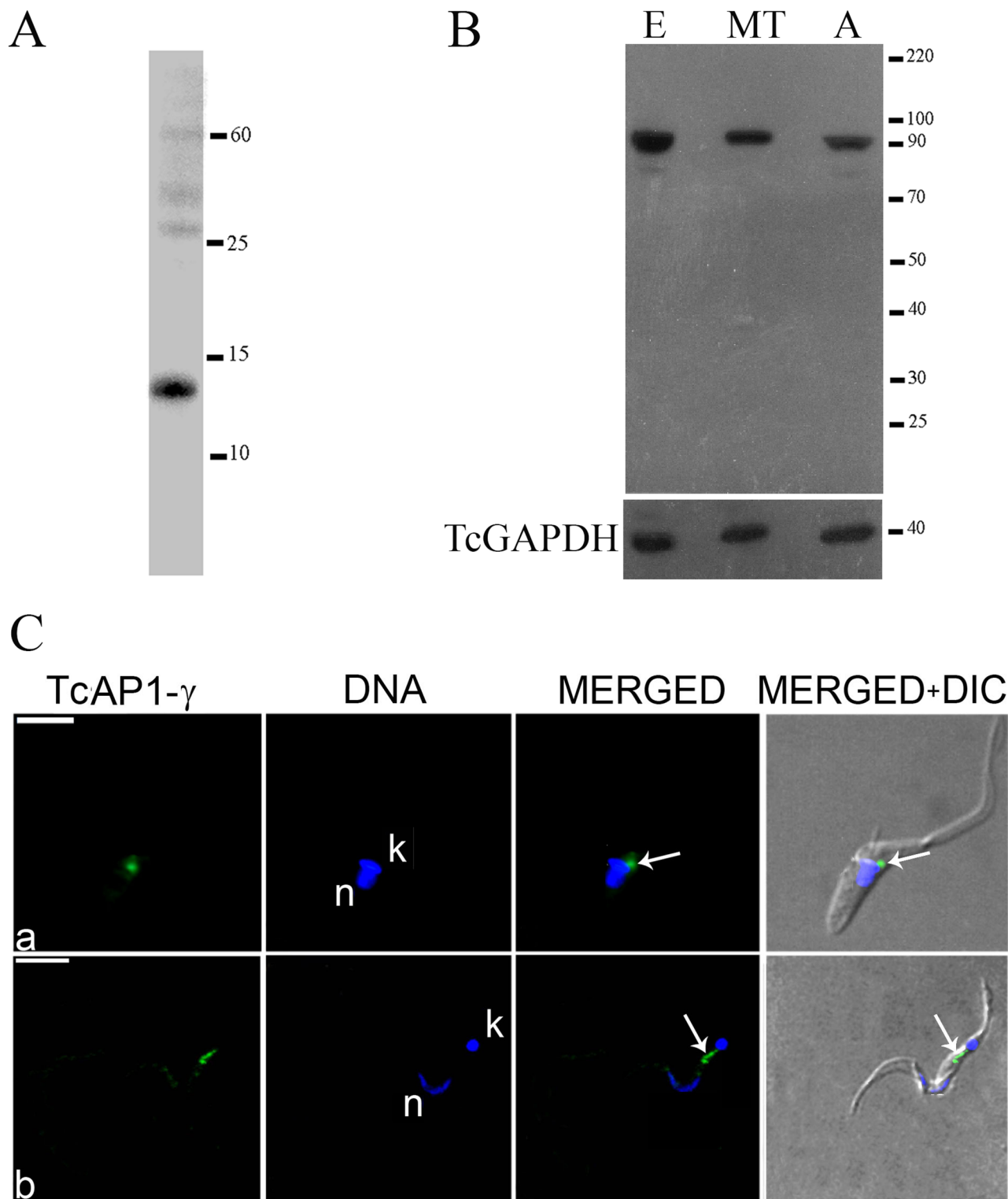
Fig 1. Expression and localization of the *Trypanosoma cruzi* AP-1 complex γ subunit (TcAP1-γ). The purified recombinant protein (histidine-tagged TcAP1-γ hinge domain) (A) and *T. cruzi* whole cell extracts (B) were resolved on 10% SDS-PAGE gels, transferred to nitrocellulose membranes and reacted with the anti-TcAP1-γ mAb 211.F7 (produced against the hinge region of TcAP1-γ). E: epimastigotes; MT: metacyclic trypomastigotes; A: amastigotes. An antiserum against the *T. cruzi* GAPDH was used as loading control. (C) Parasites were incubated with the 211.F7 mAb (1:80 dilution), followed by incubation with anti-mouse IgG conjugated to Alexa Fluor 488 (1:600 dilution). Nuclear (n) and kinetoplast (k) DNA were stained with Hoechst 33342. (a) Epimastigote and (b) metacyclic trypomastigote. TcAP1-γ labelling is indicated by arrows. DIC, differential interference contrast microscopy. Scale bar = 5μm.
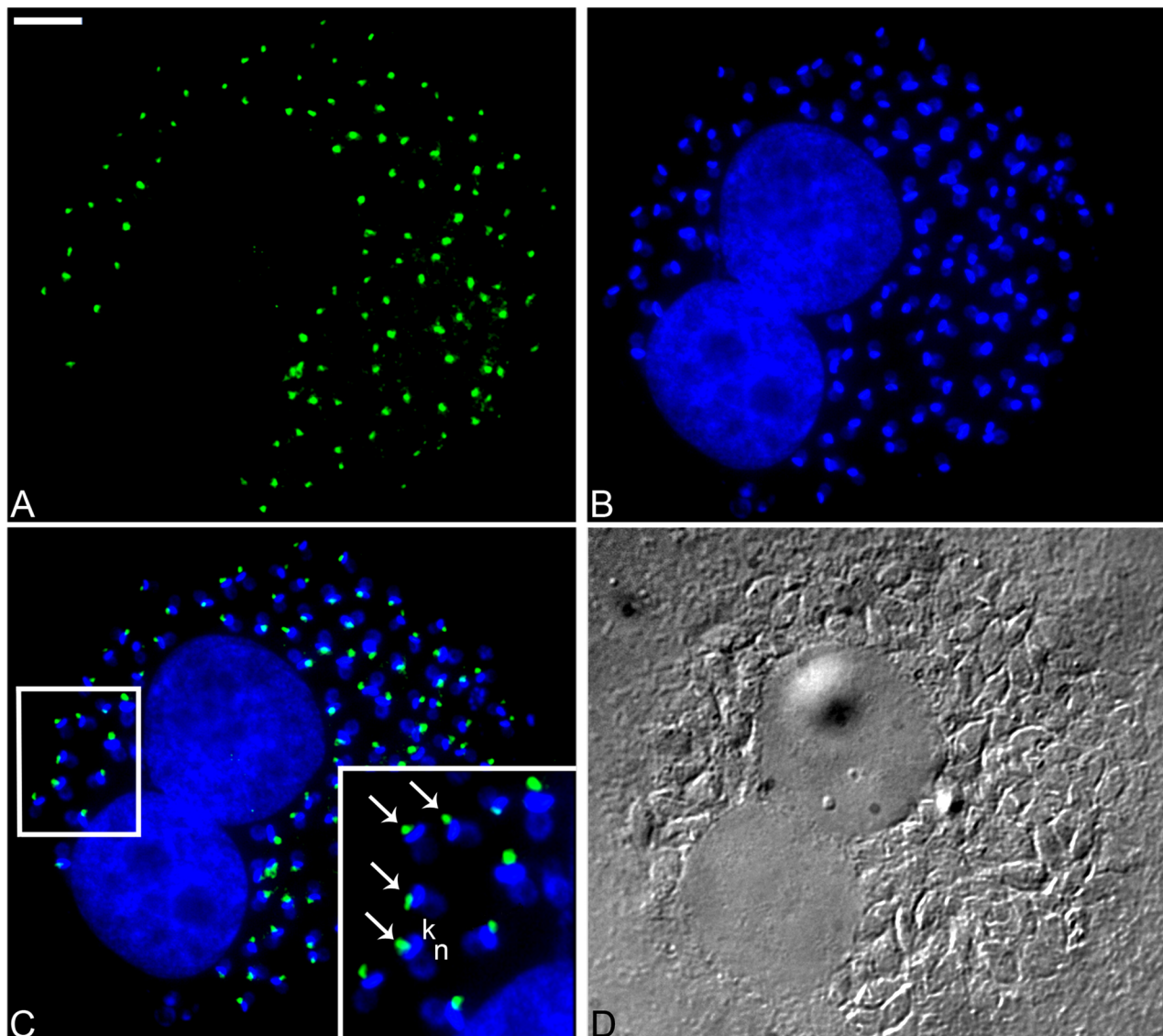
Fig 2. Immunofluorescence localization of the *Trypanosoma cruzi* AP-1 complex γ subunit (TcAP1-γ) in intracellular amastigotes. *T. cruzi*-infected VERO cells were labelled with the anti-TcAP1-γ mAb 211.F7, which was detected with anti-mouse IgG conjugated to Alexa Fluor 488. (A) Labeling for TcAP1-γ (Alexa Fluor 488). (B) Host cell and parasite DNA stained with Hoechst 33342, detecting both the nuclear (n) and the kinetoplast (k) DNA of amastigotes. (C) Overlay of A and B, showing the localization of TcAP1-γ (arrow) near the kinetoplast (k). (D) DIC, differential interference contrast microscopy. Scale bar = 10μm.

TcAP1-γ was not detected in TcγKO parasites, but it was readily detected in extracts of WT epimastigotes (Fig 4B), confirming the ablation of TcAP1-γ expression.

TcAP1-γ null mutant parasites were viable; however, growth curves of WT and TcγKO epimastigotes showed that null mutant populations grew significantly slower than wild-type cells (Fig 5A). When TcγKO epimastigotes were incubated in TAU3AAG medium (to induce metacyclogenesis *in vitro*), the ability of KO parasites to undergo differentiation into metacyclic trypomastigotes was approximately 40% lower than that of WT epimastigotes (Fig 5B). These results show that lack of TcAP1-γ significantly decreases parasite proliferation and differentiation into infective forms *in vitro*.
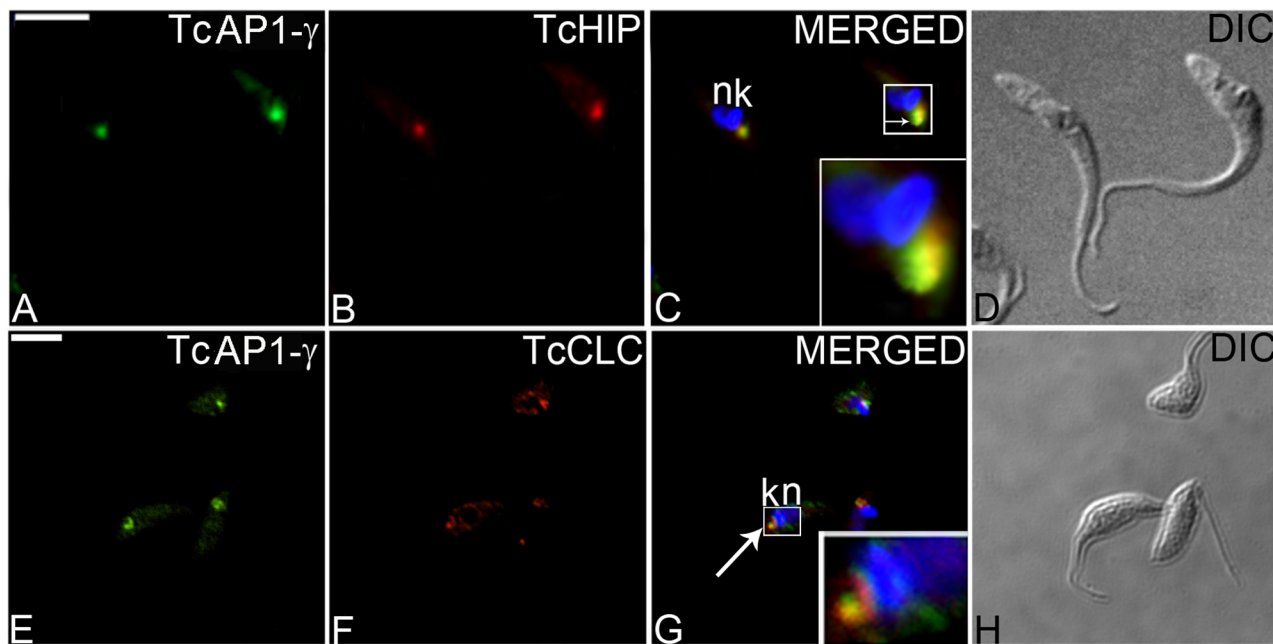
Fig 3. Co-localization of *Trypanosoma cruzi* AP-1 complex γ subunit (TcAP1-γ) with *T. cruzi* Golgi markers. Epimastigotes expressing the tagged Golgi marker Huntingtin interacting protein TcHIP-A/C (A-D) or tagged clathrin light chain TcCLC-A/C (E-H) were labelled with an anti-TcAP1-γ mAb 211.F7 that was detected with anti-mouse IgG conjugated to Alexa Fluor 488 followed by incubation with rabbit IgG anti-protein A for TcHIP-A/C and TcCLC-A/C, that were detected with anti-rabbit IgG conjugated to Alexa Fluor 546. Nuclear (n) and kinetoplast (k) DNA were stained with Hoechst 33342. Arrows indicate co-localization. DIC, differential interference contrast microscopy. Scale bar = 5μm.

TcAP1-γ knockout disturbs the maturation and targeting of cruzipain

Cruzipain is the major cysteine proteinase in *T. cruzi* and a key enzyme for nutrition, differentiation and for the establishment of host cell infection [13,56]. This hydrolase is synthesized as a zymogen of 57 kDa, from which the N-terminal pro-domain is removed autocatalytically, to generate the active enzyme (51 kDa) [57]. Once cruzipain is processed in the endoplasmic reticulum/Golgi complex, it is delivered to reservosomes, which only contain mature cruzipain [40]. Given the potential importance of TcAP1-γ in vesicular traffic from the TGN—including reservosome-bound traffic in *T. cruzi*–we investigated whether the transport of cruzipain to reservosomes was affected in TcγKO parasites. First we analyzed the expression of cruzipain in TcγKO cells using an anti-cruzipain antiserum that recognizes both the unprocessed and mature form of this enzyme [40]. Western blot analysis showed that the cruzipain zymogen form (57 kDa) was recognized by the anti-cruzipain antiserum in both WT and in TcγKO epimastigotes, although the latter had increased zymogen levels (Fig 6A). In contrast, the levels of the mature form of cruzipain (51 kDa) were clearly reduced in TcγKO cells where only a faint band corresponding to mature cruzipain was detected (Fig 6A). These data suggest that the processing of the cruzipain zymogen into mature cruzipain decreased substantially in the TcγKO mutants.

Since TcγKO parasites exhibited decreased processing of cruzipain into its mature form, we examined whether TcAP1-γ deletion affected the transport of cruzipain to reservosomes, which contain only mature cruzipain in WT epimastigotes. Indeed, immunofluorescence analysis showed that cruzipain was not detected in the reservosomes of TcγKO epimastigotes (Fig 6B). To confirm that the absence of cruzipain in the reservosomes of TcγKO parasites was due the lack of TcAP1-γ expression, we transfected TcγKO parasites with an episomal construct
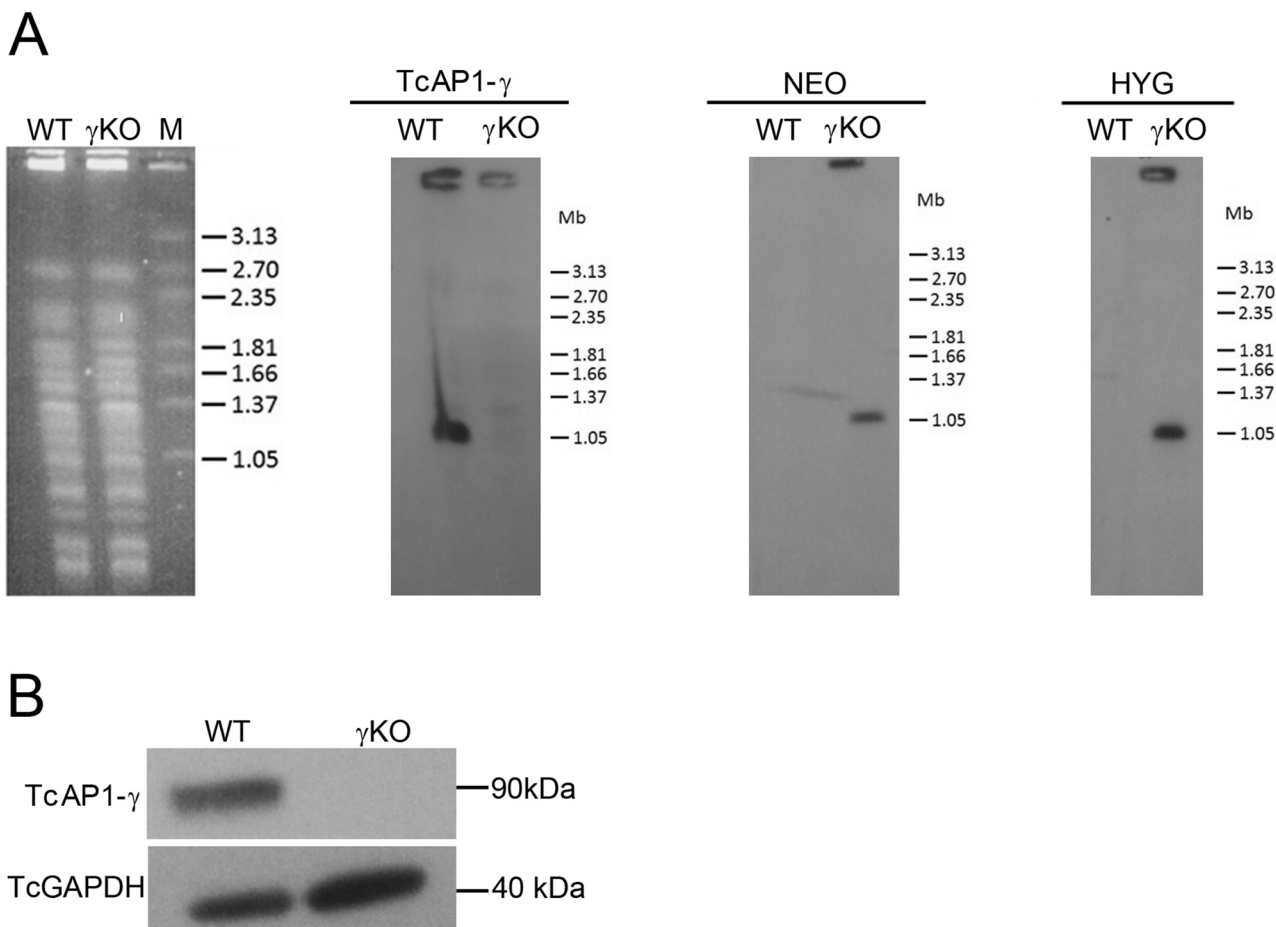
Fig 4. Evaluation of *Trypanosoma cruzi* AP-1 γ subunit (TcAP1-γ) gene knockout. Wild type (WT) and TcAP1-γ knockout (γKO) epimastigotes were analyzed by Southern blot (A) and Western blot (B). (A) High-molecular weight DNA from epimastigotes was separated by PFGE, stained with ethidium bromide (left panel), transferred to nylon membranes and hybridized with [^{32}P]-labeled probes corresponding to the *TcAP1-γ*, *NEO* and *HYG* genes. M, molecular mass marker (*Hansenula wingei* chromosomes), in Mb. (B) Epimastigote cell lysates were separated by SDS-PAGE, transferred onto nitrocellulose membranes and incubated with the anti-TcAP1-γ mAb 211.F7 (1:300 dilution). A mouse antiserum anti-TcGAPDH (1:8,000) was used as a loading control. TcAP1-γ protein and gene sequences were detected in WT, but not detected in γKO samples.

constitutively expressing TcAP1-γ. Western blot analysis confirmed that TcAP1-γ was highly expressed in the complemented TcγKO(pTc-AP1γ) parasites and immunofluorescence analysis showed that the TcAP1-γ expressed in complemented parasites was correctly addressed to the Golgi region (close to kinetoplast) (Figs A and B in S3 Fig). The complemented parasite growth was lower than the WT parasites, however the ability to differentiate to metacyclic trypomastigote forms was higher than the TcγKO cells and comparable to the WT strain (Figs C and D in S3 Fig). Complementation of TcAP1-γ expression in γKO mutants restored maturation and cruzipain localization to the reservosomes (S4 Fig), implicating the AP-1 complex in the formation of reservosome-bound vesicles containing cruzipain, at the TGN.

We further investigated whether cruzipain was targeted to the cell surface in γKO amastigotes because intense cruzipain labeling was observed in the surface of cell-derived amastigotes [58]. Immunofluorescence assays showed that the intensity of cruzipain labeling was highly reduced in the surface of γKO amastigotes compared to WT amastigotes (S5 Fig).
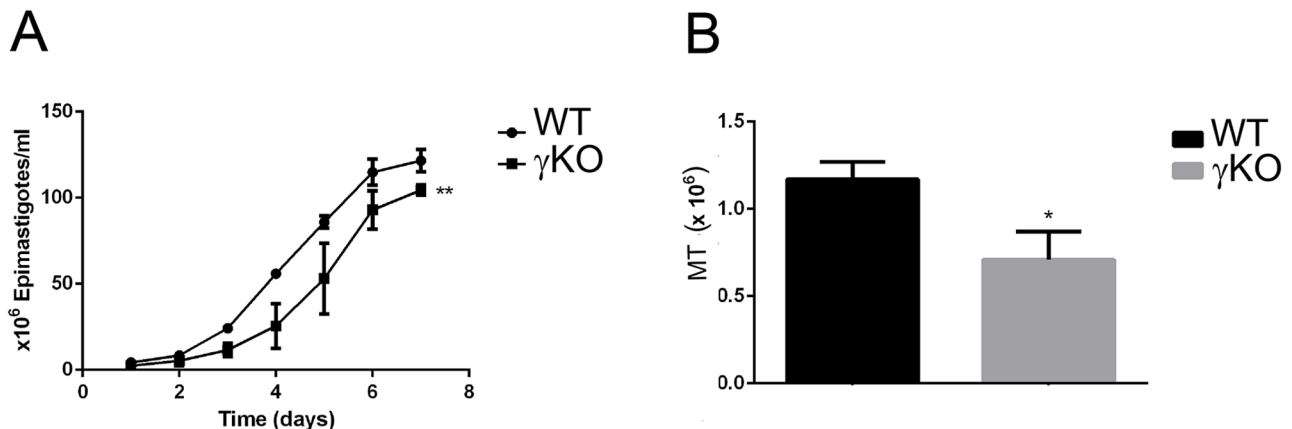
Fig 5. Effect of *Trypanosoma cruzi* AP-1 subunit γ (TcAP1-γ) gene knockout on epimastigote proliferation and differentiation into metacyclic trypomastigotes. (A) Growth curves of wild-type (WT, circles) and TcγKO (γKO, squares) epimastigotes. Data represent mean ± SD of three independent experiments. ** p < 0.05 (test-t). (B) Number of metacyclic trypomastigotes (MT) obtained after 72 h of metacyclogenesis (epimastigote to metacyclic trypomastigote differentiation) *in vitro* for WT (black column) and γKO (gray column) parasite populations. Data represent mean ± SD of three independent experiments. * P < 0.01 (test-t).

TcγKO trypomastigotes have decreased infectivity towards mammalian host cells

Cruzipain is secreted to the environment by trypomastigotes, it is also present in the amastigote surface, which is associated with increased parasite potential to infect and develop within the host cells [59,60]. Given that *T. cruzi* γKO parasites had a clear defect in cruzipain processing, we hypothesized that this mutant may have reduced ability to infect host cells. To test this hypothesis, we quantified the infectivity of WT, TcγKO and TcγKO(pTc-AP1γ) parasites towards HeLa and VERO cells (as representatives of epithelial and fibroblast cell lineages, respectively) using a high-content imaging platform with parameters optimized for the high-throughput analysis of amastigote infection in many cells (>5,000) per well.

Our data showed that knockout of AP-1γ led to a statistically significant decrease in *T. cruzi* infection in both VERO and in HeLa cells (Fig 7A and 7B). The percentage of infected cells decreased from 21.3% to 7.4% (p<0.001) and 9.6% to 6.3% (p<0.001) in HeLa and VERO cells, respectively (Fig 7B, left panel). The mean number of intracellular amastigotes per infected cell also significantly decreased, from 10.1 to 4.3 (p<0.001) and 5.6 to 3.3 (p<0.001), in HeLa and VERO cells, respectively (Fig 7B, middle panel).

Complementation of TcγKO parasites with an episomal construct expressing TcAP1-γ was sufficient to significantly restore the infection ability of TcγKO towards both mammalian cell lines; however, complementation did not fully restore parasite infectivity compared with WT parasites (Fig 7B, right panel). Trypomastigote release (by host cell bursting) was also strongly decreased (and delayed) in cultures infected with TcγKO (< 10% of the trypomastigote production of cells infected with WT parasites).

The structure of the Golgi complex and reservosomes is preserved in *T. cruzi* γKO epimastigotes

Since the TcAP1-γ knockout impairs the transport of cruzipain from TGN, we investigated whether the accumulation of the unprocessed form of this protease could cause morphological alterations in the Golgi complex of TcγKO epimastigotes. Transmission electron microscopy analysis indicated that the Golgi complex of TcγKO epimastigotes had no noteworthy
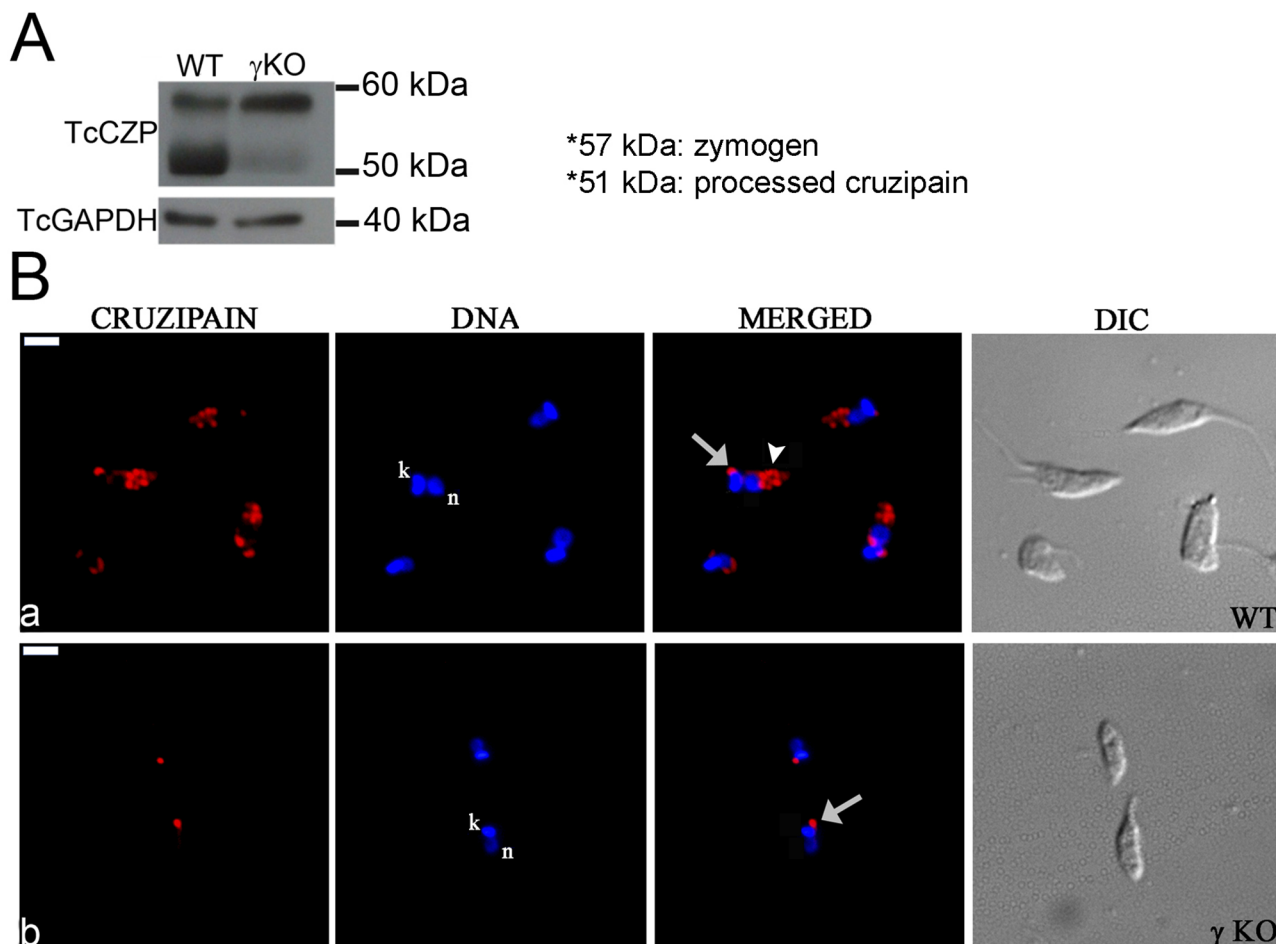
Fig 6. Effect of *Trypanosoma cruzi* AP-1 γ subunit (TcAP1-γ) gene knockout on cruzipain expression and localization. (A) Whole cell lysates from wild-type (WT) and TcγKO (γ KO) epimastigotes were separated by SDS-PAGE, transferred to nitrocellulose membranes and labeled with an anti-cruzipain (TcCZP) antiserum. In γKO epimastigotes, the levels of the zymogen form (57 kDa) of TcCZP were increased, while the levels of the mature enzyme (51 kDa) were decreased (to a faint band) compared with the WT. Labeling for the *T. cruzi* GAPDH was used as a loading control. (B) Wild-type (WT) and AP-1 γ null mutant (γ KO) epimastigotes were labeled with an anti-cruzipain antiserum and detected with anti-mouse IgG conjugated to Alexa Fluor 594. Cruzipain localized in the region of the Golgi complex (arrows) and reservosomes (arrowheads) in WT (**a**), but it appeared absent from reservosomes in the γ null mutant (b). Nuclear (n) and kinetoplast (k) DNA were stained with Hoechst 33342. DIC, differential interference contrast microscopy. Scale bar = 5μm.

https://doi.org/10.1371/journal.pone.0179615.g006

cisternae alterations (Figures A and B in S6 Fig), although the cisternae were more contrasted and easily detected. Once Golgi-derived vesicles are involved in the reservosome formation, we also examined whether reservosomes were present in TcγKO cells. Indeed, ultrastructural analysis of TcγKO epimastigotes showed the presence of reservosomes at the posterior region of these parasites (Figures C and D in S6 Fig).

Discussion

The AP-1 complex is responsible for vesicle trafficking from the TGN to endosomes in eukaryotes. Within the Trypanosomatidae, the AP-1 complex is essential in *T. brucei* and required for infectivity in *Leishmania* [30,31]. Nevertheless, the function of the AP-1 complex in the Chagas disease agent *T. cruzi* has not been examined to date. In this work we show that AP1-γ adaptin is expressed in different *T. cruzi* life stages, including parasite forms found in the invertebrate
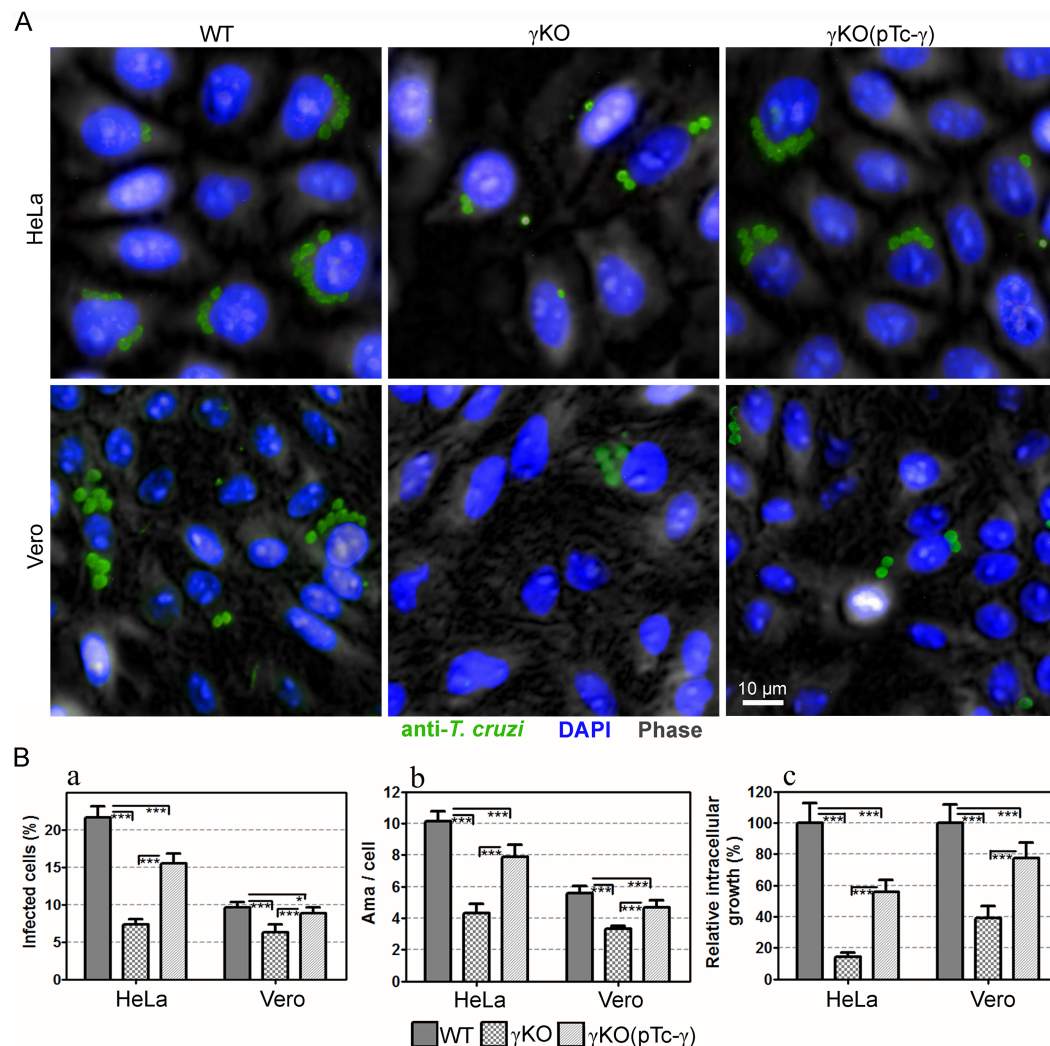
Fig 7. Effect of *Trypanosoma cruzi* AP-1 γ subunit (TcAP1-γ) gene knockout on *T. cruzi* γKO infection in mammalian cells. Vero and HeLa cells were infected with WT, TcγKO (γKO) and TcγKO(pTc-γ) (complemented TcγKO) metacyclic trypomastigotes for 72 h. Then, they were labeled with the anti-*T. cruzi* serum (anti-TEMA) (detected using anti-rabbit IgG conjugated to Alexa Fluor 488) and DAPI (for DNA detection). Cells were imaged using the Operetta Imaging System (PerkinElmer) and analyzed using the Harmony High Content Imaging and Analysis Software (Perkin Elmer). (A) Immunofluorescence images of host cells infected with intracellular amastigotes. (B) Infection quantification was performed using the Harmony High-Content Imaging and Analysis Software, which calculated the percentage of infect cells (a, left graph), mean number of amastigotes/cell (b, middle graph), and relative intracellular growth (riGF = iGF$_{mutant}$ / iGF$_{WT}$, where iGF = a x b) for ≥5000 cells/well (8 wells/experimental condition). Data represent the mean and SD of one representative experiment. ***$p < 0.001$, **$p < 0.01$ and *$p < 0.05$.

https://doi.org/10.1371/journal.pone.0179615.g007

vector (epimastigotes), metacyclic trypomastigotes (responsible for initial host infection), and the replicating intracellular stage (amastigotes).

Production of the monoclonal antibody 211.F7, which targets the hinge region of TcAP1-γ, allowed us to determine that this protein localizes to the Golgi complex, as confirmed by co-localization with the Golgi marker TcHIP, a palmitoyl acyl transferase [42]. TcAP1-γ also partially co-localized with the clathrin light chain (TcCLC), which is found (albeit not exclusively) in the TGN [43]. Recently, we showed that clathrin interacts with both AP-1 and AP-4

complexes in a clathrin interactome study [61]. These data agree with the results of the present study and suggest that an AP-1/clathrin machinery operates at the TGN, in *T. cruzi*.

Since AP-1 is responsible for addressing proteases to lysosomes [19,27], we investigated whether AP-1 was involved in the transport of the major protease cruzipain to the reservosomes, the lysosome-related organelle of *T. cruzi* epimastigotes. Cruzipain is a differentially glycoprotein expressed during the *T. cruzi* life cycle, it has higher activity in epimastigotes, where it is found in the Golgi as a pre-proprotein [16,62]. Cruzipain is then targeted to reservosomes independent from the addition of mannose-6-phosphate (M6P) residues [3,10], which target lysosomal hydrolases to endosomes in other eukaryotes [53]. The M6P biosynthetic pathway is absent in trypanosomes [28,29], which must, therefore, rely on alternative mechanisms of lysosomal hydrolase targeting. Our data strongly suggest a direct role for the AP-1 in cruzipain trafficking because ablation of TcAP1-γ leads to retention of cruzipain in the Golgi complex. Cruzipain was mostly found in its unprocessed form (57 kDa) in TcγKO epimastigotes, indicating that maturation of cruzipain occurs during its transport to the reservosomes, although it could also occur (to some degree) in the Golgi complex, as revealed by the small fraction of the mature form of this enzyme (51 kDa) detected in TcγKO parasites. As expected, complementation of TcγKO with a plasmid expressing TcAP1-γ restored the transport of cruzipain to the reservosomes. Interestingly, the AP-1/clathrin-machinery is necessary for the transporting the cysteine protease trypanopain to the lysosome in *T. brucei* procyclic forms, but it is dispensable in bloodstream forms [31].

Ablation of TcAP1-γ was not lethal, unlike that observed in *T. brucei* where TbAP1-γ is essential [31]. However, proliferation of TcγKO epimastigotes was reduced, as well as the efficiency of metacyclogenesis. It is possible that *T. cruzi* AP-1 plays a more defined role by mediating the transport of a reduced number of cargos, including cruzipain, to reservosomes. Therefore, disruption of this complex would not impair the overall metabolism of the parasite and biogenesis and full activity of reservosomes. In the absence of the specific cargos that depend on AP-1 for targeting to reservosomes, the endocytosed material in this organelle would not be fully degraded for use as an energy source by epimastigotes, reducing cell proliferation and the ability of epimastigotes to differentiate into trypomastigotes.

Reservosomes are formed by the fusion of endocytic vesicles from the flagellar pocket and cytostome with Golgi-derived vesicles. Electron microscopy analysis suggested that TcγKO parasites contain reservosomes, indicating that the biogenesis of these organelles was not fully impaired by TcAP1-γ ablation. Our results agree with a previous study showing that cruzipain inhibitors reduce *T. cruzi* growth and differentiation [56], implicating the lack of active cruzipain as a relevant consequence of TcAP1-γ knockout. However, our findings differ from those reported by Engel and co-workers [17], who showed that inhibition of cruzipain activity in epimastigotes led to cell death due to the accumulation of cruzipain in the Golgi, which was followed by large alterations in Golgi membranes. TcγKO epimastigotes in our study were viable and cisternae abnormalities in the Golgi complex were not observed, but the Golgi complex cisternae of TcγKO parasites were more contrasted and easily detected by transmission electron microscopy.

Although TcAP1-γ ablation only marginally affected the growth rate of epimastigote forms, it strongly impaired the ability of *T. cruzi* to infect host cells from two distinct cell lineages. The reduced number of infected host cells and the small number of intracellular amastigotes observed after 72 h of infection suggest that invasion and/or amastigote proliferation were affected in TcγKO parasites. Furthermore, the number of trypomastigotes released from infected cells was considerably reduced compared with that observed in cultures infected with WT parasites. We hypothesize that the major cause of these defects was the retention of cruzipain in the Golgi complex. Although this protease is expressed at lower levels in trypomastigotes

and amastigotes, compared with epimastigotes [63], cruzipain is critical for trypomastigote infectivity and for intracellular amastigote development [13,56]. Some isoforms of cruzipain are secreted by trypomastigotes [59,64] and they play an important role as virulence factors in Chagas disease [59,62]. Additionally, a striking observation is the presence of cruzipain on the surface of amastigotes [58,65], which may play an important role in parasite survival within host cells. Interestingly, in the γKO amastigotes the cruzipain expression at the cell surface was reduced.

We observed that the ability of TcγKO parasites to infect host cells was only partially restored by complementation with the episomal expression of TcAP1-γ. This result could be explained by non-uniform episomal TcAP1-γ expression within the complemented parasite population, where the maturation and transport of cruzipain in the cells expressing lower levels of TcAP1-γ levels may not have been fully restored.

In addition, we observed that whereas the metacyclogenesis rate was fully restored in the complementing strain, the growth rate of the TcγKO epimastigotes was apparently not affected by the episomal expression of TcAP1-γ. One possible reason is that the complemented TcγKO epimastigotes were grown in LIT medium supplemented with the antibiotic blasticidin to avoid the loss of the plasmid pTcGW-AP-1γ-bsd during cell proliferation.

Taken together, our results show that AP-1 machinery mediates post-Golgi sorting of cruzipain to reservosomes in *T. cruzi* and that AP-1 function is important for parasite infectivity towards host cells. Further studies are necessary to determine the other cargos that depend on AP-1 for transport within the *T. cruzi* endosomal system.

Supporting information

S1 Fig. Strategy of *TcAP1-γ* gene knockout. A) Schemes of the plasmids pTc2KO-AP-1γ-neo and pTc2KO-AP-1γ-hyg, designed to replace the two alleles of the TcAP1-γ gene, by homologous recombination for replacement with the resistance markers NEO and HYG, as depicted in B.
(TIF)

S2 Fig. Diagram of the plasmids used for complementation of TcγKO parasites. The basic structure of pTcGW 1.1 Gateway expression vectors (Kugeratski et al., 2015) were used as a backbone to construct the plasmid pTcGW-bsd (A) for Tcγ cloning. pTcGW-bsd contains the *T. cruzi* Dm28c ribosomal promoter and three distinct *T. cruzi* intergenic regions (IRs) that contain the following sequence elements for the correct processing of the transcripts of the cloned genes into the plasmid: IR1 (IR from *T. cruzi* ubiquitin locus, 278 bp), IR2 (IR between the *T. cruzi* genes TcCLB.504069.70 and TcCLB. 504069.80, 421 bp) and IR3 (IR between the *T. cruzi* genes TcCLB.506295.100 and TcCLB.506295.110, 482 bp). This plasmid also contains a selectable marker (Blasticidin resistance gene, BSD), and two recombination sites (*att*R1 and attR2) flanking the *ccdB* gene, for negative selection in *E. coli*. The Tcγ gene was amplified by PCR using primers containing the *att*B recombination sites (Table 1) and subcloned (by recombination) into *att*R1 and *att*R2 of pTcGW-bsd, resulting in the pTcGW-AP1γ-bsd plasmid (B).
(TIF)

S3 Fig. Ectopic expression of TcAP1-γ in TcγKO epimastigotes. Wild-type (WT), TcAP1-γ null mutant (γKO) and TcAP1-γ-complemented TcγKO [γKO(pTc-γ)] epimastigotes were analyzed for Western blot expression (A) and, localization of TcAP1-γ by immunofluorescence microscopy (B), using the anti-TcAP1-γ mAb 211.F7 as well as the abilities for proliferation (C) and differentiation (D). **A)** Western blot analysis using whole cell lysates. TcAP1-γ was not

detected in γKO parasites, but was highly expressed in the complemented γKO(pTc-γ) cells, compared with WT parasites. An antiserum against GAPDH of *T. cruzi* was used as a loading control. **B)** Immunolocalization of TcAP1-γ. The anti-TcAP1-γ mAb 211.F7 (1:80 dilution) was detected with an anti-mouse IgG conjugated to Alexa Fluor 594 (1:600 dilution). In the complemented γKO(pTcγ) parasite, TcAP1-γ is localized near the kinetoplast as in control WT cells (arrows), indicating that the overexpressed TcAP1-γ is correctly addressed to the Golgi. Nuclear (n) and kinetoplast (k) DNA were stained with Hoechst 33342. DIC, differential interference contrast microscopy. Scale bars = 5μm. **C)** Growth curves of wild-type (WT, circles) and complemented γKO(pTcγ) (squares) epimastigotes. Data represent the mean ± SD of three independent experiments. ** p < 0.05 (test-t). **D)** Number of metacyclic trypomastigotes (MT) obtained after 72 h of metacyclogenesis (epimastigote to metacyclic trypomastigote differentiation) *in vitro*, for the WT (black column) and the complemented γKO(pTcγ) (gray column) parasite populations. Data represent mean ± SD of three independent experiments. * P < 0.01 (test-t). (TIF)

S4 Fig. The cruzipain maturation and reservosome targeting are restored in the complemented γKO(pTcγ) strain. A) Whole cell lysates from wild-type (WT) and the complemented γKO(pTcγ) epimastigotes were separated by SDS-PAGE, transferred to nitrocellulose membranes and labeled with an anti-cruzipain (TcCZP) antiserum. In γKO(pTcγ) epimastigotes, the processing of cruzipain was restored as observed by the presence of a band of 51 kDa corresponding to the mature form of the enzyme. Labeling for the *T. cruzi* GAPDH was used as a loading control. **B)** Wild-type (WT) and γKO(pTcγ) epimastigotes were labeled with an anti-cruzipain antiserum, detected with anti-mouse IgG conjugated to Alexa Fluor 594. Cruzipain localized in the region of the Golgi complex (arrows) and reservosomes (arrowheads) in WT and the complemented strain. Nuclear (n) and kinetoplast (k) DNA were stained with Hoechst 33342. DIC, differential interference contrast microscopy. Scale bar = 5μm (TIF)

S5 Fig. Effect of *Trypanosoma cruzi* AP-1gamma subunit (TcAP1-γ) gene knockout on cruzipain localization in amastigote surface. Wild-type (WT) and AP-1 γ null mutant (γKO) amastigote (not permeabilized) were labelled with anti-cruzipain antiserum and, detected with anti-mouse IgG conjugated to Alexa Fluor 594. A strong labelling was localized in the WT surface (A), whereas the γKO amastigote surface was faintly labelled (B). Nuclear (n) and kinetoplast (k) DNA were stained with Hoechst 33342. DIC, differential interference contrast microscopy. Scale bar = 5μm (TIF)

S6 Fig. Ultrastructural analysis of *T. cruzi* epimastigote forms from wild-type (WT) and TcAP1-γ knockout (TcγKO) parasites. The Golgi complex (arrow) is observed at the anterior region of both WT (**a**) and TcγKO (**b**) parasites. No noticeable morphological alteration is observed, except that the Golgi cisternae are more contrasted and easily detected in TcγKO parasites. Reservosomes (*) with electron-dense matrix are found at the cell posterior region in both WT (**c**) and TcγKO (**d**) parasites, with no remarkable difference in size, shape and density. N = nucleus, K = kinetoplast. (TIF)

Acknowledgments

Author Contributions

Conceptualization: Claudia Maria do Nascimento Moreira, Maurilio José Soares, Stenio Perdigão Fragoso.

Formal analysis: Claudia Maria do Nascimento Moreira, Rafael Luis Kessler.

Funding acquisition: Maurilio José Soares, Stenio Perdigão Fragoso.

Investigation: Claudia Maria do Nascimento Moreira, Cassiano Martin Batista, Jessica Chimenes Fernandes, Rafael Luis Kessler.

Methodology: Claudia Maria do Nascimento Moreira, Stenio Perdigão Fragoso.

Project administration: Stenio Perdigão Fragoso.

Resources: Maurilio José Soares, Stenio Perdigão Fragoso.

Supervision: Maurilio José Soares, Stenio Perdigão Fragoso.

Validation: Claudia Maria do Nascimento Moreira, Stenio Perdigão Fragoso.

Visualization: Claudia Maria do Nascimento Moreira, Cassiano Martin Batista.

Writing – original draft: Claudia Maria do Nascimento Moreira.

Writing – review & editing: Maurilio José Soares, Stenio Perdigão Fragoso.

References

1. Tyler KM, Olson CL, Engman DM. The life cycle of *Trypanosoma Cruzi*. In: Tyler KM, Miles MA, editors. American Trypanososomiasis. Springer Science+Business Media, LLC; 2003. pp. 1–11.

2. Sant'Anna C, Parussini F, Lourenço D, De Souza W, Cazzulo JJ, Cunha-E-Silva NL. All Trypanosoma cruzi developmental forms present lysosome-related organelles. Histochem Cell Biol. 2008; 130: 1187–1198. https://doi.org/10.1007/s00418-008-0486-8 PMID: 18696100

3. Soares MJ, Souto-Padrón T, De Souza W. Identification of a large pre-lysosomal compartment in the pathogenic protozoon *Trypanosoma cruzi*. J Cell Sci. 1992; 102 (1): 157–167.

4. Cunha-e-Silva N, Sant´Anna C, Pereira MG, Porto-Carreiro I, Jeovanio AL, De Souza W. Reservosomes: Multipurpose organelles? Parasitol Res. 2006; 99: 325–327. https://doi.org/10.1007/s00436-006-0190-3 PMID: 16794853

5. de Souza W, Sant'Anna C, Cunha-e-Silva NL. Electron microscopy and cytochemistry analysis of the endocytic pathway of pathogenic protozoa. Prog Histochem Cytochem. 2009; 44: 67–124. https://doi.org/10.1016/j.proghi.2009.01.001 PMID: 19410686

6. Soares MJ, Souto-Padrón T, Bonaldo MC, Goldenberg S, de Souza W. A stereological study of the differentiation process in *Trypanosoma cruzi*. Parasitol Res. 1989; 75: 522–527. PMID: 2549536

7. Soares MJ. The reservosome of *Trypanosoma cruzi* epimastigotes: An organelle of the endocytic pathway with a role on metacyclogenesis. Mem Inst Oswaldo Cruz. 1999; 94: 139–141.

8. Contreras VT, Morel CM, Goldenberg S. Stage specific gene expression precedes morphological changes during *Trypanosoma cruzi* metacyclogenesis. Mol Biochem Parasitol. 1985; 14: 83–96. PMID: 3885031

9. Vidal JC, Alcantara CDEL, Souza WDE, Cunha-e-silva NL. Lysosome-like compartments of *Trypanosoma cruzi* trypomastigotes may originate directly from epimastigote reservosomes. Parasitology. 2017; 1–10.

10. Cazzulo JJ, Cazzulo Franke MC, Martínez J, Franke de Cazzulo BM. Some kinetic properties of a cysteine proteinase (cruzipain) from *Trypanosoma cruzi*. Biochim Biophys Acta (BBA)/Protein Struct Mol. 1990; 1037: 186–191.

11. Santos CC, Sant'anna C, Terres A, Cunha-e-Silva NL, Scharfstein J, de A Lima APC. Chagasin, the endogenous cysteine-protease inhibitor of *Trypanosoma cruzi*, modulates parasite differentiation and

invasion of mammalian cells. J Cell Sci. 2005; 118: 901–915. https://doi.org/10.1242/jcs.01677 PMID: 15713748

12. Cazzulo J. Proteinases of *Trypanosoma Cruzi*: Potential targets for the chemotherapy of Chagas disease. Curr Top Med Chem. 2002; 2: 1261–1271. PMID: 12171584

13. Meirelles MNL, Juliano L, Carmona E, Silva SG, Costa EM, Murta ACM, et al. Inhibitors of the major cysteinyl proteinase (GP57/51) impair host cell invasion and arrest the intracellular development of *Trypanosoma cruzi* in vitro. Mol Biochem Parasitol. 1992; 52: 175–184. PMID: 1620157

14. Figueiredo RCBQ, Rosa DS, Gomes YM, Nakasawa M, Soares MJ. Reservosome: an endocytic compartment in epimastigote forms of the protozoan *Trypanosoma cruzi* (Kinetoplastida: Trypanosomatidae). Correlation between endocytosis of nutrients and cell differentiation. Parasitology. 2004; 129: 431–438. PMID: 15521631

15. Duschak VG, Couto AS. Cruzipain, the major cysteine protease of *Trypanosoma cruzi*: a sulfated glycoprotein antigen as relevant candidate for vaccine development and drug target. A review. Curr Med Chem. 2009; 16: 3174–3202. PMID: 19689291

16. Branquinha MH, Oliveira SSC, Sangenito LS, Sodre CL, Kneipp LF, d'Avila-Levy CM, et al. Cruzipain: An update on its potential as chemotherapy target against the human pathogen *Trypanosoma cruzi*. Curr Med Chem. 2015; 22: 2225–2235. PMID: 25994861

17. Engel JC, Doyle PS, Palmer J, Hsieh I, Bainton DF, McKerrow JH. Cysteine protease inhibitors alter Golgi complex ultrastructure and function in *Trypanosoma cruzi*. J Cell Sci. 1998; 111 (5): 597–606.

18. Sant'Anna C, de Souza W, Cunha-e-Silva N. Biogenesis of the reservosomes of *Trypanosoma cruzi*. Microsc Microanal. 2004; 10: 637–646. https://doi.org/10.1017/S1431927604040863 PMID: 15525436

19. Guo Y, Sirkis DW, Schekman R. Protein sorting at the trans-Golgi network. Annu Rev Cell Dev Biol. 2014; 30: 169–206. https://doi.org/10.1146/annurev-cellbio-100913-013012 PMID: 25150009

20. De Matteis MA, Luini A. Exiting the Golgi complex. Nat. Rev. Mol. Cell Biol. 2008; 9: 273–284. https://doi.org/10.1038/nrm2378 PMID: 18354421

21. Bonifacino JS, Glick BS. The mechanisms of vesicle budding and fusion. Cell. 2004; 116: 153–166. PMID: 14744428

22. Boehm M, Bonifacino JS. Adaptins: The final recount. Mol Biol Cell. 2001; 12: 2907–2920. PMID: 11598180

23. Hirst J, Barlow LD, Francisco GC, Sahlender D a, Seaman MNJ, Dacks JB, et al. The fifth adaptor protein complex. PLoS Biol. 2011; 9: e1001170. https://doi.org/10.1371/journal.pbio.1001170 PMID: 22022230

24. Canagarajah BJ, Ren X, Bonifacino JS, Hurley JH. The clathrin adaptor complexes as a paradigm for membrane-associated allostery. Protein Sci. 2013; 22: 517–529. https://doi.org/10.1002/pro.2235 PMID: 23424177

25. Manna PT, Kelly S, Field MC. Adaptin evolution in kinetoplastids and emergence of the variant surface glycoprotein coat in African trypanosomatids. Mol Phylogenet Evol. 2013; 67: 123–128. https://doi.org/10.1016/j.ympev.2013.01.002 PMID: 23337175

26. Corrêa JR, Atella GC, Menna-Barreto RS, Soares MJ. Clathrin in *Trypanosoma cruzi*: in silico gene identification, isolation, and localization of protein expression sites. J Eukaryot Microbiol. 2007; 54: 297–302. https://doi.org/10.1111/j.1550-7408.2007.00258.x PMID: 17552985

27. Le Borgne R, Hoflack B. Mannose 6-phosphate receptors regulate the formation of clathrin-coated vesicles in the TGN. J Cell Biol. 1997; 137: 335–345. PMID: 9128246

28. Lefkir Y; Chassey B; Dubois A, Bogdanovic A, Brady R, Destaing O; Bruckert F, O'Halloran TJ; Cosson P, Letourneur F. The AP-1 clathrin-adaptor is required for lysosomal enzymes sorting and biogenesis of the contractile vacuole complex in Dictyostelium cells. Mol Biol Cell. 2003; 14: 1835–1851. https://doi.org/10.1091/mbc.E02-10-0627 PMID: 12802059

29. Touz M, Kulakova L, Nash T. Adaptor protein complex 1 mediates the transport of lysosomal proteins from a Golgi-like organelle to peripheral vacuoles in the primitive eukaryote *Giardia lamblia*. Mol Biol Cell. 2004; 15: 3053–3060. https://doi.org/10.1091/mbc.E03-10-0744 PMID: 15107467

30. Allen CL, Liao D, Chung W-L, Field MC. Dileucine signal-dependent and AP-1-independent targeting of a lysosomal glycoprotein in *Trypanosoma brucei*. Mol Biochem Parasitol. 2007; 156: 175–190. https://doi.org/10.1016/j.molbiopara.2007.07.020 PMID: 17869353

31. Tazeh NN, Silverman JS, Schwartz KJ, Sevova ES, Sutterwala SS, Bangs JD. Role of AP-1 in developmentally regulated lysosomal trafficking in *Trypanosoma brucei*. Eukaryot Cell. 2009; 8: 1352–1361. https://doi.org/10.1128/EC.00156-09 PMID: 19581441

32. Gokool S. Sigma 1- and mu 1-Adaptin homologues of *Leishmania mexicana* are required for parasite survival in the infected host. J Biol Chem. 2003; 278: 29400–9. https://doi.org/10.1074/jbc.M304572200 PMID: 12730207

33. Vince JE, Tull DL, Spurck T, Derby MC, McFadden GI, Gleeson P a, et al. Leishmania adaptor protein-1 subunits are required for normal lysosome traffic, flagellum biogenesis, lipid homeostasis, and adaptation to temperatures encountered in the mammalian host. Eukaryot Cell. 2008; 7: 1256–1267. https://doi.org/10.1128/EC.00090-08 PMID: 18515754

34. Contreras VT, Salles JM, Thomas N, Morel CM, Goldenberg S. In vitro differentiation of *Trypanosoma cruzi* under chemically defined conditions. Mol Biochem Parasitol. 1985; 16: 315–327. PMID: 3903496

35. Bonaldo MC, Souto-Padron T, De Souza W, Goldenberg S. Cell-substrate adhesion during *Trypanosoma cruzi* differentiation. J Cell Biol. 1988; 106: 1349–1358. PMID: 3283152

36. de Sousa MA. A simple method to purify biologically and antigenically preserved bloodstream trypomastigotes of *Trypanosoma cruzi* using Deae-cellulose columns. Mem Inst Oswaldo Cruz. 1983; 78: 317–333. PMID: 6361445

37. de Souza FSP, Rampazzo RDCP, Manhaes L, Soares MJ, Cavalcanti DP, Krieger MA, et al. Knockout of the gene encoding the kinetoplast-associated protein 3 (KAP3) in *Trypanosoma cruzi*: effect on kinetoplast organization, cell proliferation and differentiation. Mol Biochem Parasitol. 2010; 172: 90–98. https://doi.org/10.1016/j.molbiopara.2010.03.014 PMID: 20363262

38. Mazzarotto GACA, Raboni SM, Stella V, Carstensen S, de Noronha L, Levis S, et al. Production and characterization of monoclonal antibodies against the recombinant nucleoprotein of *Araucaria hantavirus*. J Virol Methods. 2009; 162: 96–100. https://doi.org/10.1016/j.jviromet.2009.07.022 PMID: 19654026

39. Sambrok J., Fritisch E., Maniatis T. Molecular Cloning: a laboratory manual 2nd ed. 2nd ed. Cold Spring Harbor, editor. 1989.

40. Batista CM, Medeiros LCS, Eger I, Soares MJ. MAb CZP-315.D9: An antirecombinant cruzipain monoclonal antibody that specifically labels the reservosomes of *Trypanosoma cruzi* epimastigotes. Biomed Res Int. 2014; 2014.

41. Gradia DF, Rau K, Umaki ACS, de Souza FSP, Probst CM, Correa A, et al. Characterization of a novel Obg-like ATPase in the protozoan *Trypanosoma cruzi*. Int J Parasitol. Australian Society for Parasitology Inc.; 2009; 39: 49–58.

42. Batista CM, Kalb LC, Moreira CM do N, Batista GTH, Eger I, Soares MJ. Identification and subcellular localization of TcHIP, a putative Golgi zDHHC palmitoyl transferase of *Trypanosoma cruzi*. Exp Parasitol. Elsevier Inc.; 2013; 134: 52–60.

43. Kalb LC, Frederico YCA, Batista CM, Eger I, Fragoso SP, Soares MJ. Clathrin expression in *Trypanosoma cruzi*. BMC Cell Biol. 2014; 15: 1–11.

44. Schimanski B, Nguyen TN, Günzl A, Gu A. Highly efficient tandem affinity purification of Trypanosome protein complexes based on a novel epitope combination. Eukaryot Cell. 2005; 4: 1942–1950. https://doi.org/10.1128/EC.4.11.1942-1950.2005 PMID: 16278461

45. Pavani RS, da Silva MS, Fernandes CAH, Morini FS, Araujo CB, Fontes MR de M, et al. Replication protein A presents canonical functions and is also involved in the differentiation capacity of *Trypanosoma cruzi*. Buscaglia CA, editor. PLoS Negl Trop Dis. 2016; 10: e0005181. https://doi.org/10.1371/journal.pntd.0005181 PMID: 27984589

46. Kessler RL, Gradia DF, de Pontello Rampazzo RC, Lourenço ÉE, Fidêncio NJ, Manhaes L, et al. Stage-regulated GFP expression in *Trypanosoma cruzi*: applications from host-parasite interactions to drug screening. PLoS One. 2013; 8. e67441 https://doi.org/10.1371/journal.pone.0067441 PMID: 23840703

47. Batista M, Marchini FK, Celedon P a F, Fragoso SP, Probst CM, Preti H, et al. A high-throughput cloning system for reverse genetics in *Trypanosoma cruzi*. BMC Microbiol. 2010; 10:1–12.

48. Kugeratski FG, Batista M, Inoue AH, Ramos BD, Krieger MA, Marchini FK. pTcGW plasmid vectors 1.1 version: A versatile tool for *Trypanosoma cruzi* gene characterisation. Mem Inst Oswaldo Cruz. 2015; 110: 687–690. https://doi.org/10.1590/0074-02760150074 PMID: 26200713

49. Ter Haar E, Harrison SC, Kirchhausen T. Clathrin from the cover: peptide-in-groove interactions link target proteins to the beta -propeller of clathrin. Proc. Natl. Acad. Sci. U.S.A. 1999; 97: 1096–1100.

50. Doray B, Kornfeld S. Gamma Subunit of the AP-1 adaptor complex binds clathrin: implications for cooperative binding in coated vesicle assembly. Mol Biol Cell. 2001; 12: 1925–1935. PMID: 11451993

51. Yeung BG, Payne GS. Clathrin interactions with C-terminal regions of the yeast AP-1 b and g subunits are important for AP-1 association with clathrin coats. Traffic. 2001; 2: 565–576. PMID: 11489214

52. Kent HM, McMahon HT, Evans PR, Benmerah A, Owen DJ. Gamma-adaptin appendage domain: structure and binding site for Eps15 and gamma-synergin. Structure. 2002; 10: 1139–48. PMID: 12176391

53. Bonifacino JS, Traub LM. Signals for sorting of transmembrane proteins to endosomes and lysosomes. Annu Rev Biochem. 2003; 72: 395–447. PMID: 12651740

54. Park SY, Guo X. Adaptor protein complexes and intracellular transport. Biosci Rep. 2014; 34: 381–390.

55. Girard-Dias W, Alcantara CL, Cunha-e-Silva N, De Souza W, Miranda K. On the ultrastructural organization of *Trypanosoma cruzi* using cryopreparation methods and electron tomography. Histochem Cell Biol. 2012; 138: 821–831. https://doi.org/10.1007/s00418-012-1002-8 PMID: 22872316

56. Franke De Cazzulo BM, Martlnez J, North MJ, Coombs GH, Cazzulo J-J. Effects of proteinase inhibitors on the growth and differentiation of *Trypanosoma cruzi*. FEMS Microbiol Lett. 1994; 124: 81–86. d PMID: 8001773

57. Murta ACM, Persechini PM, Padron T de S, de Souza W, Guimarães JA, Scharfstein J. Structural and functional identification of GP57/51 antigen of *Trypanosoma cruzi* as a cysteine proteinase. Mol Biochem Parasitol. 1990; 43: 27–38. PMID: 1705310

58. Souto-Padrón T, Campetella OE, Cazzulo JJ, de Souza W. Cysteine proteinase in *Trypanosoma cruzi*: immunocytochemical localization and involvement in parasite-host cell interaction. J Cell Sci. 1990; 96 (3): 485–490.

59. Aparicio IM, Scharfstein J, a APC, Lima APC a. A new cruzipain-mediated pathway of human cell invasion by *Trypanosoma cruzi* requires trypomastigote membranes. Infect Immun. 2004; 72: 5892–5902. https://doi.org/10.1128/IAI.72.10.5892-5902.2004 PMID: 15385491

60. Osorio L, Ríos I, Gutiérrez B, González J. Virulence factors of *Trypanosoma cruzi*: Who is who? Microbes Infect. 2012; 14: 1390–1402. https://doi.org/10.1016/j.micinf.2012.09.003 PMID: 23006853

61. Kalb LC, Frederico YCA, Boehm C, Moreira CM do N, Soares MJ, Field MC. Conservation and divergence within the clathrin interactome of *Trypanosoma cruzi*. Sci Rep. Nature Publishing Group; 2016; 6: 1–12.

62. Alvarez VE, Niemirowicz GT, Cazzulo JJ. The peptidases of *Trypanosoma cruzi*: Digestive enzymes, virulence factors, and mediators of autophagy and programmed cell death. Biochim Biophys Acta—Proteins Proteomics. Elsevier B.V.; 2012; 1824: 195–206.

63. Cazzulo JJ, Stoka V, Turk V. Cruzipain, the major cysteine proteinase from the protozoan parasite *Trypanosoma cruzi*. Biol Chem. 1997; 378: 1–10. PMID: 9049059

64. Yokoyama-Yasunaka JKU, Pral EMF, Oliveira OC, Alfieri SC, Stolf AMS. *Trypanosoma cruzi*: Identification of proteinases in shed components of trypomastigote forms. Acta Trop. 1994; 57: 307–315. PMID: 7810387

65. Tomas a M, Miles M a, Kelly JM. Overexpression of cruzipain, the major cysteine proteinase of *Trypanosoma cruzi*, is associated with enhanced metacyclogenesis. Eur J Biochem. 1997; 244: 596–603. PMID: 9119029

SUPPORTING INFORMATION

S1 Fig. Strategy of *TcAP1-γ* gene knockout
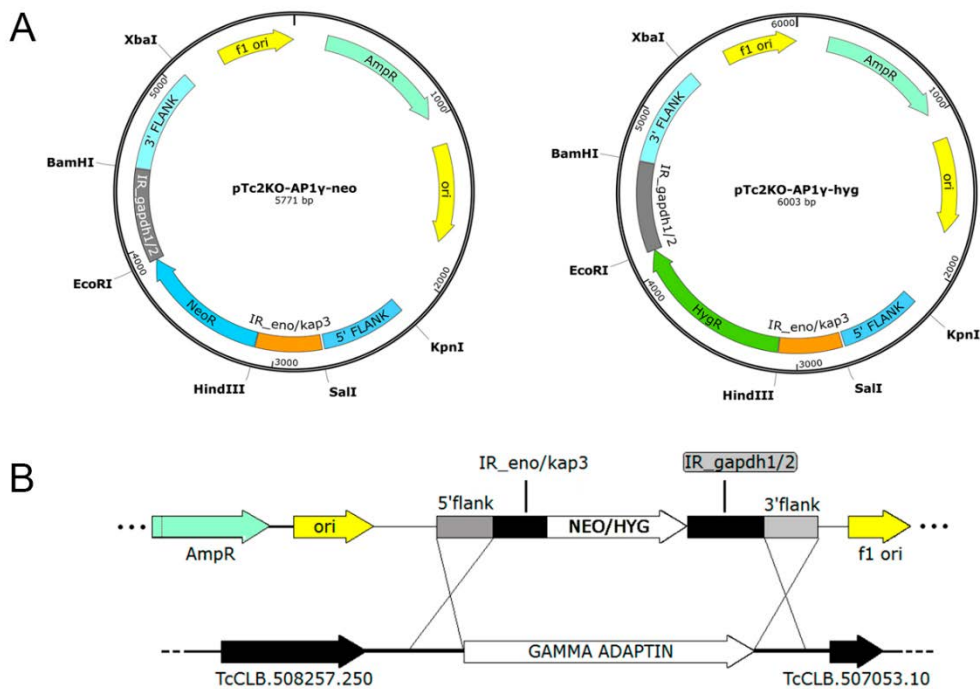
S2 Fig. Diagram of the plasmids used for complementation of TcγKO parasites
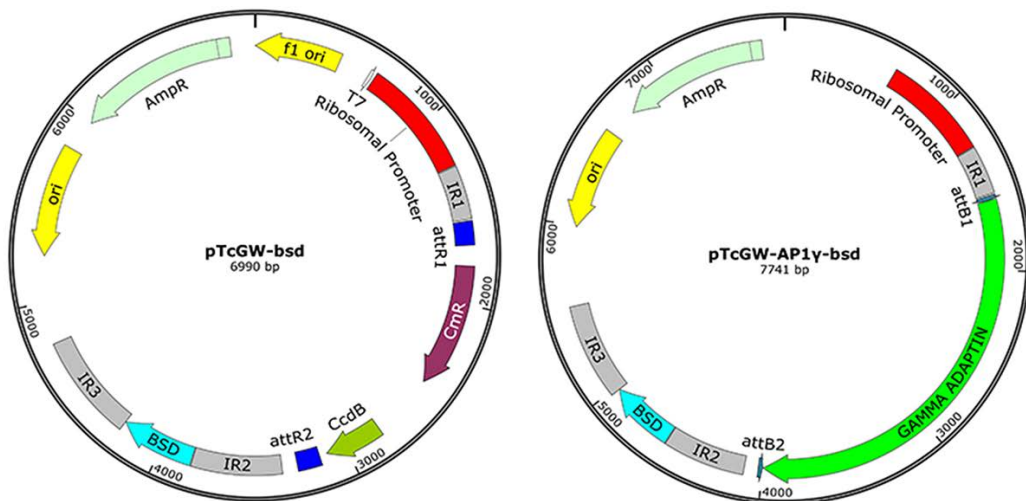
S3 Fig. Ectopic expression of TcAP1-γ in TcγKO epimastigotes.
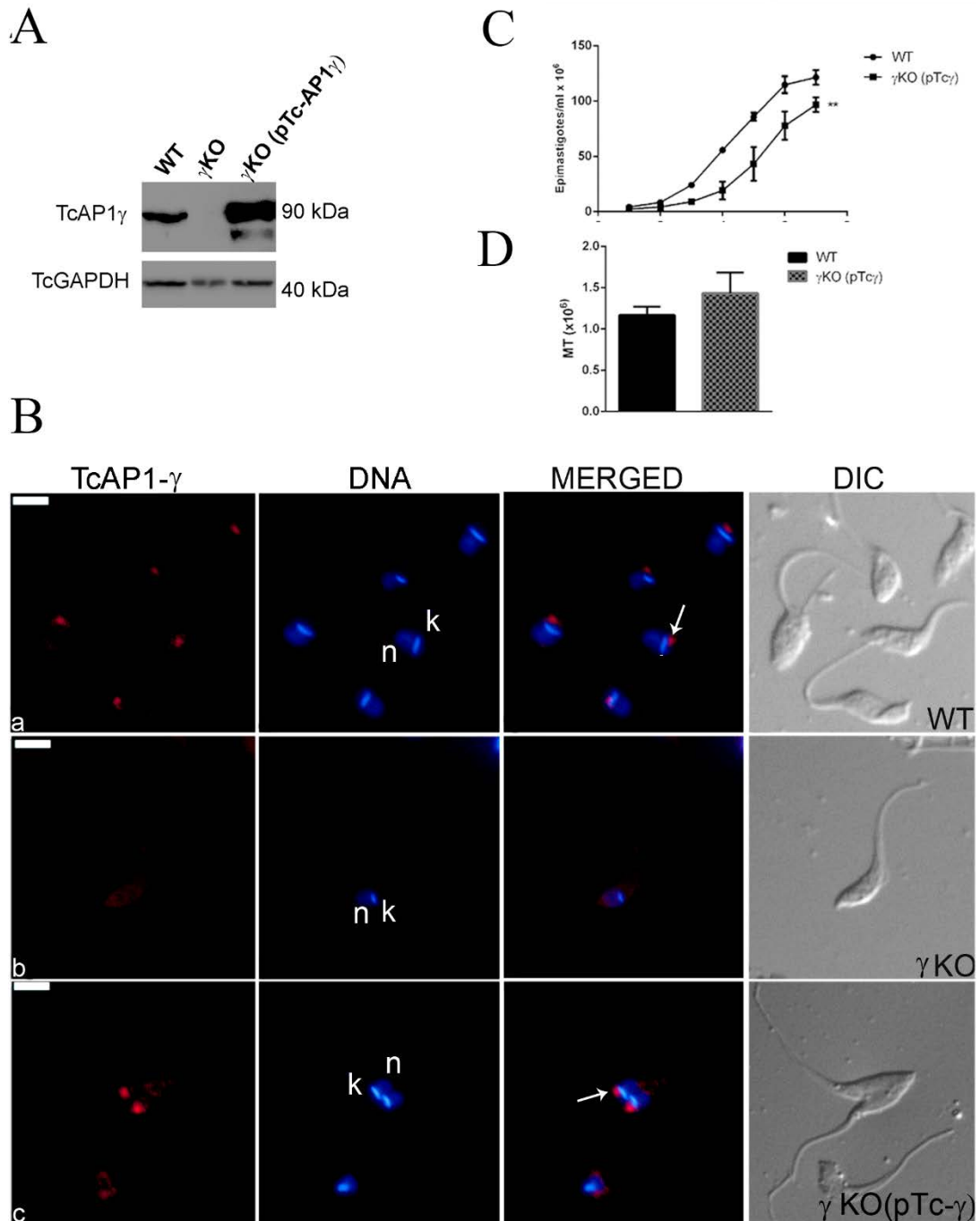
S4 Fig. The cruzipain maturation and reservosome targeting are restored in the complemented γKO(pTcγ) strain.

A

TcCZP

TcGAPDH

60 kDa
50 kDa
40 kDa

zymogen（57 kDa）
processed cruzipain（51 kDa）

B

CRUZIPAIN   DNA   MERGED   DIC

WT

γKO(pTcγ)
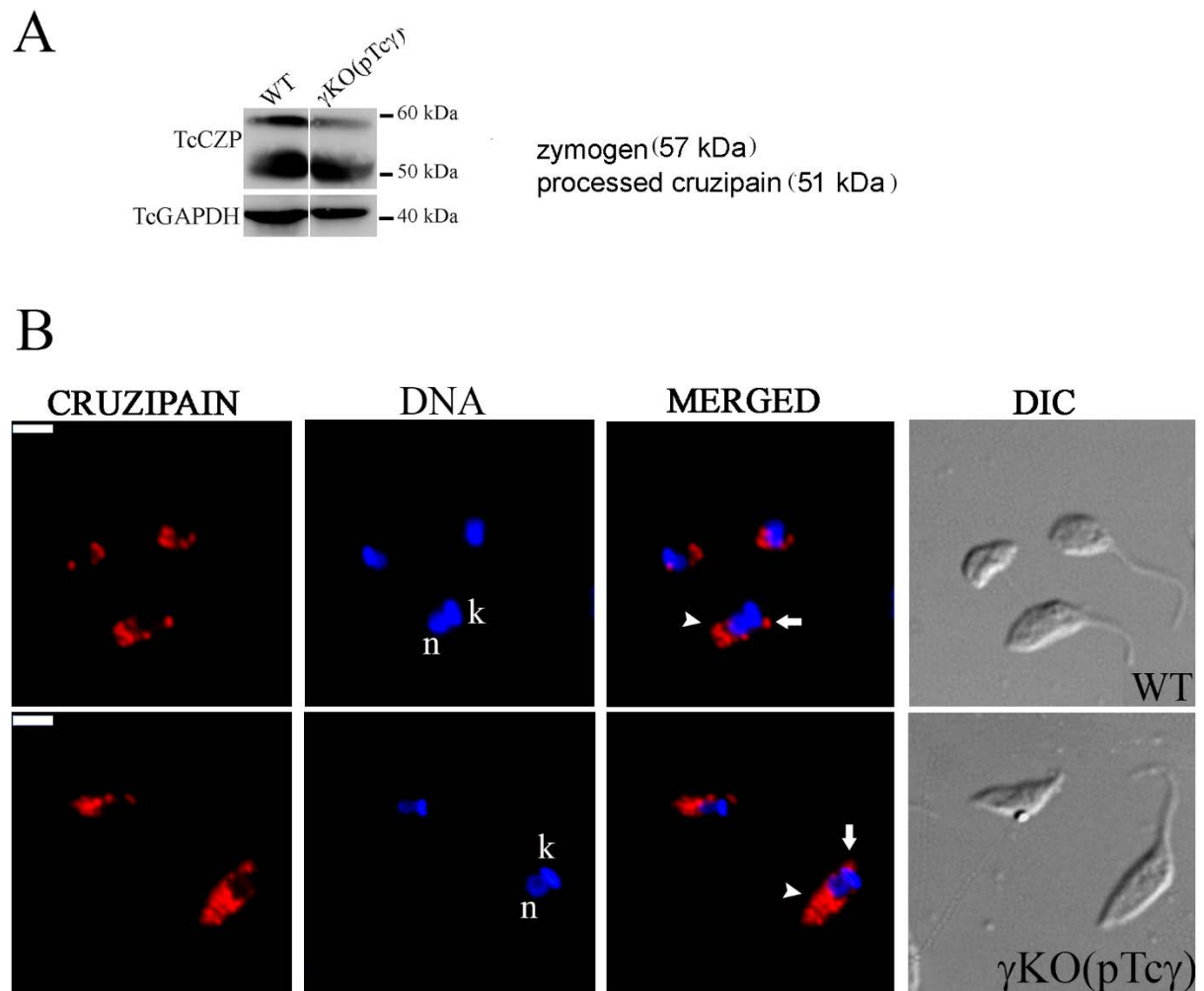
S5 Fig. Effect of *Trypanosoma cruzi* AP-1gamma subunit (TcAP1-γ) gene knockout on cruzipain localization in amastigote surface.
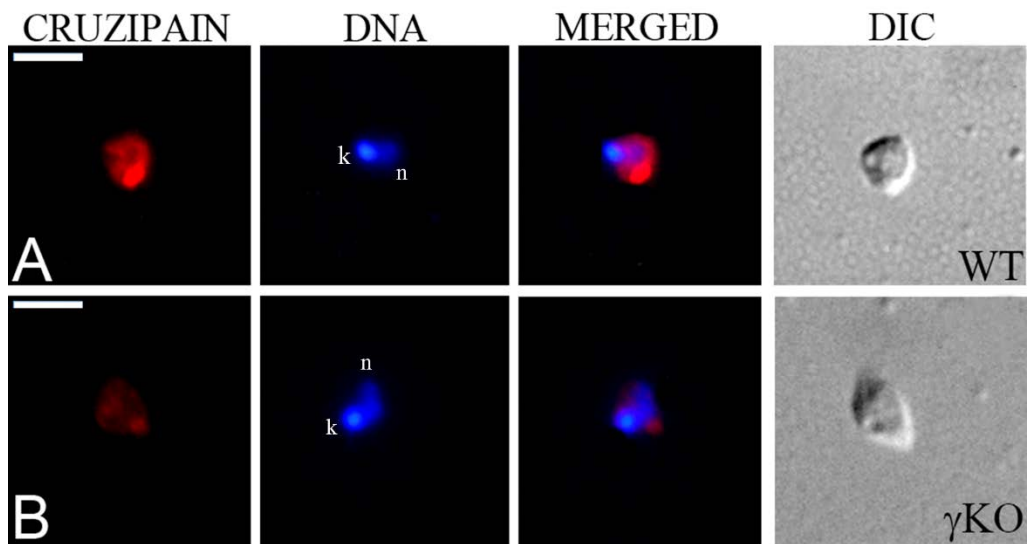
S6 Fig. Ultrastructural analysis of *T. cruzi* epimastigote forms from wild-type (WT) and TcAP1-γ knockout (TcγKO) parasites.
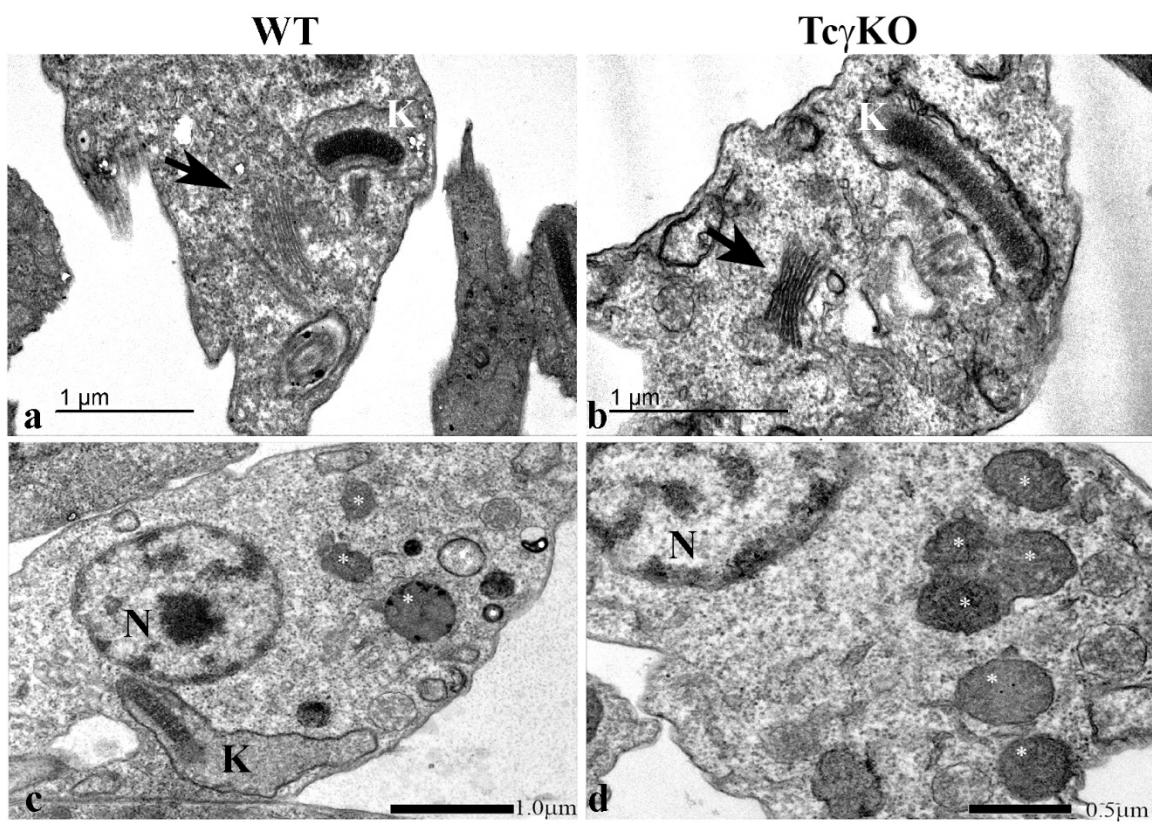
3 RESULTADOS SUPLEMENTARES E DISCUSSÃO REFERENTES AO CAPÍTULO 1

3.1 Expressão e imunolocalização da cruzipaína processada no parasita mutante

Para confirmar os resultados utilizando o soro anti-cruzipaína nos parasitas AP1-γKO, utilizamos o anticorpo monoclonal mAb anti-cruzipaina (CZP 315-D9) que reconhece majoritariamente a cruzipaína processada (51 kDa) residente nos reservosomos de formas epimastigotas de *T. cruzi* (BATISTA *et al*., 2014). Através de ensaio de western blot, utilizando extrato total de formas epimastigotas WT e γKO de *T. cruzi*, observamos que o parasita mutante possui níveis extremamente reduzidos da cruzipaína processada quando comparado ao parasita selvagem (Fig. 4.1A), corroborando o que já havíamos observado no ensaio onde utilizamos o soro anti-cruzipaína e sugerindo fortemente que o nocaute de AP1-γ interfere no processamento da cruzipaína no CG.

No ensaio de localização da cruzipaína madura por imunofluorescência, além dos parasitas selvagem (Fig. 4.1Ba) e nocaute (Fig. 4.1Bb) analisamos também o parasita complementado (Fig. 1Bc). Confirmamos que a cruzipaína madura, presente nos reservosomos do parasita selvagem (Fig. 4.1Ba), não é mais encontrada no parasita nocaute (Fig. 4.1Bb), voltando a aparecer na linhagem mutante, quando esta foi complementada com o plasmídeo pTcGW-AP1γ-bsd expressando a subunidade AP1-γ, sugerindo que AP-1 é responsável pelo transporte da cruzipaina para os reservossomos.
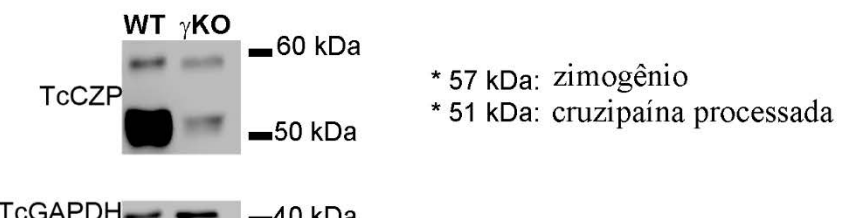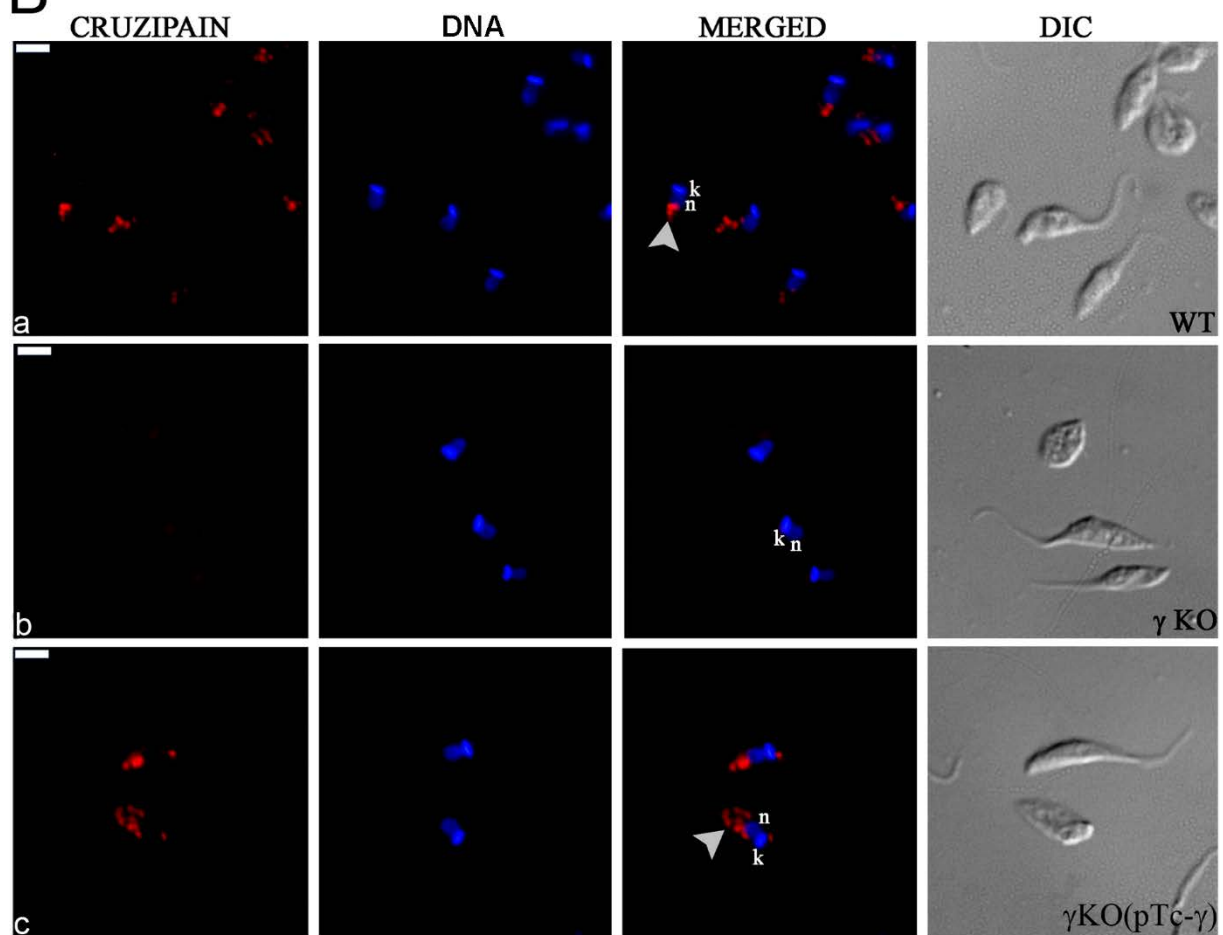
Figura 4.1. Efeito do nocaute do gene que codifica a subunidade AP-1 γ (TcAP1-γ) na expressão e localização da cruzipaína processada em *Trypanosoma cruzi*.

A) Extratos proteícos totais de epimastigotas de *T. cruzi* (WT) e TcγKO (γ KO) foram separados por SDS-PAGE, transferidos para membranas de nitrocellulose e marcados com mAb anti-cruzipaína (TcCZP) (diluição 1:500). Nos parasitas epimastigotas γKO, os níveis da forma madura da enzima (51 kDa) estavam claramente diminuídas comparada com o WT. GAPDH de *T. cruzi* foi usada como controle de corrida. **B)** Formas epimastigotas do wild-type (WT), mutante nulo de AP-1 γ (γ KO) e o complementado (γ KO (pTc-γ)) foram marcadas com mAb anti-cruzipaína (diluição 1:200) e detectada com anti-mouse IgG conjugado com Alexa Fluor 594. A cruzipaína foi localizada nos reservossomos apenas nos

parasitas WT (**a**) e no γKO (pTc-γ) (**c**) e ausente nos parasitas mutante nulo γKO (**b**). O DNA do nucleo (n) e do cinetoplasto (k) foram corados com Hoechst 33342**.** DIC, microscopia de contraste de interferência diferencial, Scale bar = 5µm

3.2 Expressão e localização da cruzipaína no parasita mutante tripomastigota metacíclico (TM)

A cruzipaína é um conhecido fator de virulência para o *T. cruzi* (CAZZULO, 2002; YOSHIDA, 2006). Ensaios por imunoeletromicroscopia mostraram que cruzipaína está presente na superfície de epimastigotas e também das formas amastigotas e tripomastigotas obtidos de cultivo celular (SOUTO-PADRÓN *et al.*, 1990). Contudo, dados sobre a localização e expressão dessa proteína nas formas tripomastigotas metacíclicas (TM) não são conhecidos. Nossos resultados, usando ensaios de western blot, mostraram que nas formas tripomastigotas metacíclicas, a cruzipaína é encontrada quase que exclusivamente na forma processada (51 kDa) e está praticamente ausente nos tripomastigotas metacíclicos da linhagem mutante para AP1-γ (Fig. 4.2A), refletindo, possivelmente, o fato de que, nas formas epimastigotas da linhagem mutante, o processamento da cruzipaína já estava reduzido drasticamente em comparação com a linhagem selvagem.

Análises por microscopia de imunofluorescência mostraram que a cruzipaína se localiza majoritariamente na região posterior das formas tripomastigotas metacíclicas (Fig. 4.2B/+triton), local onde se concentram organelas possivelmente remanescentes dos reservossomos (VIDAL *et al.*, 2017). Contudo, na linhagem mutante para AP1-γ, a cruzipaína está localizada na região entre o núcleo e o cinetoplasto, que corresponde a localização do CG nessa forma (TEIXEIRA *et al.*, 2011), sugerindo que também nas formas tripomastigotas metacíclicas do parasita nocaute a cruzipaína não processada (zimogênio) se acumula no CG.

Nossos resultados também mostraram que a cruzipaína também está localizada na superfície das formas tripomastigotas metacíclicas (Fig. 4.2B/-triton), mas está praticamente ausente na superfície das formas tripomastigotas metacíclicas da linhagem mutante. Nossos resultados de infecção de linhagens celulares usando essas formas mostraram que a linhagem mutante é pouco infectiva em comparação com a linhagem selvagem, sugerindo que a presença de cruzipaína na superfície das formas metacíclicas possa ter papel importante no processo de infecção.

A

TM
WT γKO

TcCZP   ▬ 60kDa

               ▬ 50kDa

TcGAPDH   ▬ 40kDa

* 57 kDa: zimogênio
* 51 kDa: cruzipaína processada

B

CRUZIPAIN	DNA	MERGED	DIC	
		k n	WT	+TRITON
		n k	AP1-γ KO	
		n k	WT	-TRITON
		k n	AP1-γ KO	
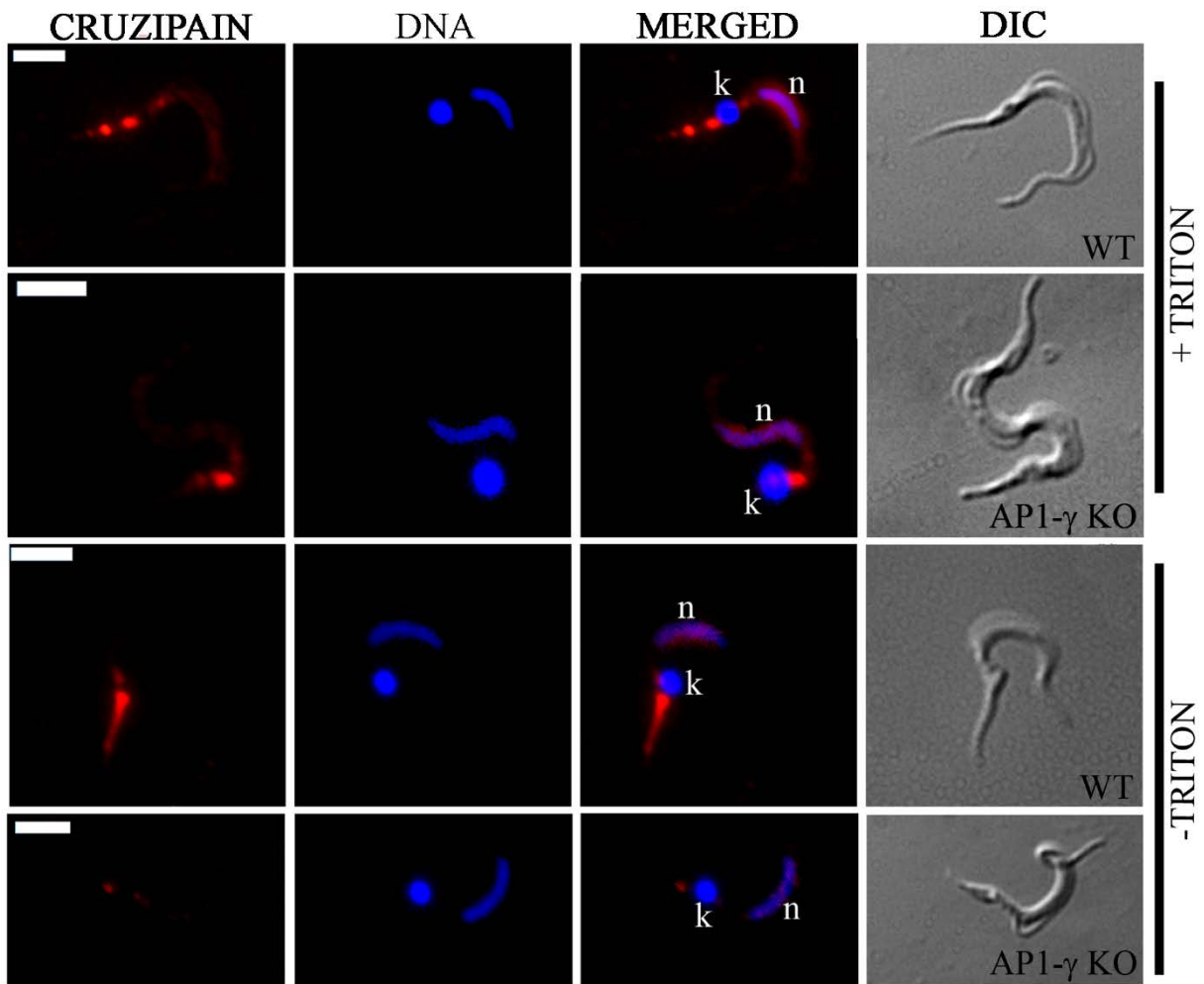
Fig. 4.2. Efeito do nocaute do gene que codifica a subunidade AP-1 γ (TcAP1-γ) na expressão e localização da cruzipaína em forma tripomastigota metacíclica de *Trypanosoma cruzi*. A) Extratos proteícos totais de tripomastigotas metacíclicos (TM) de *T. cruzi* (WT) e TcγKO (γ KO) foram separados por SDS-PAGE, transferidos para membranas de nitrocelulose e marcados com soro anti-cruzipaína (TcCZP) (diluição 1:2500). Nos parasitas γKO, os níveis da forma madura da enzima (51 kDa) estavam claramente diminuídas comparada com o WT. GAPDH de *T. cruzi* foi usada como controle de corrida. **B**) Formas

TM do wild-type (WT) e do mutante nulo de AP-1 γ (γ KO) permeabilizadas (+triton) ou sem permeabilização (-triton) foram marcadas com soro anti-cruzipaína (diluição 1:200) e detectada com anti-mouse IgG conjugado com Alexa Fluor 594. A cruzipaína foi localizada nos reservossomos e CG a nos parasitas WT e somente no CG nos parasitas mutante nulo γ. Nos parasitas não permeabilizados foi possível observar a cruzipaína na superfície do parasita WT enquanto que no parasita γKO a detecção é drasticamente diminuída. O DNA do núcleo (n) e do cinetoplasto (k) foram corados com Hoechst 33342. DIC, microscopia de contraste de interferência diferencial, barra de escala = 5μm

CAPÍTULO 2

Identificação de complexos associados ao complexo adaptador 1 (AP-1) em *Trypanosoma cruzi*

Os dados referentes a esse capítulo foram publicados no periódico Nature/Scientific Reports, no ano de 2016.

Essa etapa do projeto foi desenvolvida na Universidade de Dundee, na Escócia, em colaboração com o Prof. Mark C. Field. O financiamento foi concedido pela CAPES através do programa de doutorado sanduíche no exterior (PDSE) que teve duração de seis meses.

RESUMO: Diversas características indicam que os tripanossomatídeos divergiram muito cedo durante a evolução dos eucariotos. Com base em banco de dados genômicos, estima-se que mais de 50% dos genes que codificam proteínas nesses protozoários sejam divergentes dos eucariontes superiores, sugerindo que vias metabólicas e outros processos celulares, mesmo que ubíquos, operam por mecanismos moleculares com características únicas a esses protozoários. Em *Trypanosoma cruzi*, o conhecimento acerca dos complexos protéicos que estão envolvidos com o tráfego vesicular ainda é escasso. Porém, é possível, a partir de uma proteína conservada, isolar possíveis proteínas associadas a ela através de técnicas, tal como imunoprecipitação e, posteriormente, identificá-las por análise por espectrometria de massas.

O artigo relacionado a esse capítulo é resultado de um dos objetivos da tese de doutorado de Lígia Cristina Kalb (KALB, 2015), que tratou da identificação das proteínas parceiras de clatrina e epsinaR em *T. cruzi*. Fui co-autora desse trabalho, pois ele também envolveu a identificação de proteínas associadas ao complexo adaptador 1 (AP-1) de *T. cruzi*, por espectrometria de massas, que é um dos objetivos da minha tese de doutorado. A metodologia se baseou na obtenção de extratos proteicos do parasita através da técnica de moagem em temperaturas criogênicas (- 196 °C) (criomoagem) (*cryogriding*), desenvolvida pelo Dr. Mark C. Field, possibilitando a detecção de interações protéicas de curta duração e a redução das ligações inespecíficas existentes em processos dinâmicos, como é o caso da formação de revestimento de vesículas. Para isso, parasitas transfectantes expressando as proteínas TcClatrina (CLC, cadeia leve da clatrina) e TcEpsinaR fusionadas com etiquetas, foram

congelados rapidamente com nitrogênio líquido e depois moídos, para obtenção do extrato proteíco total em forma de um pó extra-fino. O pó obtido foi utilizado em ensaios de imunoprecipitação e, por espectrometria de massas, foi possível identificar que o complexo AP-1 interage tanto com a clatrina como com a epsinaR em *T. cruzi*. Também foi possível identificar que duas proteínas de reservosomo em *T. cruzi*, a cruzipaína e a GLP-1 podem ser carreadas por vesículas revestidas por clatrina/AP-1 a partir do complexo de Golgi.

A parte final desse capítulo, está relacionada com a identificação de proteínas parceiras de TcAP-1 utilizando as subunidades TcAP1-β e TcAP1-μ fusionadas à uma etiqueta GFP e expressas em formas epimastigotas de *T. cruzi*. Foi possível demonstrar a localização dessas duas adaptinas no complexo de Golgi de *T. cruzi* através da co-localização com a subunidade TcAP1-γ. Os extratos protéicos desses parasitas transfectantes, obtidos por criomoagem, foram utilizados em ensaios de imunoprecipitação e análise por espectrometria de massas.

SCIENTIFIC REP⚙RTS

OPEN

Conservation and divergence within the clathrin interactome of *Trypanosoma cruzi*

Ligia Cristina Kalb[1,2], Yohana Camila A. Frederico[1], Cordula Boehm[3], Claudia Maria do Nascimento Moreira[2,3], Maurilio José Soares[1] & Mark C. Field[3]

Trypanosomatids are parasitic protozoa with a significant burden on human health. African and American trypanosomes are causative agents of Nagana and Chagas disease respectively, and speciated about 300 million years ago. These parasites have highly distinct life cycles, pathologies, transmission strategies and surface proteomes, being dominated by the variant surface glycoprotein (African) or mucins (American) respectively. In African trypanosomes clathrin-mediated trafficking is responsible for endocytosis and post-Golgi transport, with several mechanistic aspects distinct from higher organisms. Using clathrin light chain (TcCLC) and EpsinR (TcEpsinR) as affinity handles, we identified candidate clathrin-associated proteins (CAPs) in *Trypanosoma cruzi;* the cohort includes orthologs of many proteins known to mediate vesicle trafficking, but significantly not the AP-2 adaptor complex. Several trypanosome-specific proteins common with African trypanosomes, were also identified. Fluorescence microscopy revealed localisations for TcEpsinR, TcCLC and TcCHC at the posterior region of trypomastigote cells, coincident with the flagellar pocket and Golgi apparatus. These data provide the first systematic analysis of clathrin-mediated trafficking in *T. cruzi*, allowing comparison between protein cohorts and other trypanosomes and also suggest that clathrin trafficking in at least some life stages of *T. cruzi* may be AP-2-independent.

Transfer of proteins and lipids between intracellular compartments by vesicular transport is a fundamental process and central to many eukaryotic cellular functions[1]. Multiple compartments and pathways comprise the exo- and endocytic arms of the endomembrane system. Transport between these compartments involves budding of protein-coated vesicles from donor membranes, a process essential for cargo sorting[2]. One of the best characterised coat proteins is clathrin[3,4]. Assembly of clathrin into lattices in higher eukaryotes serves to select cargo proteins, in part by incorporation of cargo receptor complexes and proteins into the growing clathrin coat. Lattice formation also facilitates membrane deformation and clathrin participates in sorting at the plasma membrane, endosomes and *trans* face of the Golgi complex, contributing in a wide range of individual sorting and transport events[5,6].

In Saccharomyces *cerevisiae* over 60 proteins are transiently associated with endocytic sites, in a highly dynamic and orchestrated process consistent with clathrin-mediated endocytosis (CME) as tightly regulated and modular[7,8]. Similarly, in mammalian cells over 40 proteins are recruited in a precise sequence to CME sites[9]. A network initially assembles around FCHO proteins, phosphatidylinositol 4,5-phosphate and receptors at the plasma membrane, and rapidly recruits adaptor proteins including DAB2, eps15 and intersectin[10]. AP complexes, Epsin, AP180 and many other cargo receptors are incorporated into the clathrin lattice. Dynamins are recruited by the accessory proteins amphiphysin, sorting nexin-9 and/or intersectin to the neck of the vesicle to enact membrane scission on GTP hydrolysis, whereas auxilin and the ATPase Hsc70 are involved in clathrin uncoating. The CME protein requirement is variable between cell types, suggesting adaptation to the ligands endocytosed and specific dynamic requirements, although the precise relationships between the proteins mediating CME and function are not always clear[8].

[1]Laboratory of Cell Biology, Instituto Carlos Chagas/Fiocruz-PR, Rua Prof. Algacyr Munhoz Mader 3775, Cidade Industrial, 81350-010 Curitiba, PR Brazil. [2]Laboratory of Molecular Biology of Trypanosomes, Instituto Carlos Chagas/ Fiocruz-PR, Rua Prof. Algacyr Munhoz Mader 3775, Cidade Industrial, 81350-010 Curitiba, PR Brazil. [3]School of Life Sciences, University of Dundee, Dundee, DD1 5EH, UK. Correspondence and requests for materials should be addressed to M.J.S. (email: maurilio@fiocruz.br) or M.C.F. (email: mfield@mac.com)

In trypanosomatids, a group of pathogenic protozoa afflicting much of the world's population, clathrin-based trafficking represents an important interface with the host and plays multiple roles in immune evasion and host cell invasion vital for effective infection and persistence[11]. The American trypanosome, *Trypanosoma cruzi,* is both a hemoflagellate and intracellular pathogen and causes Chagas disease in South and Central America[12]. All evidence is consistent with clathrin-mediated endocytosis (CME) being restricted to the flagellar pocket, a common feature of trypanosomatids[13].

Membrane transport is well characterised in African trypanosomatids and lacks multiple proteins that are otherwise widely conserved. This includes the AP-2 complex, a major mediator of clathrin sorting in endocytic systems many organisms[14–16]. More broadly, several proteins, including FCHO, Epsin and several monomeric adaptor proteins are restricted to animals or animals and fungi. These divergent features result in a predicted clathrin network for trypanosomes that is rather sparse, suggesting either massive simplification, extreme sequence divergence preventing *in silico* identification or the presence of alternate components[16]. Significantly, many clathrin-associated proteins, or CAPs, are present in parasitic protozoa, of which several are trypanosomatid specific[17–19].

Many observations indicate the presence of distinct compartments and structures within the *T. cruzi* endomembrane system which are distinct from African relatives, indicating that comparative analysis between trypanosomes is of significance. For example a feature differentiating *T. brucei* and *T. cruzi* is clathrin-independent endocytosis, that in the latter operates mainly through the cytostome/cytopharynx[20,21]. This structure is an invagination of the plasma membrane close to the flagellar pocket and which penetrates deep into the cytoplasm, frequently terminating at the posterior end of the cell and distal to the nucleus[22–24]. Interestingly, clathrin is found at the contractile vacuole complex in *T. cruzi*[25] similar to *Dictyostelium discoideum*[26,27], while AP180, a clathrin assembly protein, is also present in *T. cruzi* clathrin coated vesicles[25]. Uptake of extracellular material is restricted to the flagellar pocket and the cytostome in epimastigotes[28,29], but in trypomastigotes, which lack a cytostome, endocytosis appears to be largely absent[30]. Molecules ingested through the cytostome are internalized by endocytic vesicles, and it has been proposed that cargo enters the cytostome and passes through an early endosomal network before storage or degradation in reservosomes[29]. However, it has been also suggested that endocytic vesicles derived from the cell surface transfer their contents directly to the reservosome without passing through any intermediate compartments[31]. The presence of orthologs of Rab proteins associated with early and intermediate endosomes of other organisms in *T. cruzi* argues for a complex endomembrane system, and this matter has yet to be resolved.

Overall, these observations indicate considerable morphological and mechanistic divergence between the trafficking systems of trypanosomes and their hosts within trypanosome lineages. Here we characterised the clathrin interactome of *T. cruzi* using affinity isolation/proteomics in epimastigotes expressing fusion protein forms of clathrin light chain or EpsinR. Over 30 distinct proteins were identified, several of which are novel and/or trypanosome-specific. These data provide the first proteomic analysis of clathrin-mediated trafficking in *T. cruzi* and allow a detailed comparison of this protein cohort with other trypanosomes and the host.

Results

Isolation of clathrin-interacting proteins from *Trypanosoma cruzi*.
To initiate a systematic and unbiased identification of proteins interacting with the clathrin in *T. cruzi* we created transgenic epimastigotes harbouring epitope-tagged forms of the clathrin light chain (CLC) and EpsinR, both of which interact with the clathrin heavy chain. Both were tagged at the N-terminus, and expressed in cells as GFP::TcEpsinR or Protein A::TcCLC.

Initially, using TcCLC as affinity handle, coupled with cryomilling, we identified a large cohort of candidate interacting proteins using label-free proteomics. Cryomilling provides a robust method by which one can preserve protein-protein interactions in the cell and has been applied to many organisms and systems (see Obado *et al.*, 2016 for an example in trypanosomes). Analysis of these complexes by 1D SDS-PAGE and visualisation by Silver staining indicated multiple co-isolated proteins (Fig. 1). Significantly, a prominent band was observed at ~200 kDa in the electrophoretogram, and which was subsequently identified as the clathrin heavy chain by Western blotting with monoclonal antibody to TcCHC[21] and subsequently by mass spectroscopy (Fig. 1A, Table 1). Neither TcCLC or TcCHC were detected in control isolates. Following mass spectrometric analysis of these isolations and comparisons with the untagged control, we observed that the affinity-tagged isolations included both conserved and novel clathrin-associated proteins (CAPs) (Table 1). Similar protein profiles were obtained in two independent immunoprecipitations for TcCLC and three for TcEpsin, indicating that the isolation procedure was reproducible and thus likely robust.

Peptide sequences predicted by MS were used to query the *T. cruzi* predicted proteome in order to identify proteins that copurified with Protein A::TcCLC. Besides TcCHC (TcCLB.506167.50), over 30 additional proteins were identified (Table 1). Amongst these were TcEpsinR, subunits of the AP-1 and AP-4 complexes and AP180. We applied a cutoff criterion of five-fold greater emPAI score in the test versus the control isolation, together with an exclusion of 0.1 emPAI (see Supplementary data for full MS reporting). The vast majority of proteins was identified in both replicates, with the exception of some low abundance SNARE and Rab proteins and dynamin (TcCLB.508153.20). This latter protein is a frequent contaminant in membrane fractions[32] and whilst it may be involved in endocytic functions, it is unclear from these data.

The second highest ranked protein in the TcCLC isolation was the *T. cruzi* ortholog of EpsinR. Tagging of this protein with GFP at the N-terminus to produce GFP::TbEpsinR and immunofluorescence using anti-GFP and anti-clathrin heavy chain monoclonal antibody demonstrated significant colocalisation for these two proteins, at the anterior region of the cell and close to the flagellar pocket (Fig. 1B). Whilst the resolution of light microscopy is insufficient to confirm a direct interaction, these data do indicate that TcEpsinR and TcCLC have the potential
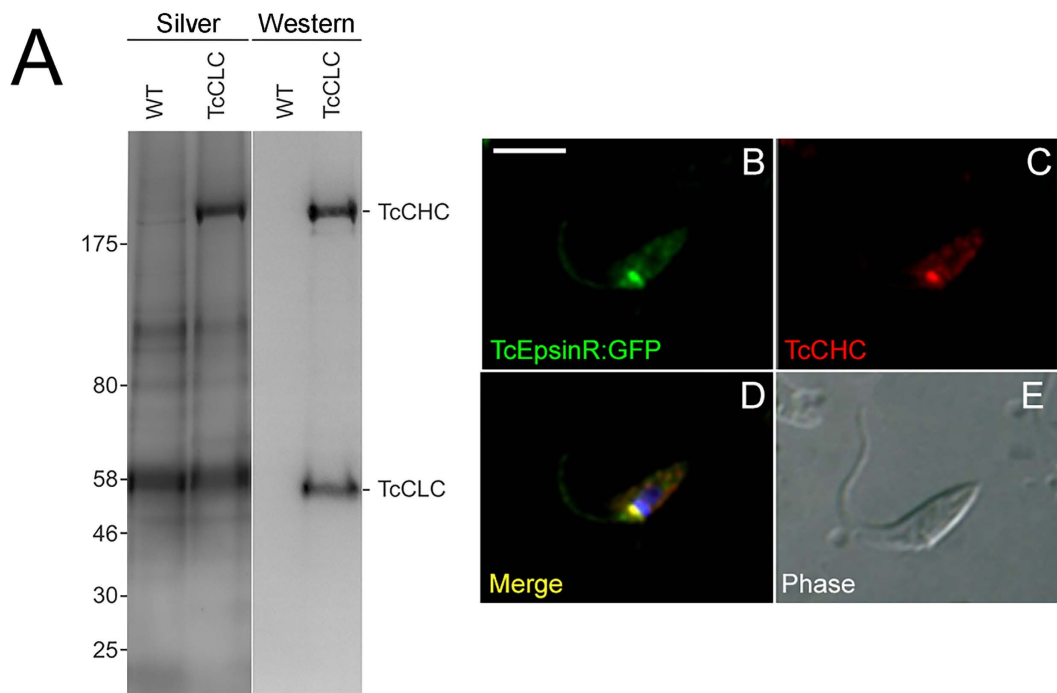
Figure 1. Immunoprecipitation of *T. cruzi* clathrin-associated proteins (TcCAPs). Panel (**A**) Protein complexes isolated by immunoprecipitation from cryolysates of *T. cruzi* epimastigotes expressing Protein A:TcCLC (+) using Dynabeads M280 coupled to sheep anti rabbit-IgG were resolved by 4–12% gradient SDS-PAG. Wild-type cell lysate (WT) was used as a negative control. Coomassie staining showed the presence of a prominent 192 kDa band (TcCHC), but not in the negative control. Visualization of TcCHC (192 kDa) was by reaction with a monoclonal antibody against TcCHC and the visualization of TcCLC/AC (55 kDa) was by reaction with an anti-rabbit secondary antibody, which has affinity for protein A. Panels (**B–E**) Immunocolocalization of clathrin heavy chain (TcCHC) and TcEpsinR in *Trypanosoma cruzi* epimastigotes. Nucleus and kinetoplast DNA were stained with Hoechst 33342.Transfected epimastigote expressing EpsinR-GFP incubated with antibody against GFP (TcEpsinR) and TcCHC monoclonal antibody (clathrin). Note co-localization of the GFP and TcCHC signals (**D**). (**E**) Differential interference contrast (DIC) image of the parasite body. Scale bar 5 μm. Images are representative of n = 10 cells.

to interact, based on proximity, and provides additional support for this connection. This is also consistent with previous work in *T. brucei*[18].

Isolation of TcEpsinR-interacting proteins from *Trypanosoma cruzi*.
To strengthen the evidence that the proteins identified by immuno-isolation of TcCLC complexes are genuine clathrin interaction partners, a reciprocal co-immunoprecipitation was performed using GFP::TcEpsinR. Immunoprecipitation of GFP::TcEpsinR using magnetic beads covalently coupled to llama anti-GFP antibody successfully co-precipitated clathrin heavy and light chains from tagged *T. cruzi* epimastigotes (Fig. 2A). Again LCMS[2] was used to identify the proteins in these complexes using three replicates, and besides TcCHC (TcCLB.506167.50), over 30 additional proteins were confidently identified (Table 2, Fig. 3).

A cohort of endocytic proteins in *T. cruzi*.
It is significant that a great many proteins identified using GFP::CLC and Protein A::EpsinR were in common (Fig. 3). This orthogonal identification supports the hypothesis that these are indeed *bona fide* endocytic proteins in *T. cruzi*. Of these, TcCHC was recovered from all five isolations (two × GFP::CLC and three × Protein A::EpsinR) while TcCLC was also found in all three TbEpsinR isolates. The ortholog of AP180/CALM (TcCLB.503449.30) was recovered from four of five experiments. Together with TcEpsinR these proteins are involved in AP-2-independent clathrin-mediated endocytosis in *T. brucei*[13], and the data here suggest a similar configuration in *T. cruzi*. A clathrin-uncoating protein, the trypanosome auxilin ortholog (TcCLB.510045.30) was also found in four of five independent experiments.

Four candidate clathrin-associated proteins (CAPs) encoded by TcCLB.503595.10 (TcCAP80), TcCLB.507221.70 (TcCAP141), TcCLB.510057.30 (TcCAP37) and TcCLB.507895.170 (TbCAP30) all encode hypothetical proteins (Fig. 3). Apart from a similar structure of predominantly β-sheet at the N-terminus and disordered/α-helical at the C-terminus for TcCAP80 and TcCAP141, these proteins appear quite divergent in secondary structure. All are essentially restricted to trypanosomatids, and even absent from the heterolobosid *Naegleria gruberi*, a sister lineage (Fig. 3). Orthologs of TcCAP80 and TcCAP141 have also been identified in *T. brucei* through affinity isolat using the TbCHC as the affinity handle, and mediate endocytosis and morphological features of the flagellar pocket (Manna *et al.*, 2016 submitted), suggesting that this cohort are also likely *bona fide* players in endocytosis in *T. cruzi*.

Accession	Annotation	Rep 1	Con 1	Rep 2	Con 2
Clathrin					
TcCLB.506167.50	**Clathrin HC**	**268,81**	**0,86**	**54,01**	**0,19**
TcCLB.506211.240	**Clathrin LC**	**15,81**	**0**	**2,17**	**0**
TcCLB.510045.30	**Auxilin**	**2,78**	**0**	**0,5**	**0**
Adaptor complex 1					
TcCLB.508257.260	**AP-1γ**	**1,78**	**0**	**0,68**	**0**
TcCLB.506247.200	**AP-1β**	**1,65**	**0,2**	**0,15**	**0**
TcCLB.510533.40	**AP-1μ**	**0,96**	**0**	**0,53**	**0**
TcCLB.509623.19	**AP-1σ**	**0,36**	**0**	**0**	**0**
Adaptor complex 4					
TcCLB.511751.200	**AP-4ε**	**0,98**	**0**	**0,12**	**0**
TcCLB.506525.104	AP-4σ	0,77	0	0	0
TcCLB.504137.60	AP-4β	0,74	0	0,07	0
TcCLB.509911.70	**AP-4μ**	**0,7**	**0**	**0,11**	**0**
Other adaptors					
TcCLB.506925.70	**EpsinR**	**12,11**	**0,9**	**3,03**	**0**
TcCLB.504105.120	**Tepsin**	**5,7**	**0**	**1,2**	**0**
TcCLB.503449.30	**AP180/CALM**	**1,15**	**0**	**0,24**	**0**
SNAREs					
TcCLB.508465.120	**Syntaxin 16**	**1,15**	**0**	**0**	**0**
TcCLB.508955.10	**Qc**	**0,41**	**0**	**0**	**0**
TcCLB.506855.140	**Vamp7c**	**0**	**0**	**0,25**	**0**
TcCLB.507795.50	**Syntaxin 7**	**0**	**0**	**0,22**	**0**
Rabs					
TcCLB.509805.60	**Rab5**	**0,64**	**0**	**0**	**0**
TcCLB.508461.270	Rab7	0,36	0	0,23	0,11
TcCLB.511621.120	Rab14	0,87	0,46	0,29	0
TcCLB.511711.80	Rab2	0,3	0		
Scission proteins					
TcCLB.508153.20	Dynamin	1,41	0	0	0
Cargo proteins					
TcCLB.511391.180	**GLP-1**	**3,92**	**1,12**	**1,12**	**0,05**
TcCLB.507537.20	Cruzipain	0,53	0	0,13	0
Trypanosome-specific clathrin-associated proteins					
TcCLB.503595.10	**CAP80**	**0,92**	**0**	**0,18**	**0**
TcCLB.507221.70	**CAP141**	**1,81**	**0**	**0,14**	**0**
TcCLB.510057.30	CAP37	0	0	1,25	0
Others					
TcCLB.509319.40	**DUF846**	**0**	**0**	**0,24**	**0**
TcCLB.503791.49	**Vps45**	**1,25**	**0**	**0,1**	**0**

Table 1. TriTrypDB accessions and annotations for TcCLC-associated proteins identified from mass spectrometry. The emPai scores for three independent replicate (Rep) isolations are shown in columns C to F together with concurrent control isolations using cryolysates from untagged cells under the same buffer conditions. Isolation buffer used was 20 mM Hepes 7.4, 250 mM citrate, 0.1% CHAPS, 1 mM MgCl$_2$ 10 μM CaCl$_2$, plus protease inhibitor cocktail. Accessions in bold are in common with the TbEpsinR isolation (Table 2). Only proteins identified with a five-fold greater emPai against the control and greater than 0.1 are shown.

Two heterotetrameric adaptor complexes were recovered with both affinity handles, the AP-1 (TcCLB.508257.260, TcCLB.510533.40, TcCLB.506247.200 and TcCLB.509623.19), which is involved in clathrin-mediated traffic from the Golgi complex and the AP-4 (TcCLB.511751.200, TcCLB.509911.70, TcCLB.504137.60 and TcCLB.506525.104). Significantly, we also recovered Tepsin (TcCLB.504105.120), a central component of AP-4-containing vesicles[33]. This protein is broadly conserved and present in most kinetoplastids except for the *Phytomonas* and *Leishmania* lineages, which significantly also lack the AP-4 complex, evidence that Tepsin is likely also associated with AP-4 in trypanosomatids[34]. In addition, Tepsin represents an additional member of the ANTH/ENTH family of phosphoinositide-binding trafficking proteins, beyond those characterised so far in trypanosomes, i.e. TbEpsinR and TbCALM.

Unexpectedly, we found no evidence in any of our isolations for AP-2, the adaptin complex that in higher eukaryotes associates with clathrin at the plasma membrane. In African trypanosomes this entire complex is absent from the genome[34], but all subunits are present in the *T. cruzi* genome. A trivial explanation is that AP-2
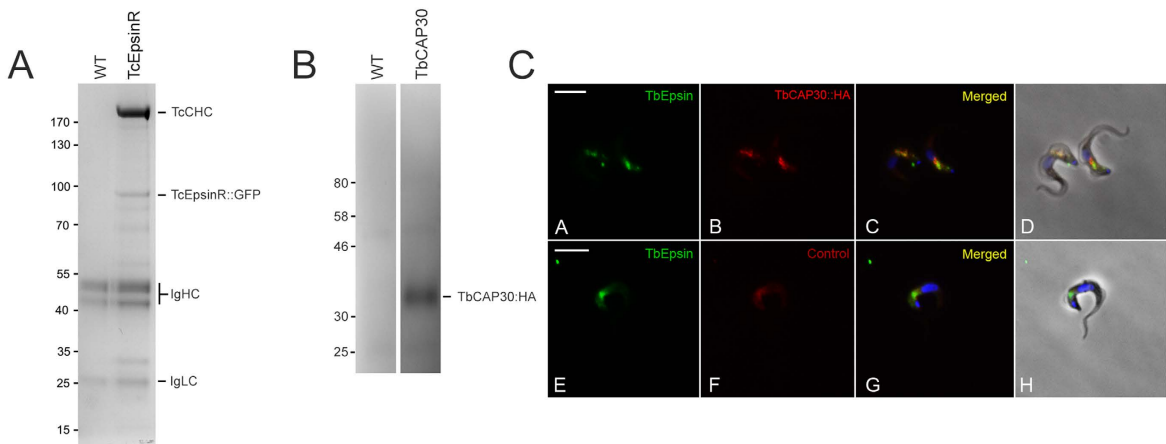
Figure 2. Immunoprecipitation of TcEpsinR-interacting proteins. (Panel **A**) Protein complexes isolated by immunoprecipitation from *T. cruzi* epimastigotes expressing GFP::TcEpsinR (lane2) using Dynabeads M270 coupled to llama anti-GFP and resolved 4–12% SDS-PA. Wild-type cell lysate (WT) was used as control. Coomassie staining showed the presence of the 192 kDa TcCHC, but not in the control. (Panel **B**) Correct tagging of TbCAP30. WT: wild forms of *T. brucei*. TbCAP30: protein extract of *T. brucei* bloodstream forms expressing TbCAP30::HA (Gene ID Tb927.8.7230, 30 kDa). Analysis with anti-HA antibody showed reaction with a polypeptide with molecular mass (33 kDa) compatible with that predicted from the gene sequence in *T. brucei* (30 kDa) plus an HA-tag (3 kDa). (Panel **C**) Immunocolocalization of Tb927.8.7230 and TbEpsinR in *Trypanosoma brucei* bloodstream forms. Transfected bloodstream forms expressing Tb927.8.7230 fused with HA incubated with rat anti-HA antibody (**B,F**) and TbEpsinR polyclonal rabbit antibody (**A,E**); note partial co-localization of the HA and TbEpsinR signals (**C,G**). Nucleus and kinetoplast DNA were stained with Hoechst 33342 (**C,G**). Differential interference contrast (DIC) images of the parasite body (**D,H**). Scale bar 5 μm.

is simply down-regulated in the epimastigote stage. To at least partially approach this question, we analysed the mRNA levels of AP-2 transcripts in epimastigotes and trypomastigotes using qRT-PCR (Fig. 4). AP-2 mRNA was easily detected in both of these life stages, and which is also consistent with a recent transcriptome study of *T. cruzi*[35]. Therefore, it appears that the failure to capture AP-2 in these pullouts is unlikely due simply to an absence of expression, and raises the possibility that CME in *T. cruzi* epimastigotes is, similarly to *T. brucei*, also AP-2 independent.

Five Rab proteins were recovered. TcCLB.509805.60 (Rab5) was recovered by both TcCLC and TcEpsinR; TcCLB.511621.120 (Rab14), TcCLB.508461.270 (Rab7) and TcCLB.511711.80 (Rab2) were isolated only for TcCLC and Rab4 (TcCLB.510911.30) only for TcEpsinR. We also recovered seven SNAREs: TcCLB.506855.140 (SNARE Vamp7c), TcCLB.507795.50 (Syntaxin 7), TcCLB.508465.120 (Syntaxin 16), TcCLB.508955.10 (Qc SNARE) from both TcCLC and TcEpsinR and TcCLB.511627.60 (SNARE VAMP7a), TcCLB.507811.60 (SNARE Vamp7b), TcCLB.506401.130 (Qa-SNARE) only in the TcEpsinR list. Several proteins that are likely cargo, i.e. TcCLB.511391.180, which encodes GLP-1, and TcCLB.507537.20 that encodes cruzipain, were also recovered using both affinity handles (Fig. 3). Finally we also recovered the product of TcCLB.509319.40, a *trans*-membrane-domain protein that is associated with the Golgi complex in *S. cerevisiae*. Significantly orthologs of TcCLB.509319.40 are widely distributed across eukaryotes.

Localisation of *TcCAP30.* From the TcEpsinR isolation we selected the hypothetical protein TcCLB.507895.170, on account of its apparent novelty as a candidate clathrin-associated protein in this protozoan, the fact that it has not previously been localied (unlike CAP80 and CAP141, where this has been done in *T. brucei* (Manna *et al.*, 2016 under revision)) and exclusive presence in trypanosomatids. However, it was more convenient to investigate this protein in *T. brucei* (Tb927.8.7230: TbCAP30, 30 kDa) bloodstream forms, where clathrin localizes to endomembrane compartments restricted to the region between the kinetoplast and nucleus. As the general organisation of the endosomal system of *T. cruzi* is similar, we anticipated that *bona fide* CAP proteins should localize to this region. We determined the location of the gene product TbCAP30 by expression of a C-terminally haemagglutinin (HA)-tagged version of the protein. We verified that the tagged protein had the correct apparent molecular weight (Fig. 2B), and that TbCAP30-HA localized in the region between the nucleus and the kinetoplast, with signal distribution overlapped with TbEpsinR (Fig. 2C). This supports the possibility that TcCAP30 has the potential to interact with clathrin/EpsinR.

Discussion

The surface of infectious organisms forms the interface between the pathogen and host and represents the primary target of immune attack. The trypanosome surface composition[36,37] is highly specialised, and the flagellar pocket constitutes a specific region that facilitates efficient internalization of host macromolecules and restricts

Accession	Annotation	Rep 1	Con1	Rep 2	Con 2	Rep 3	Con 3
Clathrin							
TcCLB.506167.50	**Clathrin HC**	**82,17**	**0**	**26,32**	**0,59**	**21,94**	**0,49**
TcCLB.506211.240	**Clathrin LC**	**1,79**	**0**	**2,61**	**0**	**3,66**	**0,14**
TcCLB.510045.30	**Auxilin**	**0,27**	**0**	**0**	**0**	**0,17**	**0**
Adaptor complex 1							
TcCLB.508257.260	**AP-1γ**	**1,71**	**0**	**1,45**	**0,32**	**1,06**	**0,23**
TcCLB.506247.200	**AP-1β**	**0,88**	**0**	**1,36**	**0**	**0,93**	**0**
TcCLB.510533.40	**AP-1μ**	**0,85**	**0**	**1,22**	**0**	**1,09**	**0,2**
TcCLB.509623.19	**AP-1σ**	**0,36**	**0**	**0,59**	**0**	**0,17**	**0**
Adaptor complex 4							
TcCLB.511751.200	**AP-4ε**	**0,11**	**0**	**0,12**	**0**	**0**	**0**
TcCLB.509911.70	**AP-4μ**	**0,05**	**0**	**0,24**	**0**	**0,11**	**0**
Other adaptors							
TcCLB.506925.70	**EpsinR**	**12,83**	**0**	**17,08**	**0**	**13,59**	**0**
TcCLB.504105.120	**Tepsin**	**0,39**	**0**	**1,2**	**0**	**1,2**	**0**
TcCLB.503449.30	**AP180/Calm**	**0,18**	**0**	**0,12**	**0**	**0**	**0**
SNAREs							
TcCLB.511627.60	VAMP7a	1,26	0	0,59	0	0,26	0
TcCLB.506855.140	**Vamp7c**	**0,74**	**0**	**0,95**	**0**	**0,95**	**0**
TcCLB.507811.60	Vamp7b	0,45	0	0,85	0	0,85	0
TcCLB.507795.50	**Syntaxin 7**	**0,22**	**0**	**0,11**	**0**	**0,22**	**0**
TcCLB.508955.10	**Qc**	**0,22**	**0**	**0,58**	**0**	**0,41**	**0**
TcCLB.506401.130	Qa	0,16	0	0,57	0	0	0
TcCLB.508465.120	**Syntaxin 16**	**0,09**	**0**	**0,53**	**0,09**	**0,29**	**0**
Rabs							
TcCLB.509805.60	**Rab5**	**0**	**0**	**0,64**	**0**	**0,85**	**0**
TcCLB.510911.30	Rab4	0,49	0	0	0	0,49	0
Cargo proteins							
TcCLB.511391.180	**GLP-1**	**0,19**	**0**	**2,77**	**0,42**	**3,5**	**0,42**
Recycling system							
TcCLB.506925.100	SCAMP domain	0,15	0	0	0	0,15	0
Trypanosome specific clathrin-associated proteins							
TcCLB.503595.10	**CAP80**	**0,18**	**0**	**0,28**	**0**	**0,13**	**0**
TcCLB.507221.70	**CAP141**	**0,18**	**0**	**0,26**	**0**	**0,22**	**0**
TcCLB.507895.170	CAP30	0,22	0	0,22	0	0,22	0
Others							
TcCLB.509319.40	**DUF846**	**0,24**	**0**	**0,53**	**0**	**0,53**	**0**
TcCLB.503791.49	**Vps45**	**0,21**	**0**	**0,4**	**0**	**0,47**	**0**

Table 2. TriTrypDB accessions and annotations for TcEpsinR-associated proteins identified from mass spectrometry. The emPai scores for three independent replicate (Rep) isolations are shown in columns C to H together with concurrent control isolations using cryolysates from untagged cells under the same buffer conditions. Isolation buffer used was 20 mM Hepes 7.4, 250 mM citrate, 0.1% CHAPS, 1 mM $MgCl_2$ 10 μM $CaCl_2$, plus protease inhibitor cocktail. Accessions in bold are in common with the clathrin light chain isolation (Table 1). Only proteins identified with a five-fold greater emPai against the control and greater than 0.1 are shown.

access of host immune factors to the exposed, endocytic receptors of the parasite[13,38]. This paradigm is probably common to all pathogenic trypanosomes, but variation in surface molecules indicates fundamental adaptation to the specific demands of the parasite/host interaction. *In silico* analysis suggests that several major proteins of the endocytic pathway characterised in animals and fungi are absent[16].

It remains unknown how much diversity is present between the trypanosomatids, but considering the remarkable differences in lifestyles and surface proteins, adaptations are predicted. For example, *T. cruzi* possesses AP-1 to 4, distinct from *Leishmania* which lacks AP-4 and *T. brucei* lacking AP-2. *T. cruzi* also possesses Rab14, which functions in Golgi to endosome transport[39] and Rab32, which has many roles including phagocytosis[40]; these are additional to the Rab set shared with *T. brucei*[41]. Both Rab14 and Rab32 are present in the last common eukaryotic ancestor, suggesting that *T. brucei* lost these genes, indicating a likely more sophisticated endomembrane system in *T. cruzi*, and providing evidence for significant divergence. Similar variance has been reported in the Apicomplexa[42].
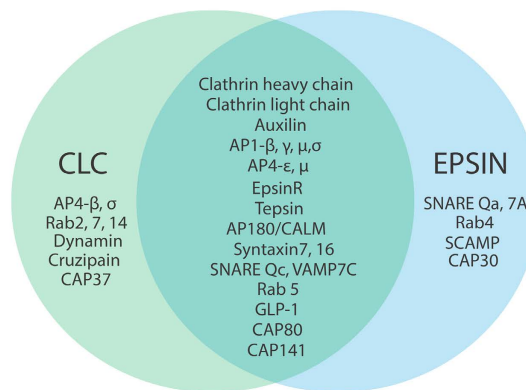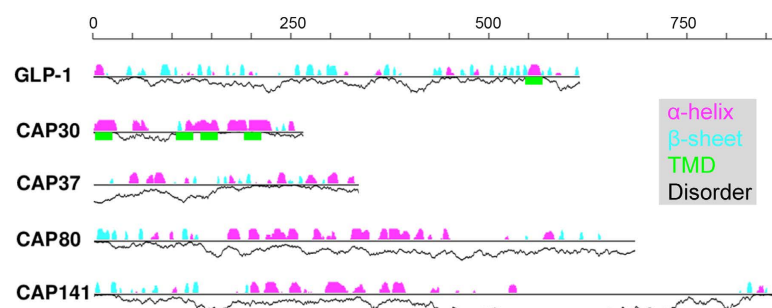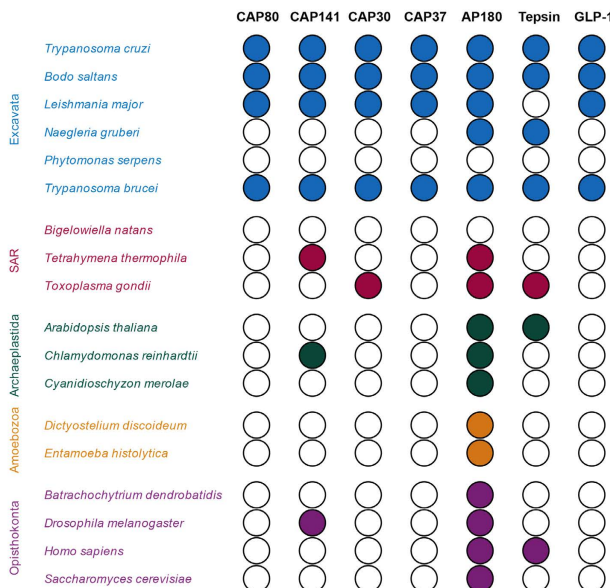
Figure 3. Proteins identified by TcCLC and TcEpsinR. (Panel **A**) Venn diagram of the most significant proteins identified with either GFP::TcCLC or Protein A:TcEpsinR. See also Tables 1 and 2 for statistical data and supplementary data for full information. (Panel **B**) Predicted secondary structures of GLP-1 and TcCAP30, 30, 80 and 141. α and β secondary structure probability is indicated above the line in purple or cyan respectively. *Trans*-membrane domains and disorder probability are shown below the lines in green and as a black line respectively. The scale bar is protein length in amino acid residues. (Panel **C**) Coulson plot of novel proteins identified by proteomics. The genomes of select taxa were searched using reciprocal BLAST, together with manual inspection of the alignment as a test for the presence of an ortholog. Filled circles indicate that a high confidence ortholog was found, and open circles indicate that an ortholog was not identified.
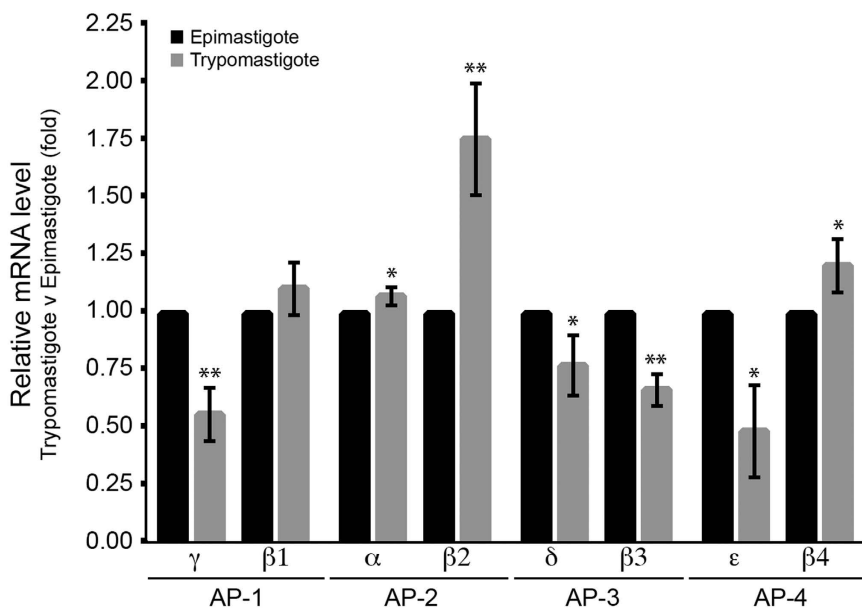
Figure 4. Relative mRNA expression of heavy chain subunits of adaptor complexes AP-1 to 4 in trypomastigote and epimastigote forms of *T. cruzi*. Data normalization for RNA was relative to the telomerase reverse transcriptase (TERT) gene. Epimastigote form level was set at 1.0 and data are presented as mean ($\pm$SD). Data analyses were performed as Livak and Schmittgen, 2001. The asterisks represent significant (*$p < 0.05$) or very significant (**$p < 0.01$) expression level differences between two life stages of each adaptin gene of *T. cruzi*. The experiment was performed in technical triplicate. The sequences of oligonucleotides used in this analysis are given in Table S1.

We exploited two conserved proteins within the clathrin-mediated transport system of *T. cruzi*: the light chain of clathrin (TcCLC) and EpsinR (TcEpsin). We identified cohorts of candidate proteins for both TcCLC and TcEpsinR. The clathrin heavy chain (TcCHC) is the most abundant protein[43] and other candidate interacting partners appear to be sub-stoichiometric, similar to CCV isolations from metazoa and trypanosomes, reflecting promiscuity of clathrin interactions[19,44,45]. A range of additional proteins with clear roles in transport also identified.

Surprisingly AP-2 was not present in any of our isolations. While the genes encoding the four subunits of this adaptor complex are absent from the genome of *T. brucei*[34], they are present in *T. cruzi*[20,41]. We predicted AP-2 to be identified, since this complex facilitates clathrin-mediated endocytosis and the pathway is active in *T. cruzi* epimastigotes[20,21]. Some unicellular organisms, including yeast, can survive without AP-2[46,47] while very rapid neuronal endocytosis is also AP-2 independent[48]. Specific cargo adaptors support clathrin-mediated endocytosis in the absence of AP-2[49], and therefore, the AP-2 complex is not mandatory. For *T. brucei* alternate adaptors, such as TbEpsinR and TbCALM, must support clathrin-mediated endocytosis[13]. Since we failed to recover AP-2, but did identify AP-1 and AP-4, this suggests that the result is likely real and unlikely simply failure to maintain clathrin-AP complexes. Therefore the dominant form of endocytosis in *T. cruzi* may be AP-2 independent, suggesting an unexpected mechanistic similarity to African trypanosomes. This is a surprising finding, potentially unifying AP-2 endocytic mechanisms across a broader range of taxa.

In contrast to AP-2, we recovered all AP-1 subunits with both affinity handles. This complex is mainly associated with transport at the *trans*-Golgi network and late endosomes in mammalian cells[49,50] and *T. brucei*[51,52]. It is possible that AP-1 has related functions in *T. cruzi*, such as targeting lysosomal enzymes like cruzipain and chagasin[53] to reservosomes. It is of interest that cruzipain (TcCLB. 507537.20) was also found and that may represent cargo *en route* to the lysosome[54]. The precise function of AP-4 is not well defined[55], but significantly the ε-subunit of AP-4 complex was also identified in a *T. cruzi* contractile vacuole proteome along with clathrin and AP180[25], also found here. Significantly, we also recovered Tepsin, a central component of AP-4-containing vesicles[33]. Tepsin and AP-4 have coevolved and organisms lacking AP-4 also lack Tepsin[55]. These data robustly confirm these earlier observations for AP-4. Significantly, we also identified orthologs of TbCAP80 and TbCAP141, recently shown to be involved in endocytosis in African trypanosomes (Manna *et al.*, 2016 under revision), suggesting that these proteins are part of a conserved trypanosome-specific endocytic mechanism.

In conclusion, we report an interactome for clathrin for *T. cruzi*. The cohort contains many highly conserved members, but also several trypanosome-specific factors. Taken together with recent evidence from African trypanosomes, these data indicate the presence of divergent mechanisms for clathrin function in these pathogenic protozoa.

Materials and Methods

Parasites. Cultured epimastigote forms of *Trypanosoma cruzi*, clone Dm28c[56], were grown at 28 °C with weekly passages in liver infusion tryptose (LIT) medium[57] supplemented with 10% fetal bovine serum (FBS).

T. brucei bloodstream forms (BSF) strain 427 were maintained in HMI-9 medium supplemented with 10% fetal bovine serum. Cells were subcultured when cell density reached a maximum of 2×10^6 cells.

Cloning and expression of *Trypanosoma cruzi* TcCLC and TcEpsinR.

To generate transgenic epimastigotes stably expressing TcCLC (Clathrin Light Chain, TcCLB.506211.240) with a protein A and C amino-terminal fusion (TcCLC/AC), TcCLC cDNA was cloned into the pTcGWPTP expression vector. The pTcGWPTP vector encodes proteins A and C and is a modification of the previously described pTcGWGFP vector[58]. The TcCLC gene was used to design forward (5′-ATGGACCCTTTTGAAGGAAGC-3′) and reverse (5′-TTATTGAGCGGTTTCGCCCT-3′) primers flanked by sequences compatible with the Gateway (Invitrogen, USA) cloning platform to enable subsequent subcloning into the target vector. The resulting pTcGWPTP plasmid encoding the TcCLC gene fused to proteins A and C was used to transfect parasites.

To generate transfected *T. cruzi* epimastigotes expressing TcEpsinR (epsin-related) with a GFP amino-terminal fusion (TcEpsinR/GFP), TcEpsinR cDNA (TcCLB.506925.70) was cloned into the pTcG-WGFP expression vector with resistance to neomicin[58]. This vector was kindly provided by Dr. Michel Batista, Instituto Carlos Chagas/Fiocruz-Paraná, Brazil). The TcEpsinR gene was used to design forward (5′-TCATGAGTATTCCAACCTCCATTCA-3′) and reverse (5′-CCCTCAGACTGTCGGCGCT-3′) primers flanked by sequences compatible with the Gateway cloning platform to enable subsequent subcloning into the target vector (Invitrogen, USA). The resulting pTcGWGFP plasmid encoding the TcEpsinR gene fused to GFP protein was used to transfect parasites.

T. cruzi transfection.

T. cruzi epimastigote cultures were grown at 28 °C in LIT medium supplemented with 10% FBS to a density of approximately 3×10^7 cells/ml. Parasites were then harvested by centrifugation at 3,000 g for 5 min at room temperature, washed once in phosphate-buffered saline (PBS, pH 7.2) and resuspended in 0.4 ml of electroporation buffer (140 mM NaCl, 25 mM HEPES, 0.74 mM Na_2HPO_4, pH 7.5) at a density of 1×10^8 cells/ml. Cells were then transferred to a cuvette (0.2 cm gap width) and 10-15 μg DNA was added. The mixture was placed on ice for 10 min and then subjected to two pulses of 450 V/500 μF using the Gene Pulser II (Bio-Rad, Hercules, CA, USA). Following electroporation, cells were cultured in 10 ml LIT medium containing 10% FBS and incubated for 24 h at 28 °C. The antibiotic G418 (500 μg/ml) was then added to the culture medium and stable, resistant cells were obtained approximately 20 days after transfection. Stably transfected cells were maintained in cultures containing 250 μg/ml G418.

One-step PCR-mediated transfection of *T. brucei* BSF cells for *in-situ* tagging.

To generate transfected *T. brucei* BSF cells expressing TbCAP30 with a 3xHA carboxy-terminal fusion (TbCAP30/HA), TbCAP30 cDNA (Tb927.8.7230) was cloned into the pMOTag2H (kindly provided by George Cross, Addgene plasmid #26296) with a puromycin selectable marker and a 3xHA-tag[59]. The TbCAP30 gene sequence was used to design forward (5′-GTTGACGTTGACCGTGTTTACGTACCAGGGACGGTGGAGGCCGCTAAGGC GCTCGGCACTTCTGAGAAGCAGGGGTACAATGCGGTTGTTGGTACCGGGCCCCCCCTCGAG-3′) and reverse (5′-TGCCCATTTCAACCGCTTTCACTGCTTGCCCTTTCCCTTTTCCCCTCTTTCTTTATATAT ATATATATATCCCCAACCTTCCTCGAAGTGGCGGCCGCTCTAGAACTAGTGGAT-3′) primers. By using one-step PCR the 3′ UTR of the target gene was replaced by a heterologous intergenic region. This replacement directs the correct splicing of the downstream antibiotic resistance marker.

T. brucei transfection: At a cell density of $1.0–1.5 \times 10^6$ cells/ml, 3.5×10^7 BSF were harvested by centrifugation for 10 minutes, 800 g at 4 °C. The supernatant was removed and the cells resuspended in 100 μl of Amaxa buffer (Lonza; Basel, Switzerland), mixed with 30 μg of ethanol precipitated linear PCR product and transferred into a sterile cuvette. Electroporation was performed using an Amaxa Nucleofector II (Lonza) as described. Cells were immediately transferred into pre-warmed HMI-9 and cultured at 37 °C to recover. After 6 hours, the antibiotic puromycin (2 μg/ml) was added and the cells were transferred to 24 well plates to enable the isolation of clonal-antibiotic resistant populations after 7–14 days, and were further expanded in continuous presence of antibiotic.

Immunofluorescence in *T. cruzi*.

For colocalisation of endogenous TcCHC (clathrin heavy chain) with exogenously expressed TcEpsin/GFP in transfected *T. cruzi* epimastigotes, 3-day-old cells were washed twice with PBS, fixed for 30 min with 4% paraformaldehyde and adhered to poly-L-lysine coated slides and incubated for 1 h at 37 °C with anti-GFP antibody (1:100) and TcCHC monoclonal antibody[21]. After three washes in PBS, the samples were incubated under the same conditions with a secondary Alexa Fluor 488-conjugated goat anti-rabbit antibody (1:600) and an Alexa Fluor 594-conjugated anti-mouse antibody (1:600). A negative control was performed by incubating anti-GFP antibody with wild-type epimastigotes (data not shown). Nuclear and kinetoplast DNA were stained with Hoechst 33342. After extensive washes, the slides were prepared with mounting medium containing N-propyl-gallate as an anti-fade agent. The samples were examined using a Leica SP5 confocal laser-scanning microscope (Leica Microsystems, Mannheim, Germany) at the Microscopy Facility of the Carlos Chagas Institute, Fiocruz-PR. Acquired images were processed for presentation using Adobe Photoshop CS5 (Adobe Systems Incorporated, USA).

Immunofluorescence in *T. brucei*.

Mid-log phase cells were harvested and washed with Voorheis' PBS (PBS supplemented with 10 mM glucose and 46 mM sucrose, pH 7.6: vPBS). The cells were subsequently fixed in 4% paraformaldehyde (w/v) and adhered to poly-L-lysine coated slides. For permeabilization and staining of internal structures, cells were incubated with 0.1% Triton X-100 (v/v) in vPBS, washed with vPBS and blocked with 20% fetal bovine serum in PBS. For co-staining, the fixed cells were incubated with a polyclonal rabbit anti-serum anti-TbEpsinR conjugated to AlexaFluor 488 and a rat antibody against HA conjugated to AlexaFluor 594.

The slides were dried and mounted with a drop of Vectashield supplemented with 4,6-diamidino-2-phenylindole (DAPI) (Vector Laboratories, USA) to stain DNA. Images were acquired on a Nikon Eclipse E600 epifluorescence microscope with a Hammamatsu ORCA CCD camera and images captured using Metamorph software. Final processing for presentation was done using Adobe Photoshop CS5 (Adobe Systems Inc.).

Cryomilling.   To identify the proteins associated with clathrin in coated vesicles, *T. cruzi* epimastigotes expressing TcCLC/AC, *T. cruzi* epimastigotes expressing TcEpsinR/GFP and *T. cruzi* wild-type epimastigotes were submitted to cryomilling with subsequent immunoprecipitation of associated complexes[32]. This method requires substantial quantities of starting material, but allows retention of protein-protein interactions not otherwise preserved. Briefly, a total of 5×10^{10} cells were harvested by centrifugation at 3000 g for 10 s and the cells snap frozen in liquid nitrogen and milled using a ball mill in liquid nitrogen (Retsch Planetary Ball Mill PM100, Haan, Germany) to produce a cryogrindate, under essentially native conditions.

Immunoprecipitation and identification of TcCLC associated proteins by mass spectrometry (MS).   A total of 350 μg of cell powder was resuspended in 1 ml of CHC buffer (20 mM Hepes 7.4, 250 mM citrate, 0.1% CHAPS, 1 mM $MgCl_2$ 10 μM $CaCl_2$, plus protease inhibitor cocktail) and complexes were subsequently bound to 350 μl of Dynabeads M280 coupled to sheep anti rabbit-IgG (Life Technologies, USA). A grindate prepared from wild type cells was used as a negative control. After incubation the beads were washed in the same buffer and eluted in 50 μl of elution buffer (20 mM Tris pH 8, 2% SDS) for 30 min at 72 °C. From the supernatant 5 μl were used to SDS-PAGE, stained with Coomassie and 5 μl Western blotted. To the remaining 40 μl, 427 μl of ethanol was added and incubated for 16 h at −20 °C and then the sample was centrifuged at 20,000 g for 30 minutes at 4 °C. The resulting pellet was analysed by LCMS[2].

Reverse co-immunoprecipitation (TcEpsinR/GFP).   Immunoprecipitation using a llama polyclonal anti-GFP antibody was performed using *T. cruzi* epimastigotes expressing TcEpsinR/GFP. For TcEpsinR immunoisolation, 350 μg of cell grindate was ressuspended in CHC Buffer and complexes were subsequently bound to 35 μl of Dynabeads M270 epoxy coupled to llama anti-GFP. After incubation the beads were washed in the same buffer and then processed as described above.

Mass spectrometry.   Liquid chromatography tandem mass spectrometry (LC-MS/MS) was performed by the Proteomic Facility at the University of Dundee. To separate proteins for mass spectrometry analysis, the samples were run 2 cm on a 10% SDS gel (NuPAGE® Bis-Tris 10% gels, Novex by Life Technologies) in a 1× MOPS SDS running buffer, fixed and stained with Coomassie. The selected 2 cm gel piece was excised and in-gel tryptic digestion (Trypsin, Modified Sequencing Grade, Roche) was carried out for 16 h at 37 °C. Peptides were extracted with 0.1% trifluoroacetic acid in 50% acetonitrile and dried in a SpeedVac. Peptides were then resuspended in 1% formic acid, centrifuged (13,000 rpm, 1 min) and transferred to an HPLC (high performance liquid chromatography) vial. Usually, 5 μl of this suspension was analysed. Samples were analysed using an Ultimate 3000 RSLC nano system coupled on-line to a LTQ OrbiTrap Velos Pro equipped with an Easy-Spray source (Thermo Scientific). Peptides were initially trapped and desalted using an Acclaim® PepMap100 C18 Nano-trap column (100 μM × 2 cm) with 0.1% formic acid (buffer A). After 3 min, a wash gradient was formed to separate the peptides using a 180 min gradient on an Easy-Spray PepMap RSLC C18 column (75 μM × 50 cm). Samples were transferred to the mass spectrometer via an Easy-Source with the temperature set at 50 °C and a source voltage of 1.9 kV. The mass spectrometer was operated in standard data dependent acquisition mode. Survey full scan MS spectra were acquired with a resolution of 60,000 at m/z 335-1800. The AGC was set to 1×10^6 and an ion trap Msn target value of 5000 was used. The top 15 most intense ions were targeted for CID fragmentation (2 Da isolation window), with normalized collision energy of 35% in the linear ion trap. The dynamic exclusion time window was set to 45 sec, with an isowidth of 2 Da. Once part of the mass range has been excluded for the set time it is released again[60]. Lock mass of 445.120024 was enabled for all experiments.

The mass spectra was analyzed using the Mascot search engine tool (Version 2.3.2) (http://www.matrixscience.com/) against the database of protein sequences from *T. cruzi* UniProt (54,500 sequences) of five different strains of *T. cruzi* (CL Brener Esmeraldo-like, CL Brener non Esmeraldo-like, Sylvio, Dm28c and Marinkellei). This strategy was used to increase the coverage of identified peptides. The abundance of proteins was deduced from the total number of MS /MS spectra generated from the same related peptides[61]. The approximate relative quantification of these proteins in complex was estimated in label-free mode and through the exponentially modified protein abundance index (emPAI)[62].

Relative quantitative real time (qRT)-PCR.   Total RNA was extracted using the RNeasy mini kit (Qiagen) according to the manufacturer's instructions along with DNase treatment and quantified using a ND-1000 spectrophotometer and Nanodrop software (Nanodrop Technologies). For cDNA synthesis, 2 μg RNA was diluted to 10 μl with diethylpyrocarbonate (DEPC)-treated water and denatured at 70 °C, 5 min. 15 μl of a reaction mix was added (2.5 μl dNTPs (25 mM stock), 5 μl 5× reverse transcription buffer (Invitrogen), 2 μl 100 mM DTT, 0.5 μl RNAseOUT (recombinant ribonuclease inhibitor, 5000 U/μl, Invitrogen), 2 μl oligo dT, (T_{30}VN, 10 μM stock) 0.5 μl Superscript II Reverse Transcriptase (200 U/μl Invitrogen), and 2.5 μl DEPC-treated water and incubated at 37 °C for 1 hr, heat-inactivated at 90 °C, 5 min and finally diluted to 200 μl with DEPC-treated water. For qRT-PCR, 5 μl of cDNA was used in a 25 μl reaction including IQ SYBR Green Supermix (BioRad) with 0.4 μM gene-specific forward and reverse primers. qRT-PCR reactions were performed in white thin wall polypropylene multiplate 48-well unskirted PCR plates (BioRad) sealed with microseal 'B' adhesive (BioRad). Reactions were performed in a BioRad MiniOpticon real time PCR detection system and included an initial denaturation at 95 °C for 3 min, 40 cycles of 95 °C 30 seconds, 58 °C 30 sec, 72 °C 30 sec (with a signal read at the end of each cycle). In each amplification step, a non-template control was subjected to the reaction to ensure that there was no contamination.

Comparative genomics. The predicted sequences of TcCLC and TcEpsinR-associated proteins were obtained using the Tritryp database (http://tritrypdb.org/tritrypdb/). AP180, CAP30, CAP37, CAP80, CAP141, GLP-1 and Tepsin were selected as query sequences in DELTA-BLAST interrogations. A broad range of 18 eukaryotic genomes was inspected: *Arabidopsis thaliana, Batrachochytrium dendrobatidis, Bigelowiella natans, Bodo saltans, Chlamydomonas reinhardtii, Cyanidioschyzon merolae, Dictyostelium discoideum, Drosophila melanogaster, Entamoeba histolytica, Homo sapiens, Leishmania major, Naegleria gruberi, Phytomonas serpens,* Saccharomyces cerevisiae, *Tetrahymena thermophilia, Toxoplasma gondii, T. brucei* and *T. cruzi,* spanning this domain diversity at NCBI (http://www.ncbi.nlm.nih.gov/BLAST/). The best returned candidate orthologs were recipriocal BLASTed against the protein database of *T. cruzi.* Proteins that retrieved the original query sequence were further considered, taking into account the presence of conserved domains using pfam and NCBI CDDB with default parameters. Lastly, both query and subject sequences were aligned with Clustal in order to access identity and to inspect for homology across the entire predicted sequence. Data are displayed as a Coulson plot using Coulson Plot Generator v1.4.7[63].

References

1. Bock, J. B., Matern, H. T., Peden, A. A. & Scheller, R. H. A genomic perspective on membrane compartment organization. *Nature.* **409,** 839–841 (2001).
2. Nakatsu, F., Hase, K. & Ohno, H. The role of the clathrin Adaptor AP-1: polarized sorting and beyond. *Membranes* (*Basel*). **4,** 747–763 (2014).
3. Kirchhausen, T. Clathrin. *Annu Rev Biochem.* **69,** 699–727 (2000).
4. Doherty, G. J. & McMahon, H. T. Mechanisms of endocytosis. *Annu Rev Biochem.* **78,** 857–902 (2009).
5. Brodsky, F. M. Diversity of clathrin function: new tricks for an old protein. *Annu Rev Cell Dev Biol.* **28,** 309–336 (2012).
6. Robinson, M. S. Forty Years of Clathrin-coated Vesicles. *Traffic.* **16,** 1210–1238 (2015).
7. Kaksonen, M., Toret, C. P. & Drubin, D. G. A modular design for the clathrin–and actin-mediated endocytosis machinery. *Cell.* **123,** 305–320 (2005).
8. Schmid, E. M. & McMahon, H. T. Integrating molecular and network biology to decode endocytosis. *Nature.* **448,** 883–888 (2007).
9. Taylor, M. J., Perrais, D. & Merrifield, C. J. A high precision survey of the molecular dynamics of mammalian clathrin-mediated endocytosis. *PLoS Biol.* **9,** e1000604 (2011).
10. Praefcke, G. J. *et al.* Evolving nature of the AP2 alpha-appendage hub during clathrin-coated vesicle endocytosis. *EMBO J.* **22,** 4371–4383 (2004).
11. Barrias, E. S., de Carvalho, T. M. & De Souza, W. *Trypanosoma cruzi*: Entry into Mammalian Host Cells and Parasitophorous Vacuole Formation. *Front Immunol.* **4,** 186 (2013).
12. Mandal, S. Epidemiological Aspects of Chagas Disease–a Review. *J Anc Dis Prev Rem.* **2,** 117–224 (2014).
13. Manna, P. T., Gadelha, C., Puttick, A. E. & Field, M. C. E/ANTH domain proteins participate in AP2-independent clathrin-mediated endocytosis. *J Cell Sci.* **128,** 2130–2142 (2015).
14. Morgan, G. W., Goulding, D. & Field M. C. The single dynamin-like protein of *Trypanosoma brucei* regulates mitochondrial division and is not required for endocytosis. *J Biol Chem.* **279,** 10692–10701 (2004).
15. Field, M. C. & Carrington, M. The trypanosome flagellar pocket. *Nat Rev Microbiol.* **7,** 775–786 (2009).
16. Field, M. C., Adung'a, V., Obado, S., Chait, B. T. & Rout, M. P. Proteomics on the rims; insights into the biology of the nuclear envelope and flagellar pocket of trypanosomes. *Parasitology.* **139,** 1158–1167 (2012).
17. Berriman, M. *et al.* The architecture of variant surface glycoprotein gene expression sites in *Trypanosoma brucei. Mol Biochem Parasitol.* **122,** 131–140 (2002).
18. Gabernet-Castello, C., Dacks, J. B. & Field, M. F. The single ENTH-domain protein of trypanosomes: endocytic functions and evolutionary relationship with epsin. *Traffic.* **10,** 894–911 (2009).
19. Adung'a, V. O., Gadelha, C. & Field, M. C. Proteomic analysis of clathrin interactions in trypanosomes reveals dynamic evolution of endocytosis. *Traffic.* **14,** 440–457 (2013).
20. Corrêa, J. R., Atella, G. C., Menna-barreto, R. S. & Soares, M. J. Clathrin in *Trypanosoma cruzi:* in silico gene identification, isolation, and localization of protein expression sites. *J Euk Microbiol.* **54,** 297–302 (2007).
21. Kalb, L. C. *et al.* Clathrin expression in *Trypanosoma cruzi. BMC Cell Biol.* **19,** 15–23 (2014).
22. Vataru-Nakamura, C., Ueda-Nakamura, T. & De Souza, W. Visualization of the cytostome in *Trypanosoma cruzi* by high resolution field emission scanning electron microscopy using secondary and backscattered electron imaging. *FEMS Microbiol Lett.* **242,** 227–230 (2005).
23. Ramos, T. C., Freymüller-Haapalainen, E. & Schenkman, S. Three-dimensional reconstruction of *Trypanosoma cruzi* epimastigotes and organelle distribution along the cell division cycle. *Cytometry A.* **79,** 538–544 (2011).
24. Alcantara, C. L., Vidal, J. C., De Souza, W. & Cunha-E-Silva, N. L. The three-dimensional structure of the cytostome-cytopharynx complex of *Trypanosoma cruzi* epimastigotes. *J Cell Sci.* **15,** 2227–2237 (2014).
25. Ulrich, P. N. *et al.* Identification of contractile vacuole proteins in *Trypanosoma cruzi. PLoS One.* **18,** e18013 (2011).
26. O'Halloran, T. J. & Anderson, R. G. Clathrin heavy chain is required for pinocytosis, the presence of large vacuoles, and development in Dictyostelium. *J Cell Biol.* **118,** 1371–1377 (1992).
27. Stavrou, I. & O'Halloran, T. J. The Monomeric Clathrin Assembly Protein, AP180, Regulates Contractile Vacuole Size in *Dictyostelium discoideum. MolBiol Cell.* **17,** 5381–5389 (2006).
28. De Souza, W., Sant'anna, C. & Cunha-e-Silva, N. L. Electron microscopy and cytochemistry analysis of the endocytic pathway of pathogenic protozoa. *Progress Histochem Cytochem.* **44,** 67–124 (2009).
29. Porto-Carreiro, I., Attias, M., Miranda, K., De Souza, W. & Cunha-e-Silva, N. *Trypanosoma cruzi* epimastigotes endocytic pathway: cargo enters the cytostome and passes through an early endosomal network before storage in reservosomes. *Eur J Cell Biol.* **79,** 858–869 (2000).
30. Corrêa, A. F., Andrade, L. R. & Soares, M. J. Elemental composition of acidocalcisomes of *Trypanosoma cruzi* bloodstream trypomastigote forms. *Parasitol Res.* **88,** 875–880 (2002).
31. Soares, M. J. The reservosome of *Trypanosoma cruzi* epimastigotes: an organelle of the endocytic pathway with a role on metacyclogenesis. *Mem Inst Oswaldo Cruz.* **1,** 139–141 (1999).
32. Obado, S. *et al.* Interactome mapping to reveal deep evolutionary events: The trypanosome nuclear pore complex possesses distinct features overlaying a conserved structural core. PLoS Biology (in the press) (2016).
33. Borner, G. H. *et al.* Multivariate proteomic profiling identifies novel accessory proteins of coated vesicles. *J Cell Biol.* **197,** 141–160 (2012).
34. Manna, P. T., Kelly, S. & Field, M. C. Adaptin evolution in kinetoplastids and emergence of the variant surface glycoprotein coat in African trypanosomatids. *Mol Phylogenet Evol.* **67,** 123–128 (2013).
35. Smircich, P. *et al.* Ribosome profiling reveals translation control as a key mechanism generating differential gene expression in *Trypanosoma cruzi. BMC Genomics.* **16,** 443–457 (2015).
36. Gadelha, C. *et al.* Architecture of a host-parasite interface: complex targeting mechanisms revealed through proteomics. *Mol Cell Proteomics.* **14,** 1911–1926 (2015).

37. Shimogawa, M. M. *et al.* Cell surface proteomics provides insight into stage-specific remodeling of the host-parasite interface in *Trypanosoma brucei. Mol Cell Proteomics*. **14,** 1977–1988 (2015).
38. Schwede, A., Macleod, O. J., MacGregor, P. & Carrington, M. How Does the VSG Coat of Bloodstream Form African Trypanosomes Interact with External Proteins? *PLoS Pathog*. **11,** e1005259 (2015).
39. Junutula, J. R. *et al.* Rab14 is involved in membrane trafficking between the Golgi complex and endosomes. *Mol Biol Cell*. **15,** 2218–2229 (2004).
40. Wang, C., Liu, Z. & Huang, X. Rab32 is important for autophagy and lipid storage in Drosophila. *PLoS One*. **7,** e32086 (2012).
41. Berriman, M. *et al.* The genome of the African trypanosome *Trypanosoma brucei. Science*. **309,** 416–422 (2005).
42. Nevin, W. D. & Dacks, J. B. Repeated secondary loss of adaptin complex genes in the Apicomplexa. *Parasitol Int*. **58,** 86–94 (2008).
43. Bonifacino, J. S. & Lippincott-Schwartz, J. Coat proteins: shaping membrane transport. *Nat Rev Mol Cell Biol*. **4,** 409–414 (2003).
44. Pearse, B. M. Clathrin: a unique protein associated with intracellular transfer of membrane by coated vesicles. *Proc Natl Acad Sci USA* **73,** 1255–1259 (1976).
45. Robinson, M. & Sedwick, C. Margaret Robinson: vesicles wear fancy coats. *J Cell Biol*. **206,** 692–693 (2014).
46. Baggett, J. J. & Wendland, B. Clathrin function in yeast endocytosis. *Traffic*. **2,** 297–302 (2001).
47. Reider, A. & Wendland, B. Endocytic adaptors–social networking at the plasma membrane. *J Cell Sci*. **124,** 1613–1622 (2011).
48. Jockusch, W. J., Praefcke, G. J., McMahon, H. T. & Lagnado, L. Clathrin-dependent and clathrin-independent retrieval of synaptic vesicles in retinal bipolar cells. *Neuron*. **46,** 869–878 (2005).
49. Robinson, M. S. Adaptable adaptors for coated vesicles. *Trends Cell Biol*. **14,** 167–174 (2004).
50. Ghosh, P., Dahms, N. M. & Kornfeld, S. Mannose 6-phosphate receptors: new twists in the table. *Nat Rev Mol Cell Biol*. **4,** 202–212 (2003).
51. Allen, C. L., Liao, D. J., Chung, W.-L. & Field, M. C. Dileucine signal-dependent and AP1-independent targeting of a lysosomal glycoprotein in *Trypanosoma brucei. Mol Biochem Parasitol*. **156,** 175–190 (2007).
52. Tazeh, N. N. *et al.* Role of AP-1 in developmentally regulated lysosomal trafficking in *Trypanosoma brucei. Eukaryotic Cell*. **8,** 1352–1361 (2009).
53. Santos, C. C. *et al.* Chagasin, the endogenous cysteine-protease inhibitor of *Trypanosoma cruzi*, modulates parasite differentiation and invasion of mammalian cells. *J Cell Sci*. **118,** 901–915 (2005).
54. Batista, C. M., Medeiros, L. C., Eger, I. & Soares, M. J. MAb CZP-315.D9: an anti-recombinant cruzipain monoclonal antibody that specifically labels the reservosomes of *Trypanosoma cruzi* epimastigotes. *Biomed Res Int*. **2014,** 714–749 (2014).
55. Hirst, J., Irving, C. & Borner, G. H. Adaptor protein complexes AP-4 and AP-5: new players in endosomal trafficking and progressive spastic paraplegia. *Traffic*. **14,** 153–164 (2013).
56. Contreras, V. T. *et al.* Biological aspects of the DM28c clone of *Trypanosoma cruzi* after metacyclogenesis in chemically defined media. *Mem Inst Oswaldo Cruz*. **83,** 123–133 (1988).
57. Camargo, E. P. Growth and differentiation in *Trypanosoma cruzi*. Origin of metacyclic trypanosomes in liquid media. *Rev Inst Med Trop Sao Paulo*. **12,** 93–100 (1964).
58. Batista, M. *et al.* A high-throughput cloning system for reverse genetics in *Trypanosoma cruzi. BMC Microbiol*. **13,** 259–271 (2010).
59. Oberholzer, O., Morand, S., Kunz, S. & Seebeck, T. A vector series for rapid PCR-mediated C-terminal *in situ* tagging of *Trypanosoma brucei* genes. *Mol Biochem Parasitol*. **145,** 117–120 (2006).
60. Zhang, Y., Wen, Z., Washburn, M. P. & Florens, L. Effect of Dynamic Exclusion Duration on Spectral Count Based Quantitative Proteomics. *Anal Chem*. **81,** 6317–6326 (2009).
61. Liu, H., Sadygov, R. G. & Yates, J. R. A model for random sampling and estimation of relative protein abundance in shotgun proteomics. *Anal Chem*. **76,** 4193–4201 (2004).
62. Ishihama, Y. *et al.* Exponentially modified protein abundance index (emPAI) for estimation of absolute protein amount in proteomics by the number of sequenced peptides per protein. *Mol Cell Proteomics*. **4,** 1265–1272 (2005).
63. Field, H. I., Coulson, R. M. R. & Field, M. C. An automated graphics tool for comparative genomics: the Coulson plot generator. *BMC Bioinformatics*. **14,** doi: 10.1186/1471-2105-14-141 (2013).

Acknowledgements

Author Contributions

M.J.S. and M.C.F. conceived the study, L.C.K., Y.C.A.F., C.B. and M.N.M. undertook the research. L.C.K., M.C.F and M.J.S. wrote the manuscript and Y.C.A.F., C.B. and M.N.M. provided additional text and revisions. L.C.K. and M.C.F. produced Figures 1 and 2, Y.C.A.K., L.C.K. and M.C.F. Figure 3 and M.N.M. and M.C.F. Figure 4. Tables and Supplementary data were produced by L.C.K., C.B. and M.C.F.

Additional Information

Supplementary information accompanies this paper at http://www.nature.com/srep

Competing financial interests: The authors declare no competing financial interests.

How to cite this article: Kalb, L. C. *et al.* Conservation and divergence within the clathrin interactome of *Trypanosoma cruzi*. *Sci. Rep.* **6**, 31212; doi: 10.1038/srep31212 (2016).

4 MATERIAIS E MÉTODOS REFERENTES AOS RESULTADOS SUPLEMENTARES NÃO PUBLICADOS DO CAPÍTULO 2

4.1 Cultivo dos parasitas

Formas epimastigotas do clone Dm28c de *T. cruzi* foram cultivadas a 28°C em meio LIT (liver infusion tryptose) (CAMARGO, 1964) suplementado com 10% de soro fetal bovino inativado. As passagens foram realizadas semanalmente com inóculo de 1 x 10^6 células/ml (CONTRERAS *et al.*; 1985). Para os experimentos, os parasitas na fase logarítmica de crescimento (terceiro dia de cultivo) foram coletados por centrifugação a 3.000 x *g* por 5 min.

4.2 Modificação do vetor pTcNEO3xFlag-C para pTcNEO/GFP-C

O vetor de expressão pTcNEO/GFP-C foi obtido a partir da modificação do vetor pTcNEO3xFlag-C, construído pelo nosso grupo (GONÇALVES, 2014) a partir dos plasmídeos da sériepTcGW (BATISTA et al., 2010), a fim de substituir a etiqueta 3xFLAG por GFP (Green fluorescente protein) (Fig. 1). O objetivo dessa substituição foi permitir a expressão da proteína de interesse com a etiqueta GFP na porção C-terminal. Para isso, amplificamos o gene que codifica para proteína GFP utilizando os primers GFPSpeIF 5´(**ACTAGT**AATGGTGAGCAAGGGCGAGGAGCTGTTCACC) e GFPAscIR 5´(**GGCGCGCC**CTACTTGTACAGCTCGTCCATGCCGAGAGTGATC), contendo, respectivamente, os sítios para as enzimas de restrições *Spe*I e *Asc*I (em negrito). A reação de PCR (Polymerase Chain Reaction) foi realizada com a enzima Platinum® *Taq* DNA Polymerase High Fidelity (Invitrogen) utilizando o plasmídeo pEGFP-C3 (Clontech, EUA) como molde. As condições de amplificação foram conforme segue: desnaturação a 94ºC por 4 min, seguidos de 30 ciclos (desnaturação, anelamento do oligonucleotídeos iniciador e extensão) e um último ciclo a 72ºC por 7 min. A temperatura e tempo de anelamento foram ajustados de acordo com a especificidade dos *primers* e o tempo de extensão nos ciclos foi ajustado conforme o tamanho do fragmento (1 min para cada 1.000 pares de bases). Os amplicons foram purificados com a utilização do QIAquick PCR Purification Kit (Qiagen, Alemanha). Inserto e vetor foram digeridos com as enzimas *Spe*I e *Asc*I (Biolabs, EUA) conforme orientação do fabricante, purificados e ligados com a enzima T4 DNA ligase (Thermo Scientific, EUA) segundo protocolo do fabricante. A reação de ligação do vetor ao inserto foi utilizada para transformar bactérias quimio-competentes *ccd*B resistentes (*E. coli*, linhagem *ccd*B Survival™ 2 T1^R), e os clones foram identificados pela técnica de palitagem. Esta técnica foi realizada transferindo as colônias de bactérias transformadas para tubos com

capacidade de 200 μl com o auxílio de palitos de madeira (uma colônia por tubo). Em seguida, as bactérias foram lisadas com 20 μl de tampão de lise (glicerol 5%, SDS 0,5%, EDTA 5 mM, NaOH 50 mM, azul de bromofenol) à 65 ºC por 10 min. Estas amostras foram submetidas a eletroforese em gel de agarose 0,8% juntamente com o controle negativo (plasmídeo sem a modificação). O clone positivo foi propagado em meio LB (Luria Bertani) com ampicilina (100 μg/mL) e cloranfenicol (34 μg/mL) e purificado com kit de miniprerparqação de plasmídeos "QIAprep spin miniprep kit" (QIAGEN). O plasmídeo obtido dessa modificação foi denominado pTcNEO/GFP-C.
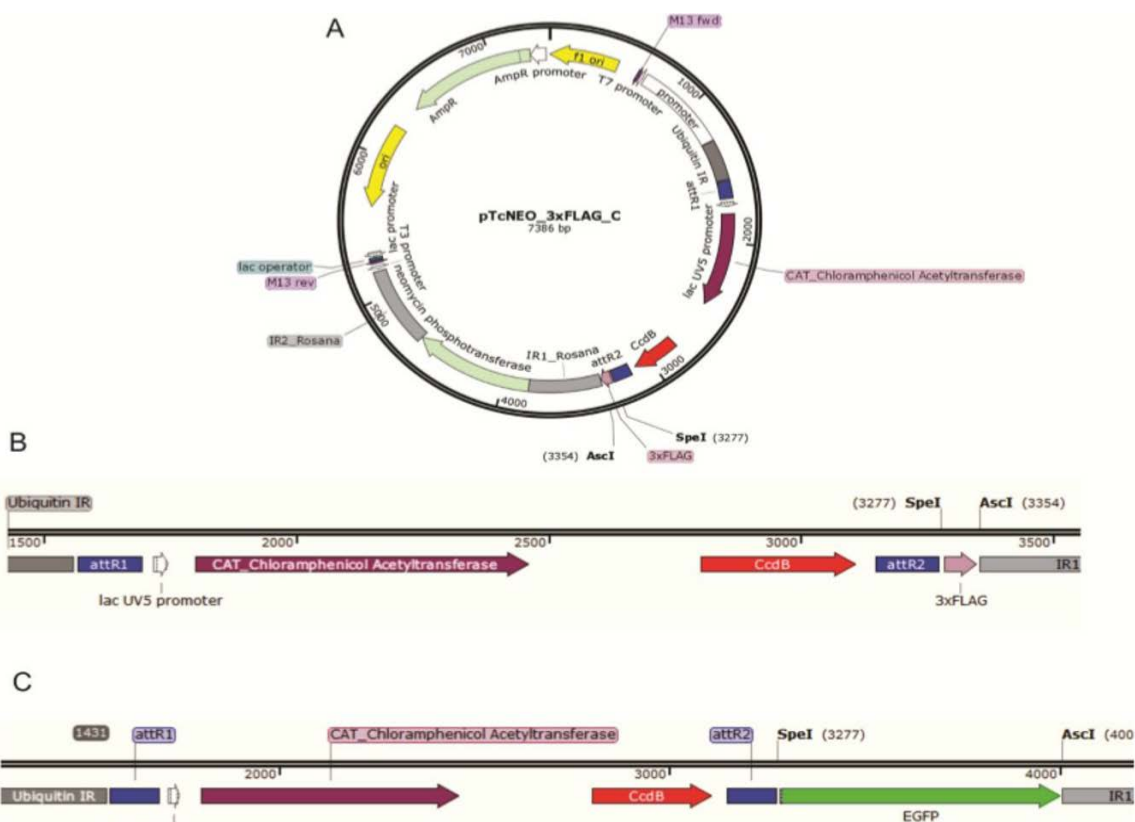
Figura 5.1. Modificação do plasmídeo pTcNEO3XFlag-C para pTcNEO/GFP-C. A. Plasmídeo contendo a etiqueta 3xFLAG para inserção na porção C-terminal da proteína. B. região do vetor mostrando os sítios de restrição utilizados para a troca de etiqueta C. Inserção do gene GFP na região de destino.

4.3 Obtenção de formas epimastigotas de *T. cruzi* expressando TcAP1-β/GFP e TcAP1-μ/GFP

Os genes TcAP1-β (Tc00.1047053506247.200) e TcAP1-μ (Tc00.1047053510533.40) foram clonados no vetor pTcNEO/GFP-C para expressão em *T. cruzi* das proteínas AP1-β e AP1-μ fusionadas à proteína GFP na sua porção C-terminal. Assim, os dois genes foram

amplificados por PCR usando os primers F e R (Quadro 1), que contem sequências *att*B1 (iniciador F) e *att*B2 (iniciador R) (em negrito) que permitem a inserção na plataforma Gateway de clonagem (Invitrogen, EUA).

Quadro 1 – Primers utilizados para amplificação dos genes TcAP1-β e TcAP1-μ.

PRIMER	SEQUENCIA (5'-3')
BetaF	**GGGGACAAGTTTGTACAAAAAAGCAGGCTT**CATGGATGCCGTATTGCGAAAGGTGCA
BetaR	**GGGGACCACTTTGTACAAGAAAGCTGGGTC**GGCAAACCTCTGGTCCAGTAC
MuF	**GGGGACAAGTTTGTACAAAAAAGCAGGCTT**CATGGCGTCAGTGTTCTACATCTTA
MuR	**GGGGACCACTTTGTACAAGAAAGCTGGGTC**ATATGTTCTTATCTGATAGTCCCC

As reações de PCR foram processadas no termociclador modelo Proflex (Thermo Scientific) nas seguintes condições: 100 ng de DNA genômico de *T. cruzi*, 10 pmol de cada primer, dNTPs 200 μM, MgSO$_4$ 1 mM,1 unidade da enzima Platinum® Taq DNA Polymerase High Fidelity (Invitrogen) em tampão apropriado (Thermo Scientific). O material foi desnaturado a 95°C por 3 min seguido da amplificação por 30 ciclos com etapa de desnaturação a 95°C por 30 s, anelamento dos primers a 55°C por 30 s e extensão a 72°C por 2 min. Os genes amplificados foram recombinados com o vetor pDONR™221 (Thermo Scientific) mediante reação de recombinação BP clonasse, para gerar os clones de entrada pDONR/AP1-β e pDONR/AP1-μ. A reação de recombinação com BP foi realizada conforme descrito a seguir: 150 ng do produto de PCR contendo os sítios *att*B1 e 2 e 150 ng do plasmídeo pDONR™221 foram misturados com 2 μl da enzima BP Clonase II (termo Scientific) em um volume final de 10 μl em TE. As reações foram incubadas a 25°C por 16 horas. As reações foram interrompidas pela adição de 2 μg (2 μl) de proteinase K por 10 min a 37°C. Bactérias *E. coli* cálcio-competentes de linhagem DH5α foram transformadas com os plasmídeos recombinados, mediante choque térmico. Os plasmídeos recombinantes foram purificados utilizando o kit QIAprep Spin Miniprep Kit (QIAGEN), conforme recomendações do fabricante. Após a entrada do gene de interesse em pDONR™221, foi feita recombinação LR para entrada no vetor de destino pTcNEO/GFP-C. Para o processo de recombinação foram usados 150 ng dos clones de entrada e 150 ng do vetor de destino, 2 μl da enzima LR Clonase II (Thermo Scientific) e o volume final de 10 μl TE. As reações foram incubadas a 25°C por 16h e inativadas com 2 μg de proteinase K por 10 min a 37°C. A recombinação LR foi utilizada para transformar células cálcio-competentes de *E.coli* da linhagem DH5α mediante choque térmico e purificados utilizando o kit QIAprep Spin Miniprep Kit (QIAGEN), conforme recomendações do fabricante. Para confirmar a correta inserção dos genes nos plasmídeos recombinantes, as amostras foram enviadas para a empresa Macrogen Korea (Coréia do Sul) para sequenciamento. Plasmídeos resultantes contendo os genes para TcAP1-

β/GFP e TcAP1-µ/GFP foram usados para transfectar formas epimastigotas de *T. cruzi*. Os parasitas transfectantes foram selecionados por resistência ao antibiótico G418 e analisadas quanto a expressão de TcAP1-β/GFP e TcAP1-µ/GFP através de ensaio western blot e imunofluorescência.

4.4 Transfecção em *T. cruzi*

Formas epimastigotas de *T. cruzi* foram cultivadas em meio LIT suplementado com 10% SFB a 28°C até densidade celular de 3 x 10^7 células/ml. Os parasitas foram coletados por centrifugação a 3000 x *g* por 5 min a temperatura ambiente. O sedimento celular foi lavado com PBS estéril e ressuspenso em solução de eletroporação (NaCl 140 mM, HEPES 25 mM, Na_2HPO_4 0.74 mM, pH 7,5) a uma densidade de 2 x 10^8 células/ml. A suspensão de células (0,4 ml) foi transferida para cubeta de eletroporação estéril (0,2 cm de gap) (BioAgency, EUA) pré-resfriadas, seguida da adição de 10-15 µg de DNA. Uma cubeta contendo igual quantidade de suspensão celular e sem adição de DNA foi usada como controle. Após 10 min no gelo, as amostras contidas nas cubetas foram submetidas a dois pulsos de 450 Volts, 500 µF, utilizando o eletroporador GenePulser (Bio-Rad, Hercules, CA, USA). Após a eletroporação, as células foram transferidas para garrafas de cultura de 25 cm^2, contendo 10 ml de meio LIT (suplementado com 10.000 U penicilina e estreptomicina a 10 µg/ml). As culturas foram então incubadas a 28°C. Após 24 horas, o antibiótico G418 (500 µg/ml) foi adicionado ao meio de cultivo. Para a seleção dos parasitas transfectantes, as culturas foram mantidas, por passagens semanais, até a ausência de proliferação celular na cultura controle (parasitas selvagens submetidos à eletroporação sem o plasmídeo).

4.5 Imunofluorescência

Formas epimastigotas de *T. cruzi* expressando TcAP-1β/GFP e TcAP-1µ/GFP em fase exponencial de crescimento (3 dias) foram lavadas 2x em PBS, fixadas por 30 min em paraformaldeido 4% e aderidas por 20 min a lamínulas recobertas com poli-L-lisina a 0,1%. As células foram permeabilizadas com Triton X-100 a 0,5% diluído em PBS por 5 min a temperatura ambiente, lavadas novamente com PBS e bloqueadas para reações inespecíficas por 1 h em solução de 1,5% de albumina bovina em PBS. Em seguida as amostras foram incubadas por 1 h com antisoro anti-GFP de coelho (Sigma) (1:100) e anticorpo monoclonal anti TcAP-1γ. Após três lavagens em PBS as amostras foram incubadas com anticorpo secundário anti-IgG de coelho conjugado a Alexa Fluor 488 (1:600) e anti-IgG de camundongo conjugado a Alexa Fluor 594 (1:600) por 45 min. O DNA do núcleo e cinetoplasto foi corado por Hoechst 33342 (Thermo Scientific). As lâminas foram lavadas em

PBS e montadas com Prolong (Life Technologies). O material foi observado no microscópio Nikon E600 (Nikon Instruments, Melville, N.Y. USA) do Centro de Microscopia do Instituto Carlos Chagas, Fiocruz-PR. As imagens adquiridas foram editadas para melhor contraste usando Adobe Photoshop CS5 (Adobe Systems Incorporated, USA).

4.6 Western blot

Extratos protéicos de *T. cruzi* foram resolvidos por SDS-PAGE (NuPAGE® Novex® 4-12% Bis-Tris) (Life Technologies) e transferidas para membranas de nitrocelulose (Hybond C, Amersham Biosciences) em tampão de transferência para western blot (Tris-base 25 mM, Glicina 192 mM, Metanol 20%). As membranas foram bloqueadas com tampão de bloqueio (Tampão PBS 1X; Tween 20 0,05%; Leite em pó desnatado 5%) e incubadas com anti-GFP (produzido em coelho, 1:500), anti TcAP-1γ (1:300) ou anticorpo monoclonal anti-TcCHC (puro, produzido em camundongo (KALB et al., 2014). As membranas foram então lavadas três vezes com PBS contendo Tween 20 0,1%, seguido de incubação com os anticorpos secundários anti-IgG de coelho ou anti-IgG de camundongo conjugados à peroxidase (Amersham Biosciences) na diluição de 1:10.000 por 1 h a 37°C. A detecção de proteínas foi feita por quimioluminescência utilizando 1:1 das seguintes soluções: solução A (2,5 mM de luminol (Sigma-aldrich), 0,4mM ácido p-cumárico (Sigma-aldrich), 100 mM de Tris-HCl pH 8,5 e água destilada) e solução B (57,6 µM de H_2O_2 a 30%, 100 mM de Tris-HCl Ph 8,5 e água destilada) e adicionados à membrana por 1 - 2 min. O sinal quimioluminescente foi detectado com a auxílio do sistema de detecção G: BOX Chemi XX6 (Syngene, UK).

4.7 Acoplamento de *nanobodies* anti-GFP a esferas magnéticas

Microesferas magnéticas (Dynabeads® M270 epoxy) (30 mg) (Life technologies) que foram lavadas com 1 ml de tampão fosfato 100 mM, pH 7,4 e ressuspendidas em 100 µl do mesmo tampão fosfato. *Nanobodies* anti-GFP (100 µl contendo 300 µg totais) foram misturados com as microesferas magnéticas, seguida da adição de 100 µl de sulftato de amônio 3 M, lentamente para evitar a precipitação de proteínas. As microesferas foram incubadas durante 72 h a 30°C, com agitação constante. Posteriormente, elas foram lavadas, sequencialmente, com 1 ml das seguintes soluções: tampão fosfato 100 mM, pH 7,4; Glicina 100 mM, pH 2,5; Tris-HCl 10 mM, pH 8,8; Trietilamina 100 mM; PBS; Triton X-100 0,5% em PBS e, novamente, PBS. As microesferas foram ressuspendidas em 150 µl de PBS e armazenadas a 4°C até o momento do uso.

4.8 Extrato protéico por moagem em temperaturas criogênicas (*cryogriding*)

Para obtenção do extrato protéico para imunoprecipição, formas epimastigotas de *T. cruzi* expressando TcAP-1β/GFP e TcAP-1μ/GFP e formas epimastigotas selvagens (aproximadamente 5 x 10^{10} células) foram coletadas por centrifugação (3.000 x *g*, 10 min, 4°C) e lavadas em PBS contendo inibidores de proteases (COMPLETE Mini Protease inhibitor cocktail tablet, Roche). O material foi centrifugado novamente (3.000 x *g*, 10 min, 4°C) e o sobrenadante foi removido. O *pellet* de células foi congelado rapidamente por gotejamento em tubo cônico contendo nitrogênio líquido. Após o congelamento, o nitrogênio foi removido por evaporação e as amostras foram mantidas a -80°C. As células congeladas foram lisadas mecanicamente pela técnica de criomoagem em moínho de bolas (Planetary Ball Mill PM100, Retsch, Haan, Alemanha), previamente resfriado em nitrogênio líquido. As amostras foram moídas a 300 rpm por 3 min. Esse procedimento foi repetido cerca de 10 vezes para obtenção de um pó de células extra-fino (< 0,1 µm). Este pó foi transferido para um tubo conico pré-resfriado e armazenado a –80°C.

4.9 Imunoprecipitação

Aproximadamente 50 µg do pó de células obtido conforme descrito no item anterior, foram ressuspensos em 1 ml de tampão (conforme o caso, num total de 11 tampões descritos abaixo) suplementado com inibidor de protease (COMPLETE Mini Protease inhibitor cocktail tablet, Roche). As amostras foram cavitadas por ultrasom três vezes em potência 4 por 2 segundos.

Quadro 2: Tampões utilizados nos ensaios de imunoprecipições.

1	Hepes 20 mM pH 7,4; Na-citrato 250 mM; CHAPS 0,1%; MgCl2 1 mM, CaCl$_2$10 μM
2	Hepes 20 mM pH 7,4, NaCl 150 mM, CHAPS 0,1%, MgCl$_2$ 1 mM, CaCl$_2$ 10 μM
3	Hepes 20 mM pH 7,4, NaCl 50 mM, CHAPS 0,1%, MgCl$_2$ 1 mM, CaCl$_2$ 10 μM
4	Hepes 20 mM pH 7,4, NaCl 100 mM, CHAPS 0,1%, MgCl$_2$ 1 mM, CaCl$_2$ 10 μM
5	Hepes 20mM pH 7.4, NaCl 100mM, Tween 0,1%, MgCl$_2$ 1mM, CaCl$_2$ 10 μM
6	Hepes20mM pH 7.4, NaCl 100mM, Triton 0.1%, MgCl$_2$ 1mM, CaCl$_2$ 10μM
7	Hepes 20mM pH 7.4, NaCl 100mM, Brij58 0.1%, MgCl$_2$ 1mM, CaCl$_2$ 10μM
8	Hepes 20 mM pH 7,4, Na-citrato 50mM, NaCl 20 mM, Tween 0,1%, MgCl$_2$ 1 mM, CaCl$_2$ 10 mM
9	Hepes 20 mM pH 7,4, Na-citrato 50mM, NaCl 20 mM, Tween 0,5%, MgCl$_2$ 1 mM, CaCl$_2$ 10 mM
10	Hepes 20 mM pH 7,4, Na-citrato 50mM, NaCl 20 mM, CHAPS 0,5%, MgCl$_2$ 1 mM, CaCl$_2$ 10 mM
11	Hepes 20 mM pH 7,4, Na-citrato 50mM, NaCl 20 mM, CHAPS 0,1%, MgCl$_2$ 1 mM, CaCl$_2$ 10 mM

O material foi centrifugado a 20.000 x *g* durante 10 min a 4°C. O sobrenadante foi coletado em novo tubo e misturado com 3 µl das microesferas magnéticas acopladas aos *nanodobies* anti-GFP. A suspensão foi incubada sob agitação constante a 4°C durante 2 h. Em seguida, com o auxílio de uma estante magnética, as esferas foram lavadas três vezes com o

mesmo tampão de suspensão e incubadas a 95°C com tampão de amostra 4x (Tris-HCl 40 mM pH 6,8, SDS 1%, β-mercaptoetanol 2,5%, glicerol 6% e azul de bromofenol 0,005%). O perfil eletroforético da amostra foi observado em matriz de acrilamida 4-12% (NuPAGE®) em coloração de Comassie (kit Staining with SimplyBlue™ SafeStain (Life technologies) ou coloração de prata.

Após a padronização do tampão, 300 µg de pó (divididos em seis tubos com capacidade de 1,5 mL) de cada uma das três amostras (*T.cruzi* selvagem, *T.cruzi* AP1-β/GPF e *T.cruzi* AP1-µ/GFP) foram usados para ligação com as microesferas acopladas aos *nanobodies* anti-GFP, seguindo o procedimento descrito acima até a etapa de lavagem das microesferas magnéticas. As proteínas ligadas aos *nanobodies* anti-GFP foram eluídas pela adição de 50 µl de tampão de eluição (Tris-HCl 20 mM pH 8,0/SDS 2%), com incubação por 30 min a 72°C. Do sobrenadante, 5 µl foram usados análise por SDS-PAGE e 5 µl para análise por western blot. O restante do material (40 µl) foi precipitado com 427 µl de etanol absoluto por 16 horas a -20ºC. As proteínas foram coletadas por centrifugação a 20.000 x *g* por 30 min a 4ºC. O sobrenadante parcialmente descartado, deixando no tubo aproximadamente 20 µl de etanol junto com o *pellet* das amostras, que foram em seguida enviadas para análise em espectrômetro de massas. Os dados referentes ao processamento das amostras e análise pelo espectômetro de massas estão descritos no artigo desse capítulo. A quantificação relativa aproximada das proteínas presentes nos complexos foi estimada de modo *label-free* e através do índice de abundância proteica exponencialmente modificado (emPAI), determinado em uma mistura baseado na cobertura dos peptídeos da proteína identificada (ISHIHAMA et al., 2005). Assim, o valor de emPAI é determinado pela fórmula:

$$emPAI = 10^{\frac{N_{obsd}}{N_{obsbl}}} - 1$$ Nobservado (Nobsd) refere-se ao número de peptídeos observados experimentalmente e Nobservável (Nobsdl) é o número calculado de peptídeos para cada proteína através de digestões determinadas *in silico*. As buscas seguiram os seguintes parâmetros: taxa de falsos positivos (FDR) de 1% e os peptídeos que apresentaram valor estatisticamente significativo de p-valor <0.05. emPAI é diretamente proporcional à abundância absoluta de uma dada proteína em uma amostra de conteúdo proteico total conhecido (ISHIHAMA et al., 2005). Desse modo, o índice absoluto de emPAI para cada proteína do controle foi utilizado para determinar o do valor considerado alta confiança obtido das amostras imunoprecipitadas no extrato testado, sendo esse valor cinco vezes maior do que no controle.

5   RESULTADOS SUPLEMENTARES REFERENTES AO CAPÍTULO 2 – IMUNOPRECIPITAÇÃO DE TCAP1-B E TCAP1-µ

5.1   Expressão e localização de TcAP1-β e TcAP1-µ fusionadas à GFP e co-localização com TcAP1-γ

O complexo adaptor 1 atua na membrana da rede trans-Golgi, onde segrega moléculas e auxilia na formação do revestimento de vesículas com clatrina. Para identificar as proteínas e complexos parceiros de TcAP1, fusionamos uma etiqueta GFP (28 kDa) às porções C-terminais das subunidades TcAP1-β (106 kDa) e TcAP1-µ (49 kDa) para ensaio de imunoprecipitação. A expressão das proteínas TcAP1-β/GFP e TcAP1-µ/GFP em *T. cruzi,* foi confirmada a partir da análise por western blot, utilizando antissoro anti-GFP para a detecção da etiqueta GFP (Fig. 6.1).
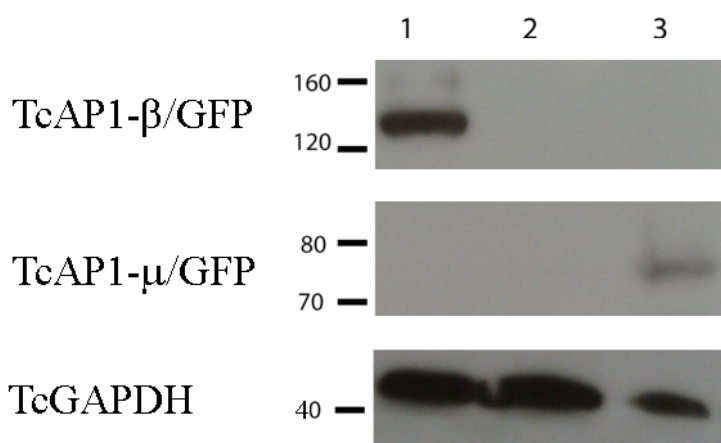
Figura 6.1. Análise da expressão de TcAP1-β/GFP e TcAP1-µ/GFP em formas epimastigotas de *Trypanosoma cruzi*, por western blot utilizando o antissoro anti-GFP. 1. Extrato proteico total dos parasitas transfectantes expressando TcAP1-β/GFP. 2. Extrato proteico total de parasitas selvagens. 3. Extrato proteico total dos parasitas transfectantes expressando TcAP1-µ/GFP. O antissoro anti-TcGAPDH foi utilizado como controle.

O complexo adaptador 1 é composto por quatro subunidades: γ, β, µ e σ. Para verificar se GFP não estava interferindo na localização de TcAP1-β/GFP e TcAP1-µ/GFP no complexo de Golgi, realizamos ensaio de co-localização destas proteínas com a subunidade TcAP1-γ. Os resultados dos ensaios de imunofluorescência mostraram que as adaptinas TcAP1-β/GFP e

TcAP1-µ/GFP estavam presentes no Golgi e se co-localizavam com a TcAP1-γ (Fig. 6.2), indicando que GFP não interferiu no direcionamento das adaptinas recombinantes.
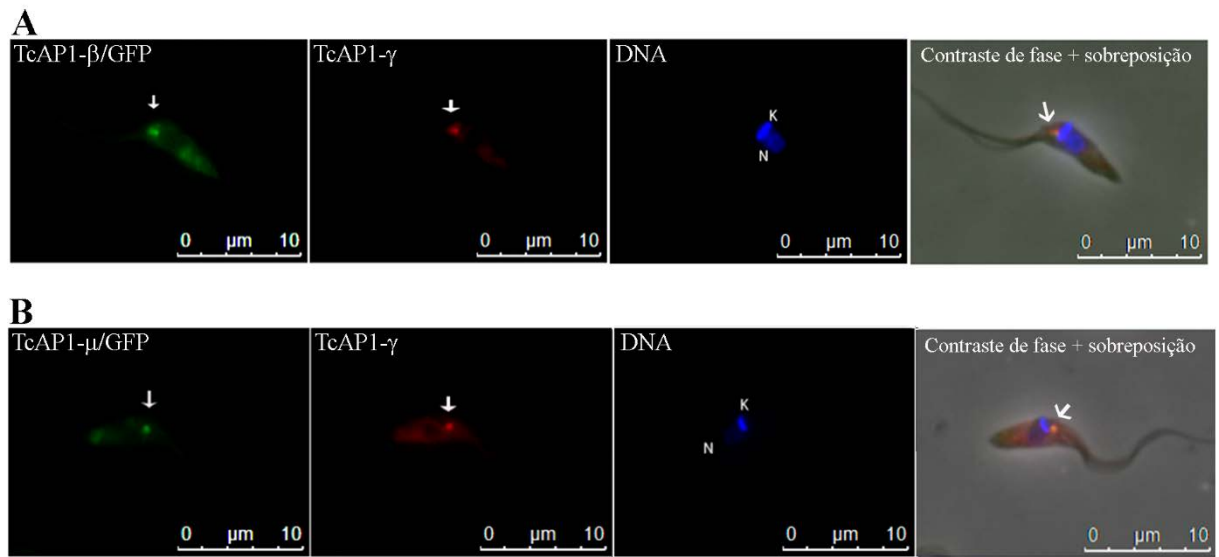
Figura 6.2. Localização de adaptinas fusionadas a GFP e co-localização com TcAP1-γ em formas epimastigotas de *T. cruzi*. Os parasitas foram incubados com antissoro anti-GFP (coelho) e com o anticorpo monoclonal anti TcAP1-γ 211-F7 (camundongo). Em verde, localização da GFP fusionada a TcAP1-β (A) e TcAP1-µ (B), revelada por anticorpo secundário anti-IgG de coelho conjugado a AlexaFluor 488. Em vermelho, localização de TcAP1-γ usando o anticorpo monoclonal anti-TcAP1-γ 211-F7, revelada por anticorpo secundário anti-IgG de camudongo conjugado a AlexaFluor 594. DNA foi corado com DAPI. Em amarelo, a co-localização entre as adaptinas na porção anterior do parasita.

5.2 Imunoprecitação de TcAP1-β e TcAP1-µ

As proteínas TcAP1-β/GFP e TcAP1-µ/GFP foram utilizadas como iscas, em ensaios de imunoprecipitação, para capturar e posteriormente identificar, por espectrometria de massas, as proteínas que interagem com AP-1 e que são necessárias para a formação do revestimento das vesículas dependentes desse complexo adaptador na rede trans-Golgi. Formas epimastigotas de *T. cruzi* expressando essas subunidades fusionadas à proteína GFP foram moídas enquanto congeladas, obtendo-se um pó extra-fino. Esse pó foi utilizado nos ensaios de imunoprecipitação juntamente com microesferas magnéticas acopladas aos *nanobodies* anti-GFP. Foram testados diferentes tampões de extração, com diferentes concentrações de sais e detergentes (Fig. 6.3). Destaca-se, entre eles, um dos tampões que foi utilizado na imunoprecipitação de clatrina e epsinaR (Hepes 20mM pH 7.4, Na-Citrato 250 mM , CHAPS 0,1%, MgCl$_2$ 1mM, CaCl$_2$ 10 µM) (vide artigo referente a esse capítulo), a

partir do qual foi possível co-imunoprecipitar o complexo AP-1. As frações eluídas das microesferas magnéticas foram separadas por SDS-PAGE, e submetidas à colocação pela prata. O extrato de parasitas selvagens foi utilizado como controle negativo dos experimentos de imunoprecipitação. Os perfis eletroforéticos das imunoprecipitações utilizando diferentes tampões estão mostrados na fig. 6.3. Podemos observar, além de várias outras proteínas co-precipitadas, a presença de um polipeptídeo com aproximadamente 130 kDa, embora não enriquecido, nos cinco primeiros tampões testados, cuja massa molecular coincide com aquela predita para TcAP1-β/GFP (134 kDa) (Fig. 6.3A). Entretanto, não foi possível identificar a subunidade TcAP1-μ/GFP (77 kDa) no material imunoprecipitado dessa subunidade, talvez devido à baixa expressão no parasita transfectante.
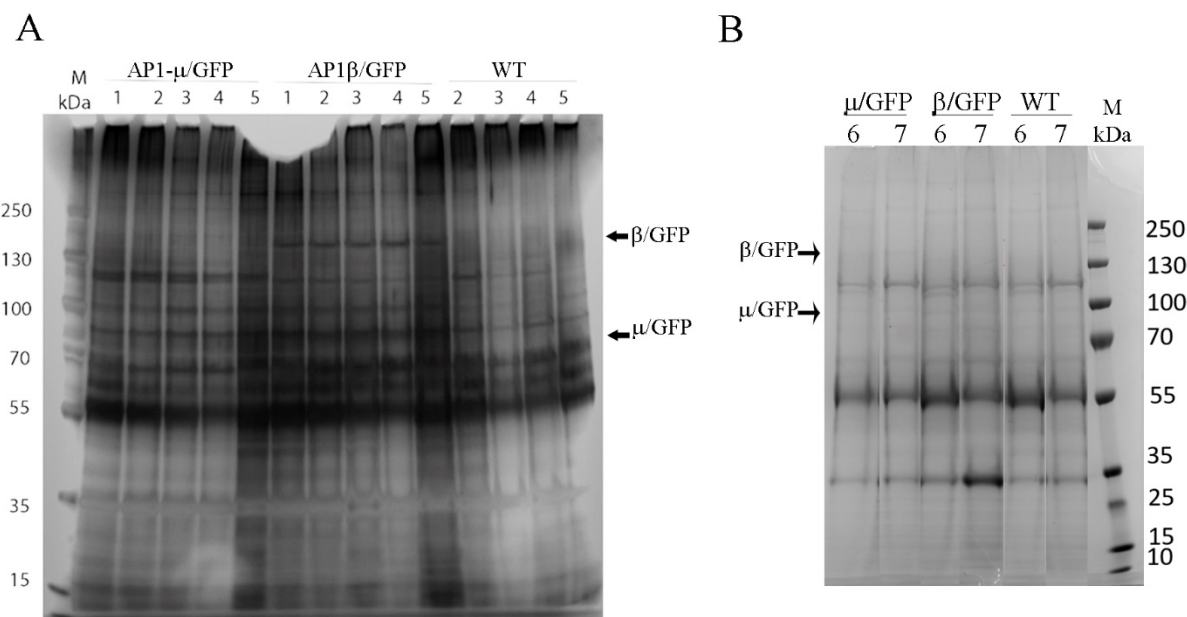
Figure 6.3. Teste de imunoprecipitação de TcAP1-β/GFP e TcAP1-μ/GFP com diferentes tampões de extração. Padrão eletrofético do material eluído das microesferas magnéticas em matriz de poliacrilamida 4%-12% corado com prata (A- tampões de 1 a 5) ou comassie (B- tampões de 6-7). Tampões:

1- Hepes 20 mM pH 7.4, NaCl 100 mM, CHAPS 0,1%, $MgCl_2$ 1 mM, $CaCl_2$, 10 μM

2- Hepes 20 mM pH 7.4, NaCl 100 mM, Tween 0,1%, $MgCl_2$ 1mM, $CaCl_2$ 10 μM

3- Hepes 20 mM pH 7.4, NaCl 100 mM, Triton 0,1%, $MgCl_2$ 1mM, $CaCl_2$ 10 μM

4- Hepes 20 mM pH 7.4, NaCl 100 mM, Brij58 0,1%, $MgCl_2$ 1mM, $CaCl_2$ 10 μM

5- Hepes 20 mM pH 7.4, Na-Citrato 250 mM, CHAPS 0,1%, $MgCl_2$ 1mM, $CaCl_2$ 10 μM

6- Hepes 20 mM pH 7.4, NaCl 50 mM, CHAPS 0,1%, $MgCl_2$ 1mM, $CaCl_2$ 10 μM

7- Hepes 20mM pH 7.4, NaCl 150 mM, CHAPS 0,1%, $MgCl_2$ 1mM, $CaCl_2$ 10 μM

Análise por western blot, utilizando o antissoro anti-GFP (1:1.000), confirmou que as proteínas TcAP1-β/GFP e TcAP1-μ/GFP estavam presentes no material eluído das microesferas, cujo extrato (pó da criomoagem) havia sido solubilizado no tampão 5 (Hepes 20 mM pH 7.4, Na-Citrato 250 mM, CHAPS 0,1%, $MgCl_2$ 1 mM, $CaCl_2$ 10 μM), a partir do qual foram identificadas proteínas do complexo AP-1 que co-precipitaram com clatrina e epsinaR (Kalb et al., 2016). Observamos também que uma fração da proteína TcAP1-μ/GFP em tampão 5 estava insolúvel (Fig. 6.4 A). Testamos diferentes condições para tentar solubilizar TcAP1-μ/GFP, tais como aumentar o tempo de sonicação ou diminuir o tempo de centrifugação. Todavia, o padrão da imunoprecipitação continuou o mesmo, ou seja, parte de TcAP1-μ/GFP permaneceu insolúvel (dados não mostrados).

Análise por ensaio de western blot, utilizando o anticorpo monoclonal 211-F7, que reconhece AP1-γ em *T. cruzi*, mostrou que essa outra subunidade do complexo AP1 também co-precipitou nos ensaios de imunoprecipitação usando tanto TcAP1-β/GFP como TcAP1-μ/GFP, sugerindo que a presença da GFP não interferiu com a montagem do complexo AP1 (Fig. 6.4B).
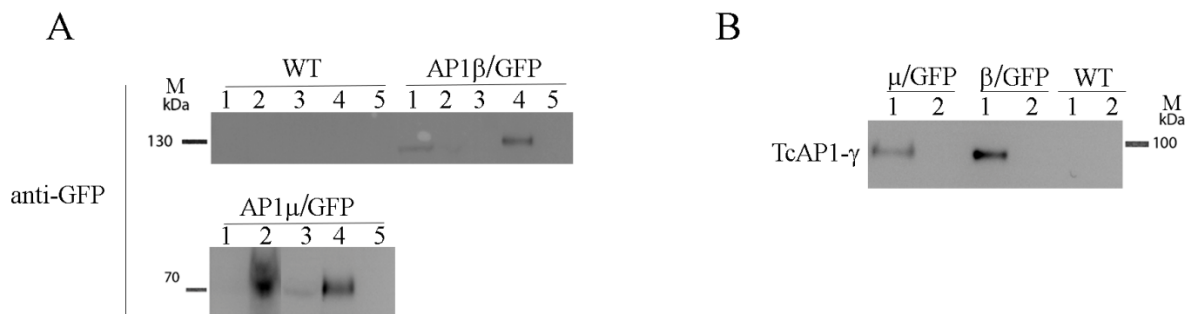
Figure 6.4. Análise da imunoprecipitação de TcAP1-β/GFP e TcAP1-μ/GFP com tampão 5 por western blot.
(**A**) Antisoro anti-GFP foi utilizado para identificar as proteínas AP1-β/GFP e AP1-μ/GFP durante a imunoprecipitação. 1. Extrato proteico total ressuspendido em tampão de extração; 2-Pellet; 3-Material não ligado nas beads magnéticas; 4. Material eluído das microesferas magnéticas; 5. Microesferas magnéticas. (**B**) Detecção da subunidade AP1-γ com anticorpo monoclonal anti-TcAP1-γ, a partir do material eluido das microesferas dos ensaios de imunoprecipitação de AP1-β/GFP e AP1-μ/GFP:1. Material eluído das microesferas magnéticas; 2. Microesferas magnéticas.

Diante dos resultados apresentados, onde a subunidade TcAP1-γ co-precipitou com as subunidades β/GFP e μ/GFP, foram selecionados os materiais eluidos a partir das microesferas incubadas com os extratos ressuspensos em dois diferentes tampões do teste apresentado na fig. 6.3 (tampão**3**: Hepes 20mM pH 7.4, NaCl 100mM, Triton 0,1%, MgCl$_2$ 1mM, CaCl$_2$ 10 μM e o tampão **5**: Hepes 20mM pH 7.4, Na-Citrato 250mM, CHAPS 0,1%, MgCl$_2$ 1 mM, CaCl$_2$ 10 μM). Essas amostras foram enviadas para análise por espectrometria de massas. Os perfis eletroforéticos das amostras imuprecipitadas estão mostrados na fig. 6.5.
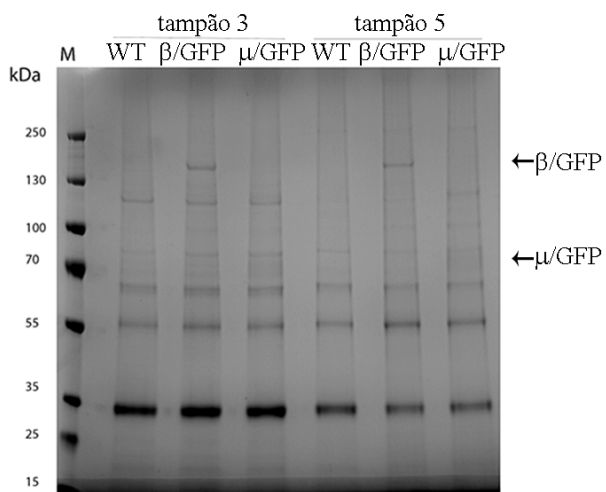
Figura 6.5. **Imunoprecipitação de TcAP1-β/GFP e TcAP1-μ/GFP**. Perfil eletroforético do material imunoprecipitado usando os tampões 3 e 5, em matriz de poliacrilamida 4-12% corado com comassie blue.

5.3   Análise de proteínas associadas à TcAP1-β e TcAP1-μ

O resultado da análise por espectrometria de massas das imunoprecipitações de TcAP1-β/GFP e TcAP1-μ/GFP com os dois diferentes tampões não trouxeram muitas informações. Primeiramente, foi possível identificar que tanto TcAP1-β/GFP como TcAP1-μ+GFP eram as proteínas mais abundantes entre as proteínas identificadas, o que era esperado já que elas foram expressas em maior quantidade nos parasitas transfectantes. Em segundo lugar, todas as outras três proteínas do complexo AP-1 co-imunoprecipitaram com a TcAP1-μ (TcAP1-β, TcAP1-γ e TcAP1-σ), enquanto que apenas duas delas co-imunoprecipitaram com a TcAP1-β (TcAP1-γ, e TcAP1- μ). Esses dados sugerem que o complexo AP-1 é altamente estável. Entretanto, supreendentemente, não identificamos a clatrina e a epsinaR, duas proteínas que interagem com AP1 conforme resultados apresentados no artigo desse capítulo. Após comparar as listas com o controle negativo

(WT) observamos que exceto as proteínas do complexo AP1, as demais proteínas eram apenas contaminantes (Fig. 6 e Fig 7).

A		
Accession	↓emPAI	Description
tr|K4E9F9	38,46	Mu-adaptin 1, putative,adaptor complex AP-1 medium subunit, putative OS=Trypanosoma cruzi GN=TCSYLVIO_001761 PE=4 SV=1
tr|V5BW37	6,24	Gamma-adaptin 1 OS=Trypanosoma cruzi Dm28c GN=TCDM_02471 PE=4 SV=1
tr|V5DDV1	5,43	Beta-adaptin OS=Trypanosoma cruzi Dm28c GN=TCDM_05969 PE=4 SV=1
tr|K4E1C8	5,1	Beta-adaptin, putative OS=Trypanosoma cruzi GN=TCSYLVIO_004597 PE=4 SV=1
tr|K4EBV2	4,06	Glycerate kinase, putative OS=Trypanosoma cruzi GN=TCSYLVIO_000880 PE=4 SV=1
tr|K4DU81	2,88	40S ribosomal protein S3, putative OS=Trypanosoma cruzi GN=TCSYLVIO_000304 PE=3 SV=1
tr|Q2TJB4	2,63	Dehydrogenase OS=Trypanosoma cruzi PE=4 SV=1
tr|Q4E4V7	2,38	Prostaglandin F2alpha synthase OS=Trypanosoma cruzi (strain CL Brener) GN=Tc00.1047053508461.80 PE=4 SV=1
tr|K4DMJ1	2,33	Retrotransposon hot spot (RHS) protein, putative (Fragment) OS=Trypanosoma cruzi GN=TCSYLVIO_009588 PE=4 SV=1
tr|K4DNQ7	1,77	Uncharacterized protein OS=Trypanosoma cruzi GN=TCSYLVIO_009135 PE=4 SV=1
tr|K4E5X1	1,68	Uncharacterized protein OS=Trypanosoma cruzi GN=TCSYLVIO_002873 PE=4 SV=1
tr|K2N8A0	1,66	RNA helicase, putative OS=Trypanosoma cruzi marinkellei GN=MOQ_005178 PE=4 SV=1
tr|Q4CX87	1,54	Tryparedoxin peroxidase, putative OS=Trypanosoma cruzi (strain CL Brener) GN=Tc00.1047053509499.14 PE=4 SV=1
tr|K2MMQ6	1,24	Adenosylhomocysteinase OS=Trypanosoma cruzi marinkellei GN=MOQ_007824 PE=3 SV=1
tr|K4DZK9	1,22	Uncharacterized protein OS=Trypanosoma cruzi GN=TCSYLVIO_005575 PE=4 SV=1
tr|Q7Z1E2	1,18	Clathrin assembly protein AP19-like protein OS=Trypanosoma cruzi GN=ClaATc PE=2 SV=1
tr|K4DSA9	1,06	Glycosomal phosphoenolpyruvate carboxykinase, putative OS=Trypanosoma cruzi GN=TCSYLVIO_007745 PE=3 SV=1
tr|V5B5L8	1,04	Pyrroline-5-carboxylate synthetase-like protein OS=Trypanosoma cruzi Dm28c GN=TCDM_02659 PE=4 SV=1

B		
Accession	↓emPAI	Description
tr|K4E9F9	117,84	Mu-adaptin 1, putative,adaptor complex AP-1 medium subunit, putative OS=Trypanosoma cruzi GN=TCSYLVIO_001761 PE=4 SV=1
tr|V5BW37	13,82	Gamma-adaptin 1 OS=Trypanosoma cruzi Dm28c GN=TCDM_02471 PE=4 SV=1
tr|K4DS68	10,56	Glucose-regulated protein 78, putative (Fragment) OS=Trypanosoma cruzi GN=TCSYLVIO_008232 PE=3 SV=1
tr|V5DDV1	10,4	Beta-adaptin OS=Trypanosoma cruzi Dm28c GN=TCDM_05969 PE=4 SV=1
tr|K4E1C8	9,51	Beta-adaptin, putative OS=Trypanosoma cruzi GN=TCSYLVIO_004597 PE=4 SV=1
tr|K2PB50	9,28	Glucose-regulated protein 78, putative OS=Trypanosoma cruzi marinkellei GN=MOQ_001461 PE=3 SV=1
tr|K2MZN4	8,92	40S ribosomal protein S3, putative OS=Trypanosoma cruzi marinkellei GN=MOQ_003638 PE=3 SV=1
tr|Q4DA	5,03	Heat shock 70 kDa protein, putative (Fragment) OS=Trypanosoma cruzi (strain CL Brener)

Z6		GN=Tc00.1047053506135.9 PE=3 SV=1
tr|Q4C QJ7	4,99	Ribosomal protein L21E (60S), putative OS=Trypanosoma cruzi (strain CL Brener) GN=Tc00.1047053507251.20 PE=4 SV=1
tr|K4E4 W4	3,88	Heat shock 70 kDa protein, mitochondrial, putative OS=Trypanosoma cruzi GN=TCSYLVIO_003281 PE=3
tr|V5BS 80	3,51	ATP-dependent RNA helicase OS=Trypanosoma cruzi Dm28c GN=TCDM_00483 PE=3 SV=1
tr|Q4C QW2	3,33	60S ribosomal protein L4, putative OS=Trypanosoma cruzi (strain CL Brener) GN=Tc00.1047053504121.30 PE=4 SV=1
sp|P334 47	2,93	Tyrosine aminotransferase OS=Trypanosoma cruzi PE=1 SV=2
tr|Q4CY Q8	2,93	Actin, putative OS=Trypanosoma cruzi (strain CL Brener) GN=Tc00.1047053510571.30 PE=3 SV=1
tr|K2M 741	2,91	ATP synthase subunit beta OS=Trypanosoma cruzi marinkellei GN=MOQ_005364 PE=3 SV=1
tr|Q4C M56	2,72	Tryparedoxin peroxidase, putative OS=Trypanosoma cruzi (strain CL Brener) GN=Tc00.1047053507259.10 PE=4 SV=1
tr|K4DT U5	2,52	Chaperone DNAJ protein, putative OS=Trypanosoma cruzi GN=TCSYLVIO_007186 PE=3 SV=1
tr|K4DN Q7	2,1	Uncharacterized protein OS=Trypanosoma cruzi GN=TCSYLVIO_009135 PE=4 SV=1
tr|V5AU M8	1,87	Uncharacterized protein OS=Trypanosoma cruzi Dm28c GN=TCDM_07430 PE=4 SV=1
tr|V5BI6 2	1,59	Ubiquinone biosynthesis protein COQ4 homolog, mitochondrial OS=Trypanosoma cruzi Dm28c GN=TCDM_14232 PE=3 SV=1
tr|Q4CX 87	1,54	Tryparedoxin peroxidase, putative OS=Trypanosoma cruzi (strain CL Brener) GN=Tc00.1047053509499.14 PE=4 SV=1
tr|Q7Z1 E2	1,54	Clathrin assembly protein AP19-like protein OS=Trypanosoma cruzi GN=ClaATc PE=2 SV=1
tr|Q1L1I 2	1,48	Tc24 protein (Fragment) OS=Trypanosoma cruzi PE=4 SV=1
tr|V5BZ 53	1,37	Glucose-regulated protein 78 OS=Trypanosoma cruzi Dm28c GN=TCDM_01248 PE=3 SV=1
tr|K2M VM1	1,26	Pyruvate phosphate dikinase, putative OS=Trypanosoma cruzi marinkellei GN=MOQ_000480 PE=4 SV=1
sp|P266 43	1,23	60S acidic ribosomal protein P1 OS=Trypanosoma cruzi PE=3 SV=1
tr|V5D6 I4	1,21	Uncharacterized protein OS=Trypanosoma cruzi Dm28c GN=TCDM_09201 PE=4 SV=1
tr|K4DT 97	1,16	Glucose-regulated protein 78, putative OS=Trypanosoma cruzi GN=TCSYLVIO_007719 PE=3 SV=1
tr|Q8T8 E0	1,07	Tryparedoxin OS=Trypanosoma cruzi GN=TPNI PE=4 SV=1

Figura 6.6. **Proteínas identificadas como associadas à TcAP1-µ**.

(A) Proteínas identificadas associadas a TcAP1-µ utilizando o tampão de extração 3 (Hepes 20 mM pH 7.4, NaCl 100 mM , Triton 0,1%, $MgCl_2$ 1 mM, $CaCl_2$ 10 µM) e em (B) com o tampão de extração 5 (Hepes 20 mM pH 7.4, Na-Citrato 250mM, CHAPS 0,1%, $MgCl_2$ 1 mM, $CaCl_2$ 10 µM). Foram selecionadas proteína com valor de emPAI≥1,0 e as que possuíam o emPAI 5 vezes maior do que no controle. emPAI indica o índice de abundância de cada proteína no imunoprecitado. As proteínas que estão destacadas na tabela são as proteínas que fazem parte do complexo TcAP-1 (Clathrin assembly protein AP-19 é a subunidade AP1-σ).

A

Accession	↓emPAI	Description
tr|V5DDV1	23	Beta-adaptin OS=Trypanosoma cruzi Dm28c GN=TCDM_05969 PE=4 SV=1
tr|K4E1C8	21,17	Beta-adaptin, putative OS=Trypanosoma cruzi GN=TCSYLVIO_004597 PE=4 SV=1
tr|B5U6U3	21,12	Elongation factor 1-alpha OS=Trypanosoma cruzi GN=G5 PE=3 SV=1
tr|K4E9F9	8,64	Mu-adaptin 1, putative,adaptor complex AP-1 medium subunit, putative OS=Trypanosoma cruzi GN=TCSYLVIO_001761 PE=4 SV=1
tr|V5BW37	8,19	Gamma-adaptin 1 OS=Trypanosoma cruzi Dm28c GN=TCDM_02471 PE=4 SV=1
tr|K4EBV2	4,06	Glycerate kinase, putative OS=Trypanosoma cruzi GN=TCSYLVIO_000880 PE=4 SV=1
tr|K4DMJ1	2,04	Retrotransposon hot spot (RHS) protein, putative (Fragment) OS=Trypanosoma cruzi GN=TCSYLVIO_009588 PE=4 SV=1
tr|K4DU81	2,03	40S ribosomal protein S3, putative OS=Trypanosoma cruzi GN=TCSYLVIO_000304 PE=3 SV=1
tr|K4DSA9	1,66	Glycosomal phosphoenolpyruvate carboxykinase, putative OS=Trypanosoma cruzi GN=TCSYLVIO_007745 PE=3 SV=1
tr|K4DX70	1,43	ATP-dependent RNA helicase, putative OS=Trypanosoma cruzi GN=TCSYLVIO_006093 PE=3
tr|K4E5X1	1,25	Uncharacterized protein OS=Trypanosoma cruzi GN=TCSYLVIO_002873 PE=4 SV=1
tr|K2NR29	1,17	ADP,ATP carrier protein 1, mitochondrial, putative,ADP/ATP translocase 1, putative OS=Trypanosoma cruzi marinkellei GN=MOQ_004780 PE=3 SV=1
tr|Q26907	1,16	Cytoplasmic repetitive antigen (CRA) protein (Fragment) OS=Trypanosoma cruzi PE=4 SV=1
tr|Q4E4E7	1,05	Tyrosine aminotransferase OS=Trypanosoma cruzi (strain CL Brener) GN=Tc00.1047053510187.30 PE=3 SV=1
tr|K4DR85	1,05	T-complex protein 1 subunit delta OS=Trypanosoma cruzi GN=TCSYLVIO_008271 PE=3 SV=1

B

Accession	↓emPAI	Description
tr|Q26973	167,23	Alpha-tubulin OS=Trypanosoma cruzi PE=2 SV=1
tr|K4DWZ6	42,95	40S ribosomal protein S2, putative OS=Trypanosoma cruzi GN=TCSYLVIO_006088 PE=3 SV=1
tr|V5DDV1	11,42	Beta-adaptin OS=Trypanosoma cruzi Dm28c GN=TCDM_05969 PE=4 SV=1
tr|K4E1C8	10,79	Beta-adaptin, putative OS=Trypanosoma cruzi GN=TCSYLVIO_004597 PE=4 SV=1
tr|K4E9F9	8,64	Mu-adaptin 1, putative,adaptor complex AP-1 medium subunit, putative OS=Trypanosoma cruzi GN=TCSYLVIO_001761 PE=4 SV=1
tr|V5BW37	5,32	Gamma-adaptin 1 OS=Trypanosoma cruzi Dm28c GN=TCDM_02471 PE=4 SV=1
tr|K4DT61	4,95	Sterol 24-c-methyltransferase, putative OS=Trypanosoma cruzi GN=TCSYLVIO_007533 PE=4
tr|G0Z1B7	4,62	Prostaglandin F2alpha synthase (Fragment) OS=Trypanosoma cruzi PE=4 SV=1
tr|K2PB50	4,22	Glucose-regulated protein 78, putative OS=Trypanosoma cruzi marinkellei GN=MOQ_001461
tr|O61083	3,69	Glutamate dehydrogenase OS=Trypanosoma cruzi PE=2 SV=1
tr|Q4CYQ8	3,22	Actin, putative OS=Trypanosoma cruzi (strain CL Brener) GN=Tc00.1047053510571.30 PE=3 S
tr|Q4DAZ6	3,05	Heat shock 70 kDa protein, putative (Fragment) OS=Trypanosoma cruzi (strain CL Brener) GN=Tc00.1047053506135.9 PE=3 SV=1
tr|I6LE92	2,93	Actin OS=Trypanosoma cruzi GN=Act PE=3 SV=1
tr|K4E4W4	2,77	Heat shock 70 kDa protein, mitochondrial, putative OS=Trypanosoma cruzi GN=TCSYLVIO_003281 PE=3 SV=1
tr|Q4D3A7	2,75	Kinetoplastid membrane protein KMP-11 OS=Trypanosoma cruzi (strain CL Brener) GN=Tc00.1047053508413.68 PE=4 SV=1
tr|V5AUM8	2,47	Uncharacterized protein OS=Trypanosoma cruzi Dm28c GN=TCDM_07430 PE=4 SV=1
tr|K2M741	2,32	ATP synthase subunit beta OS=Trypanosoma cruzi marinkellei GN=MOQ_005364 PE=3 SV=1
sp|P26643	1,91	60S acidic ribosomal protein P1 OS=Trypanosoma cruzi PE=3 SV=1
tr|V5BI62	1,59	Ubiquinone biosynthesis protein COQ4 homolog, mitochondrial OS=Trypanosoma cruzi Dm28c GN=TCDM_14232 PE=3 SV=1
tr|K4DP32	1,37	Uncharacterized protein (Fragment) OS=Trypanosoma cruzi GN=TCSYLVIO_009041 PE=4 SV=1
tr|V5C2S4	1,31	T-complex protein 1 OS=Trypanosoma cruzi Dm28c GN=TCDM_00106 PE=3 SV=1
tr|K4DZ31	1,31	T-complex protein 1, eta subunit, putative OS=Trypanosoma cruzi GN=TCSYLVIO_005772
tr|K4E544	1,2	Chaperonin HSP60/CNP60, putative OS=Trypanosoma cruzi GN=TCSYLVIO_003311 PE=3 SV=1
tr|K4DTU5	1,18	Chaperone DNAJ protein, putative OS=Trypanosoma cruzi GN=TCSYLVIO_007186 PE=3 SV=1

tr|K4DT97	1,16	Glucose-regulated protein 78, putative OS=Trypanosoma cruzi GN=TCSYLVIO_007719 PE=3 S
tr|V5BZ53	1,11	Glucose-regulated protein 78 OS=Trypanosoma cruzi Dm28c GN=TCDM_01248 PE=3 SV=1
tr|K4EDM1	1,11	T-complex protein 1 subunit gamma OS=Trypanosoma cruzi GN=TCSYLVIO_000177 PE=3 SV1

Figura 7. **Proteínas identificadas como associadas à TcAP1-β**. A. Proteínas identificadas associadas a TcAP1-μ utilizando o tampão de extração 3 (Hepes 20 mM pH 7.4, NaCl 100 mM , Triton 0,1%, MgCl$_2$ 1 mM, CaCl$_2$ 10 μM) e em B. com o tampão de extração 5 (Hepes 20 mM pH 7.4, Na-Citrato 250mM, CHAPS 0,1%, MgCl$_2$ 1 mM, CaCl$_2$ 10 μM). Foram selecionadas proteína com valor de emPAI≥1,0 e as que possuíam o emPAI cinco vezes maior do que no controle. emPAI indica o índice de abundância de cada proteína no imunoprecitado. As proteínas que estão destacadas na tabela são as proteínas que fazem parte do complexo TcAP-1.

6 DISCUSSÃO REFERENTE AOS RESULTADOS SUPLEMENTARES NÃO PUBLICADOS DO CAPÍTULO 2

O complexo adaptador 1 (AP-1) possui como uma de suas funções, realizar a interface entre componentes de membrana da rede trans-Golgi, como proteínas e lipídios e recrutar a clatrina para formar o revestimento da vesícula (PARK & GUO, 2014). Sua estrutura, em forma de bloco, incluindo duas "orelhas" ligadas por uma haste flexível (dobradiça), auxilia nessa função de adaptador (OWEN *et al.*, 2004). Cada subunidade desempenha diferentes funções e associações fora e dentro do complexo. A adaptina γ interage com a clatrina, com a GTPase Arf1 e, juntamente com a subunidade σ, interage com receptor de membrana. A subunidade β1 interage com a clatrina na região da dobradiça. A interação com a GTPase Arf1 e com receptor de membrana ocorre através da sua região N-terminal. A porção C-terminal dessa adaptina faz interação com diversas proteínas regulatórias e acessórias. A subunidade µ1 interage através da porção N-terminal, com receptor de membrana.

Em *T. cruzi*, todas as subunidades do complexo AP-1, tem ortólogos em *T. brucei* e *Leishmania* spp (MOREIRA, 2013). Porém pouco é conhecido sobre as interações de AP-1 com outras proteínas que participam do tráfego vesicular e quais os cargos que as vesículas revestidas por AP-1 transportam a partir da rede trans-Golgi nesses tripanossomatídeos. Análise das proteínas associadas a AP-1 pode indicar se o processo de formação de vesículas na rede trans-Golgi é realizado como em outros eucariotos ou se tem particularidades aos tripanossomatídeos, tal como já observado em relação à ausência de um receptor de manose-6-fosfato para reconhecimento do cargo a ser transportado por AP-1. Entretanto, a análise por imunoprecipitação a partir da utilização das adaptinas β1 e µ1 fusionadas com GFP não evidenciou outras proteínas associadas ao AP-1, sugerindo que as interações sejam muito dinâmicas ou que a introdução de uma etiqueta tal como GFP (28 kDa) possa ter dificultado a interação das subunidades do complexo AP-1 com outras proteínas, principalmente clatrina e episinaR. A introdução de etiquetas nas subunidades do complexo AP-1 possui vários problemas, pois tanto a região N-terminal quanto a região C-terminal das subunidades do complexo estão comprometidas com associações com componentes de membrana ou proteínas tais como clatrina, epsinaR e outras proteínas acessórias. Mesmo assim, optamos por adicionar a etiqueta GFP na região C-terminal das subnidades TcAP1-β e TcAP1-µ, pois poderiam estar mais acessíveis para interação com os *nanobodies* anti-GFP.

A dinâmica da montagem de vesículas com revestimento com clatrina ocorre pelo recrutamento do complexo adaptador AP-1 para membrana da rede trans-Golgi, que então precisa ser ativado para se associar com fosfolipídeos e com a carga, para somente então

recrutar a clatrina e demais proteínas acessórias para o local da montagem do revestimento (KIRCHHAUSEN, 2000). É possível que a etiqueta GFP, nos dois casos, de alguma forma, esteja inibindo a ativação do complexo e dificultado que o AP desenvolva sua função. Tanto a subunidade TcAP1-β quanto a TcAP1-μ podem se associar com componentes de membrana e essa associação acontece pela região N-terminal (TRAUB, 2009), a qual não foi modificada na construção com fusão com GFP. Isso explicaria a localização dessas proteínas no complexo de Golgi, não significando, porém, que o complexo está corretamente montado nessa região.

Por outro lado, quando imunoprecipitamos a cadeia leve de clatrina de *T. cruzi* (artigo incluído nesse capítulo), foi possível co-imunoprecipitar diversas proteínas, incluindo todas as subunidades do complexo TcAP-1. O adaptador AP1 interage com a porção globular/terminal da cadeia pesada da clatrina (BONIFACINO & TRAUB, 2003), portanto essa região estaria livre para interagir com o complexo AP-1, já que a etiqueta foi fusionada na cadeia leve de clatrina.

Apesar de não conseguirmos identificar outras proteínas nas imunoprecipitações de TcAP1-β/GFP e TcAP1-μ/GFP, além daquelas do próprio complexo, foi possível observar que a interação entre as subunidades do complexo AP1 parece ser bem estável em *T. cruzi*, mesmo na presença de uma etiqueta robusta como GFP. Além disso, em todas as condições testadas conseguimos identificar a presença de TcAP1-γ por western blot, mesmo nas condições mais estringentes.

7   CONCLUSÕES

Capítulo 1

1. TcAP1-γ não é essencial para T. cruzi;
2. O nocaute de TcAP1-γ reduziu a proliferação e diferenciação para forma tripomastigota metacíclica;
3. As formas tripomastigotas metacíclicas do mutante para TcAP1-γ tem capacidade reduzida de infectar em linhagens celulares;
4. O processamento da cruzipaína foi reduzido significantemente na ausência de TcAP1-γ;
5. O transporte da cruzipaína do complexo de Golgi para os reservossomos em epimastigotas é dependente de AP-1;
6. A cruzipaína na superfície de amastigotas e tripomastigotas metacíclicas está reduzida na linhagem mutante para AP1-γ;
7. Não foram observadas alterações ultraestruturais no complexo de Golgi e nos reservossomos do mutante TcAP1γ;
8. O parasita mutante para AP1-γ, quando complementado com o plasmídeo pTcGW-AP1γ-bsd expressando a subunidade AP1-γ, recuperou a capacidade de diferenciação, de transporte da cruzipaína processada para os reservossomos e infectividade.

Capítulo 2

1. As subunidades TcAP1-β/GFP e TcAP1-µ/GFP se encontram no complexo de Golgi, co-localizando com a subunidade TcAP1-γ;
2. Não foi possível identificar proteínas parceiras de TcAP-1 além das subunidades do próprio complexo pela técnica de cryogriding, possivelmente pelo tamanho do tag utilizado (GFP);
3. Entretanto, utilizando a cadeia leve de clatrina e epsinaR como iscas, foi possível identificar interação dessas duas proteínas com TcAP-1 (Kalb et al., 2016).
4. Os resultados da análise por espectrometria de massas da imunoprecipitação de TcAP1-β e TcAP1-µ mostraram que as quatro subunidades do complexo AP-1 se associam em *T. cruzi*.

8 REFERÊNCIAS

ALLEN, C. L. et al. Dileucine signal-dependent and AP-1-independent targeting of a lysosomal glycoprotein in Trypanosoma brucei. **Molecular and biochemical parasitology**, v. 156, n. 2, p. 175–90, dez. 2007.

ALLEN, C. L.; GOULDING, D.; FIELD, M. C. Clathrin-mediated endocytosis is essential in Trypanosoma brucei. **The EMBO journal**, v. 22, n. 19, p. 4991–5002, 1 out. 2003.

BAI, H.; DORAY, B.; KORNFELD, S. GGA1 Interacts with the Adaptor Protein AP-1 through a WNSF Sequence in Its Hinge Region. **Journal of Biological Chemistry**, v. 279, n. 17, p. 17411–17417, 2004.

BATISTA, C. M. et al. MAb CZP-315.D9: An antirecombinant cruzipain monoclonal antibody that specifically labels the reservosomes of trypanosoma cruzi epimastigotes. **BioMed Research International**, v. 2014, 2014.

BATISTA, M. et al. A high-throughput cloning system for reverse genetics in Trypanosoma cruzi. **BMC microbiology**, v. 10, n. 1, p. 259, 2010.

BOEHM, M.; BONIFACINO, J. S. Adaptins: The Final Recount. **Molecular biology of the cell**, v. 12, n. October, p. 2907–2920, 2001.

BONIFACINO, J. S.; TRAUB, L. M. Signals for sorting of transmembrane proteins to endosomes and lysosomes. **Annual review of biochemistry**, v. 72, p. 395–447, 2003.

BROOKS, D. R. et al. Processing and trafficking of cysteine proteases in Leishmania mexicana. **Journal of cell science**, v. 113 (Pt 2, p. 4035–4041, 2000.

CAMPBELL, T. N; CHOY, Y. M. Protein Trafficking in the Biosynthetic Pathway. v. 2, n. 3, p. 67–76, 2001.

CAVALIER-SMITH, T. Kingdoms Protozoa and Chromista and the eozoan root of the eukaryotic tree. **Biology Letters**, v. 6, n. 3, p. 342–345, 2010.

CAZZULO, J. Proteinases of Trypanosoma Cruzi: Potential Targets for the Chemotherapy of Chagas Disease. **Current Topics in Medicinal Chemistry**, v. 2, n. 11, p. 1261–1271, 2002.

COLE, N. B.; LIPPINCOTT-SCHWARTZ, J. Organization of organelles and membrane traffic by microtubules. **Current Opinion in Cell Biology**, v. 7, n. 1, p. 55–64, 1995.

COLLINS, B. M. et al. Molecular architecture and functional model of the endocytic AP2

complex. **Cell**, v. 109, n. 4, p. 523–35, 17 maio 2002.

CONTRERAS, V. T.; MOREL, C. M.; GOLDENBERG, S. Stage specific gene expression precedes morphological changes during Trypanosoma cruzi metacyclogenesis. **Molecular and Biochemical Parasitology**, v. 14, n. 1, p. 83–96, 1985.

CORRÊA, J. R. et al. Clathrin in Trypanosoma cruzi: in silico gene identification, isolation, and localization of protein expression sites. **The Journal of eukaryotic microbiology**, v. 54, n. 3, p. 297–302, 2007.

COURA, J. R. Chagas disease: what is known and what is needed--a background article. **Memórias do Instituto Oswaldo Cruz**, v. 102 Suppl, n. August, p. 113–22, 30 out. 2007.

COURA, J. R.; VINAS, P. A. Chagas disease: a new worldwide challenge. **Nature**, v. 465, p. 56–57, 2010.

DE SOUZA, W. Basic cell biology of Trypanosoma cruzi. **Current pharmaceutical design**, v. 8, n. 4, p. 269–85, jan. 2002a.

DE SOUZA, W. Special organelles of some pathogenic protozoa. **Parasitology research**, v. 88, n. 12, p. 1013–25, dez. 2002b.

DE SOUZA, W.; SANT'ANNA, C.; CUNHA-E-SILVA, N. L. Electron microscopy and cytochemistry analysis of the endocytic pathway of pathogenic protozoa. **Progress in histochemistry and cytochemistry**, v. 44, n. 2, p. 67–124, jan. 2009.

DENNY, P. W. et al. Leishmania major: clathrin and adaptin complexes of an intra-cellular parasite. **Experimental parasitology**, v. 109, n. 1, p. 33–7, jan. 2005.

DI PAOLO, G.; DE CAMILLI, P. Phosphoinositides in cell regulation and membrane dynamics. **Nature**, v. 443, n. 7112, p. 651–657, 2006.

DOCAMPO, R. et al. Acidocalcisomes - conserved from bacteria to man. **Nat Rev Microbiol**, v. 3, n. 3, p. 251–261, 2005.

EDELING, M. A; SMITH, C.; OWEN, D. Life of a clathrin coat: insights from clathrin and AP structures. **Nature reviews. Molecular cell biology**, v. 7, n. 1, p. 32–44, jan. 2006.

FAGONE, P.; JACKOWSKI, S. Membrane phospholipid synthesis and endoplasmic reticulum function. **Journal of lipid research**, v. 50 Suppl, p. S311-6, 2009.

FAINI, M. et al. Vesicle coats: Structure, function, and general principles of assembly. **Trends in Cell Biology**, v. 23, n. 6, p. 279–288, 2013.

FARQUHAR, M. G.; PALADE, G. E. The Golgi apparatus (complex)-(1954-1981)-from artifact to center stage. **The Journal of cell biology**, v. 91, n. 3 Pt 2, p. 77s–103s, dez. 1981.

FARQUHAR, M. G.; PALADE, G. E. The Golgi apparatus: 100 years of progress and controversy. **Trends in cell biology**, v. 8, n. 1, p. 2–10, jan. 1998.

FIELD, M. C.; CARRINGTON, M. The trypanosome flagellar pocket. **Nature reviews. Microbiology**, v. 7, n. 11, p. 775–86, 2009.

GHOSH, P.; DAHMS, N. M.; KORNFELD, S. Mannose 6-phosphate receptors: new twists in the tale. **Nature reviews. Molecular cell biology**, v. 4, n. 3, p. 202–12, mar. 2003.

GOKOOL, S. Sigma 1- and mu 1-Adaptin homologues of Leishmania mexicana are required for parasite survival in the infected host. **The Journal of biological chemistry**, v. 278, n. 32, p. 29400–9, 8 ago. 2003.

HELDWEIN, E. E. et al. Crystal structure of the clathrin adaptor protein 1 core. **Proceedings of the National Academy of Sciences of the United States of America**, v. 101, n. 39, p. 14108–13, 2004.

HIRST, J. et al. Characterization of a fourth adaptor-related protein complex. **Molecular biology of the cell**, v. 10, n. August, p. 2787–2802, 1999.

HIRST, J. et al. The fifth adaptor protein complex. **PLoS biology**, v. 9, n. 10, p. e1001170, out. 2011.

HIRST, J. et al. Distinct and Overlapping Roles for AP-1 and GGAs Revealed by the "Knocksideways" System. **Current biology : CB**, v. 22, n. 18, p. 1711–6, 25 set. 2012.

HIRST, J.; ROBINSON, M. S. Clathrin and adaptors. **Biochimica et biophysica acta**, v. 1404, n. 1–2, p. 173–93, 14 ago. 1998.

KALB, L. C. et al. Clathrin expression in Trypanosoma cruzi. **BMC cell biology**, v. 15, p. 23, 2014.

KIRCHHAUSEN, T. Three ways to make a vesicle. **Nature reviews. Molecular cell biology**, v. 1, n. 3, p. 187–98, dez. 2000.

LE BORGNE, R.; HOFLACK, B. Mannose 6-phosphate receptors regulate the formation of clathrin-coated vesicles in the TGN. **The Journal of cell biology**, v. 137, n. 2, p. 335–45, 21 abr. 1997.

MANDON, E. C.; TRUEMAN, S. F.; GILMORE, R. Protein Translocation across the Rough

Endoplasmic Reticulum. **Cold Spring Harb Perspect Biol**, v. 5, n. 2, p. 303–368, 2013.

MANNA, P. T.; KELLY, S.; FIELD, M. C. Adaptin evolution in kinetoplastids and emergence of the variant surface glycoprotein coat in African trypanosomatids. **Molecular Phylogenetics and Evolution**, v. 67, n. 1, p. 123–128, 2013.

MATTEIS, M. A. DE; LUINI, A. Exiting the Golgi complex. **Nature reviews. Molecular cell biology**, v. 9, n. April, p. 273–284, 2008.

MATTERA, R. et al. Conservation and diversification of dileucine signal recognition by adaptor protein (AP) complex variants. **Journal of Biological Chemistry**, v. 286, n. 3, p. 2022–2030, 2011.

MEYER, C. et al. mu1A-adaptin-deficient mice: lethality, loss of AP-1 binding and rerouting of mannose 6-phosphate receptors. **The EMBO journal**, v. 19, n. 10, p. 2193–2203, 2000.

MORGAN, G. W. et al. Developmental and morphological regulation of clathrin-mediated endocytosis in Trypanosoma brucei. **Journal of cell science**, v. 114, n. Pt 14, p. 2605–15, jul. 2001.

MUNRO, S. What is the Golgi apparatus, and why are we asking? **BMC biology**, v. 9, p. 63, jan. 2011.

MOREIRA C.M.N. Identificação dos genes, expressão e localização celular do complexo adaptador 1 em Trypanosoma cruzi. Dissertação de Mestrado. Pós-Graduação em Biociências e Biotecnologia, Instituto Carlos Chagas/FIOCRUZ-PR, 2013.

NAKATSU, F.; HASE, K.; OHNO, H. The role of the clathrin adaptor AP-1: Polarized sorting and beyond. **Membranes**, v. 4, n. 4, p. 747–763, 2014.

OWEN, D. J.; COLLINS, B. M.; EVANS, P. R. Adaptors for clathrin coats: structure and function. **Annual review of cell and developmental biology**, v. 20, p. 153–91, jan. 2004.

PAGE, L. J. et al. Gamma-synergin: an EH domain-containing protein that interacts with gamma-adaptin. **The Journal of cell biology**, v. 146, n. 5, p. 993–1004, 1999.

PARK, S. Y.; GUO, X. Adaptor protein complexes and intracellular transport. **Bioscience reports**, v. 34, n. 4, p. 381–390, 2014.

PEARSE, B. M. Clathrin: a unique protein associated with intracellular transfer of membrane by coated vesicles. **Proceedings of the National Academy of Sciences of the United States of America**, v. 73, n. 4, p. 1255–9, abr. 1976.

PEARSE, B. M.; ROBINSON, M. S. Purification and properties of 100-kd proteins from coated vesicles and their reconstitution with clathrin. **The EMBO journal**, v. 3, n. 9, p. 1951–7, set. 1984.

PRESLEY, J. F. et al. ER-to-Golgi transport visualized in living cells. **Nature**, v. 389, n. 6646, p. 81–85, 1997.

REN, X. et al. Structural basis for recruitment and activation of the AP-1 clathrin adaptor complex by Arf1. **Cell**, v. 152, n. 4, p. 755–767, 2013.

ROBINSON, M. S. Forty Years of Clathrin-coated Vesicles. **Traffic**, v. 16, n. 12, p. 1210–1238, 2015.

SANDERFOOT, A. A. The Specificity of Vesicle Trafficking: Coat Proteins and SNAREs. **the Plant Cell Online**, v. 11, n. 4, p. 629–642, 1999.

SANT'ANNA, C. et al. Subcellular proteomics of Trypanosoma cruzi reservosomes. **Proteomics**, v. 9, n. 7, p. 1782–94, abr. 2009.

SCOTT, C. C.; VACCA, F.; GRUENBERG, J. Endosome maturation, transport and functions. **Seminars in Cell and Developmental Biology**, v. 31, p. 2–10, 2014.

SHIH, W.; GALLUSSER, A; KIRCHHAUSEN, T. A clathrin-binding site in the hinge of the beta 2 chain of mammalian AP-2 complexes. **The Journal of biological chemistry**, v. 270, n. 52, p. 31083–90, 29 dez. 1995.

SOARES, M. J. The Reservosome of Trypanosoma cruzi Epimastigotes: An Organelle of the Endocytic Pathway with a Role on Metacyclogenesis. **Memorias do Instituto Oswaldo Cruz**, v. 94, n. SUPPL. 1, p. 139–141, 1999.

SOARES, M. J.; SOUTO-PADRÓN, T.; DE SOUZA, W. Identification of a large pre-lysosomal compartment in the pathogenic protozoon Trypanosoma cruzi. **Journal of cell science**, v. 102 (Pt 1, p. 157–167, 1992.

SOARES, M. J.; SOUZA, W. DE. Endocytosis of gold-labeled proteins and LDL by Trypanosoma cruzi. **Parasitology research**, p. 461–468, 1991.

SOUTO-PADRÓN, T. et al. Cysteine proteinase in Trypanosoma cruzi: immunocytochemical localization and involvement in parasite-host cell interaction. **Journal of cell science**, v. 96 (Pt 3), n. 2, p. 485–490, 1990.

SZUL, T.; SZTUL, E. COPII and COPI Traffic at the ER-Golgi Interface. **Physiology**, v. 26,

n. 5, p. 348–364, 2011.

TAN, H.; ANDREWS, N. W. Don't bother to knock--the cell invasion strategy of Trypanosoma cruzi. **Trends in parasitology**, v. 18, n. 10, p. 427–8, out. 2002.

TARLETON, R. L. et al. Chagas Disease and the London Declaration on Neglected Tropical Diseases. **PLoS Neglected Tropical Diseases**, v. 8, n. 10, p. 8–13, 2014.

TAZEH, N. N. et al. Role of AP-1 in developmentally regulated lysosomal trafficking in Trypanosoma brucei. **Eukaryotic cell**, v. 8, n. 9, p. 1352–61, set. 2009.

TEIXEIRA, D. E. et al. Atlas didático Ciclo de vida do Trypanosoma cruzi. p. 50, 2011.

TRAUB, L. M. Tickets to ride: selecting cargo for clathrin-regulated internalization. **Nature reviews. Molecular cell biology**, v. 10, n. 9, p. 583–96, set. 2009.

TRAUB, L. M.; KORNFELD, S. The trans-Golgi network: a late secretory sorting station. **Current opinion in cell biology**, v. 9, n. 4, p. 527–33, ago. 1997.

TRAUB, L. M.; OSTROM, J. A.; KORNFELD, S. Biochemical dissection of AP-1 recruitment onto Golgi membranes. **Journal of Cell Biology**, v. 123, n. 3, p. 561–573, 1993.

VIDAL, J. C. et al. Lysosome-like compartments of Trypanosoma cruzi trypomastigotes may originate directly from epimastigote reservosomes. **Parasitology**, p. 1–10, 2017.

VINCE, J. E. et al. Leishmania adaptor protein-1 subunits are required for normal lysosome traffic, flagellum biogenesis, lipid homeostasis, and adaptation to temperatures encountered in the mammalian host. **Eukaryotic Cell**, v. 7, n. 8, p. 1256–1267, 2008.

WANG, Y. J. et al. Phosphatidylinositol 4 phosphate regulates targeting of clathrin adaptor AP-1 complexes to the Golgi. **Cell**, v. 114, n. 3, p. 299–310, 2003.

YEUNG, B. G.; PHAN, H. L.; PAYNE, G. S. Adaptor Complex-independent Clathrin Function in Yeast. **Molecular Biology of the Cell**, v. 10, n. 11, p. 3643–3659, 1999.

YOSHIDA, N. Molecular basis of mammalian cell invasion by Trypanosoma cruzi. **Anais da Academia Brasileira de Ciências**, v. 78, n. 1, p. 87–111, 2006.

ZIZIOLI, D. et al. Early embryonic death of mice deficient in gamma-adaptin. **The Journal of biological chemistry**, v. 274, n. 9, p. 5385–5390, 1999.